# OPTIMAL ENERGY MANAGEMENT OF SOLAR-ASSISTED HEAT PUMP WATER HEATING SYSTEMS: A CASE OF STUDENT RESIDENCES AT THE CENTRAL UNIVERSITY OF TECHNOLOGY, FREE STATE

By

**TSHOLOFELO PRISCILLA GAONWE**

Dissertation submitted in fulfilment of the requirements for the degree:

**Master of Engineering in Mechanical Engineering**

In the Department of Mechanical and Mechatronic Engineering

Faculty of Engineering, Built Environment and Information Technology

Central University of Technology, Free State

Supervisor: Prof. K. Kusakana

Co-Supervisor: Dr. P.A. Hohne

July 2022

# DECLARATION

I, TSHOLOFELO PRISCILLA GAONWE, _____, do hereby declare that this research project, which has been submitted to the Central University of Technology Free State, for the degree: Master of Engineering in Mechanical Engineering, is my own independent work and complies with the Code of Academic Integrity, as well as other relevant policies, procedures, rules and regulations of the Central University of Technology, Free State. This project has not been submitted before by any person in fulfilment (or partial fulfilment) of the requirements for the attainment of any qualification.

**T.P. Gaonwe** Date: **22 July 2022**

# DEDICATION

I hereby dedicate this dissertation to my son, Motheo Osego Gaonwe, who has given the greatest enthusiasm throughout my study. Having him grow up in the absence of my presence, as I carried out my studies, has been challenging. However, your love for me has been one of my greatest motivations.

My beautiful mother, Nomathemba Irene Gaonwe, who has continuously believed in me and supported me throughout my journey. I am forever grateful to you for helping raise my son while I complete my study and encouraged me my best no matter what. You have been my greatest pillar of strength and I can never thank God enough for a God-sent Angel like you. Furthermore, to my sisters, particularly my eldest, Boingotlo Bridgette Gaonwe, for all the support that she has given me, sacrificing the most to be the support system I needed.

Above all, I thank my Heavenly Father for the strength, wisdom and knowledge throughout this journey, that has not been easy to carry alone.

# ACKNOWLEDGMENTS

I would like to express my most sincere gratitude to my supervisors, Prof. K. Kusakana and Dr P.A Hohne, for their continued support, valuable guidance, encouragement and above all, their patience throughout this challenging journey.

I acknowledge the Central University of Technology (CUT), Free State, for their financial support and assistance.

# LIST OF ABBREVIATIONS

| | |
|---|---|
| ASHPWH | Air-source heat pump water heater |
| BEP | Break-even point |
| COP | Coefficient of performance |
| DHW | Domestic hot water |
| DSM | Demand-side management |
| DR | Demand response |
| DX-SAHP | Direct-expansion solar-assisted heat pump water heaters |
| ESC | Extremum seeking control |
| ESTWH | Electric storage tank-water heater |
| ETC | Evacuated tubes collectors |
| FL | Fuzzy logic controller |
| FPC | Flat plate collector |
| GHG | Greenhouse gas emission |
| HPWH | Heat pump water heater |
| IDX-SAHP | Indirect-expansion solar-assisted heat pump water heaters |
| LCC | Life cycle costs |
| MINLP | Mixed integer nonlinear programming |
| MPC | Model predictive control |
| NLP | Nonlinear programming |
| OC | Optimal control |
| PID | Proportional integral derivative |
| PV | Photovoltaic panel/cell |
| RBC | Rule-based controller |
| SAHPWH | Solar-assisted heat pump water heaters |
| SAURAN | Southern African Universities Radiometric Network |
| SCIP | Solving constraint integer programs |

| | |
|---|---|
| SWH | Solar water heater |
| TOU | Time-of-use electricity tariff |
| WHO | World Health Organization |

# ABSTRACT

In South Africa, more than 40% of the energy produced, is estimated to be consumed in the commercial sector. Organizations, such as universities in South Africa, are faced with increased pressure to manage energy demands and escalating energy costs. This has resulted in the country currently facing ambiguous tariff increases, at short intervals, by the power utilities and rolling blackouts that could possibly lead to a grid shutdown. On the other hand, most institutions were not designed to be energy efficient, as they were mostly constructed in an era when energy optimization did not offer sufficient financial benefits. Therefore, energy efficiency is seldom viewed as a core university function.

Standard electric storage tank-water heaters (ESTWHs) are the most used systems for sanitary water heating and are a major contributor to the undesirable high morning and afternoon peaks in energy demand. Another reason is that these systems rely solely on thermostat systems for operation control, with no other energy management activities (or technologies) in place. In addition, the thermostat automatically switches ON/OFF, to heat water to the end user's set desired thermal level throughout the day, whenever the temperature drops below the set point, due to standby losses. All these things, therefore, add to the cost of the monthly bills of the users.

Using renewable energy source water heating systems, such as air-source heat pump water heaters (ASHPWHs) and solar water heaters (SWHs), may further assist to reduce excessive energy demand and the cost of hot water production. However, these stand-alone water heating systems are insufficient, in the case of a great deal of hot water production whereby continuous energy supply is needed. This is due to the slow heating processes of the ASHPWHs and SWHs being solely dependent on thermal heat from the sun to heat the water. Furthermore, like the ESTWHs, the electricity-driven HP units on the market use primary thermostat control systems, which may further contribute to the energy consumption during the peak period.

Solar-assisted heat pump water heaters (SAHPWHs), are a possible solution to the escalating electricity charges, faced by the South African community, particularly for the continuous demand for sanitary hot water in the commercial sector, such as university student residences. The solar system may provide a great amount of thermal energy to supply the heat pump unit during the time when the sun is available, while the heat pump

consumes a minimal amount of energy, during the time when there is minimal to no solar energy available, to heat the water. These SAHPWH technologies may be a solution to assist with reducing the high energy demand, which will further help alleviate the pressure on the electricity supply grid. Additionally, implementing an optimal energy control scheme, to load shifting by the TOU tariff plan, may help alleviate demand strain on the supply grid, as well as optimize energy savings, while maintaining the consumer's thermal comfort level.

In this study, an IDX-SAHPWH system, operating under an optimal energy control scheme, integrated with the load shifting by TOU pricing plan, is proposed for the commercial sector. A student residence was used as a case study. A mathematical model of the proposed system was developed, and the optimal operation control problems were formulated. The Solving Constraint Integer Programs (SCIP) solver, in the MATLAB interface optimization toolbox, was used for the simulations, with the considered computational variables taken at 20-minute intervals. The baseline model was further simulated using the same component sizing, as well as under the same climate conditions.

From the simulation results, the proposed system, under the optimal energy control scheme integrated with the load shifting by TOU pricing plan, operates optimally, as it avoids the peak and standard periods of the TOU tariffs, which guarantees savings in energy and costs, as compared to the baseline ESTWH. The proposed system ensures that water is heated during the off-peak period to the highest temperature that will be able to maintain the thermal level of the consumers, throughout the high TOU tariff periods.

The techno-economic analysis of the optimally controlled proposed system and the baseline systems were conducted and presented for a project lifespan of 20 years. All cost aspects were considered in the analysis and, from the results obtained, the IDX-SAHPWH system showed significant savings. The cost savings obtained from the winter and summer seasons, as well as annual, are 76.0 %, 75.6 % and 75.8 %, respectively. The break-even point of the project is during the 9th month of the first year of the project, with a possible savings of 71.5 % at the end of the project's lifetime.

It may therefore be concluded that the aim of this study has been met as the IDX-SAHPWH system, when operated with the optimal energy control scheme, integrated with the load shifting by TOU pricing plan, shows a very significant savings in costs, while

maintaining the thermal comfort level of the consumers. Furthermore, the system may contribute to the load reduction during peak energy usage periods on the electricity grid supply. As a result, this system can be used in any commercial enterprise, that has a high demand for sanitary water heating.

# TABLE OF CONTENTS

# LIST OF FIGURES

# LIST OF TABLES

# CHAPTER 1: INTRODUCTION

## 1.1 BACKGROUND

Global energy consumption is increasing, while conventional energy sources are no longer sufficient to meet the energy demand, triggering as energy crisis [1]. Since the electricity generation in South Africa, is through the burning of fossil fuels, such as coal [2], it has negative environmental effects (such as greenhouse gas (GHG) emission) and promotes health risks to South Africa's citizens [3], with the country being one of the top 20 GHG emitters in the world [4]–[6]. Unfortunately, to most of South Africa's poverty-stricken citizens, this has become costly [7]. In South Africa, more than 40% of the energy production is estimated to be consumed in the commercial sector [8]. During peak demand periods, where the high demand of energy is incurred, electricity is charged at significantly higher rates, as compared to standard and low demand periods [9].

South African Universities, alike to other organisations, households and businesses are further faced with increasing pressure to manage the energy demand and escalating energy costs [10]. Most university campuses were not designed to be energy efficient, as they were mostly constructed in an era when energy optimization did not offer sufficient financial benefits. Therefore, energy efficiency is seldom viewed as a core university function, prioritizing it is a new concept [11]. As a result of electricity shortage and outages in South Africa, coupled with an ambiguous tariffs increase within short intervals by the power utilities, this has resulted in high maintenance costs (e.g. generator running and fuel cost) and reduced capital expenditure for the universities [12].

In the commercial building sector, water heating is the fourth largest of the energy consumers, after space heating, air-conditioning and lighting [13]. The sanitary hot water consumption is one of the largest contributors of the energy demand to the undesirable high morning and afternoon peaks [14]. In South Africa, the mostly common devices for heating water have been the standard electric storage tank-water heaters (ESTWHs), further known as "geysers" and "boilers". These systems may have been popular in the past, owing to their low implementation and low electricity prices. Electricity rates were low enough at the time, that energy costs were not considered. As a result of the rising

population, economy and living standards, the electricity price continues to rise, resulting in a high demand for electricity and shortage of energy. consequently, the country is currently faced with rolling blackouts, which could possibly lead to a grid shutdown [15].

Aiming to mitigate the high energy consumed during the water heating process, Eskom, the electricity supplier in South Africa, introduced energy conservation practices for electricity consumers, which includes lowering the temperature of the thermostat in the ESTWHs, to reduce standby energy loss [15]. This practice, however, increases the chance of a pathogenic bacterium, called Legionella pneumophila, which grows at temperatures ranging from 20 ºC to 45 ºC [16]. However, a temperature as low as 40°C, is thought to be suitable for user satisfaction [17]. A set point temperature suitable to prevent the breeding of Legionella pneumophila, is often greater than or equal to 55 °C, however, less than or equal to 65°C [8].

Investing in renewable energy is important in reducing the negative economic, social and environmental impacts of energy production and consumption, in South Africa [12]. Using the renewable energy sourced water heating systems, such as air-source heat pump water heaters (ASHPWHs) and solar water heaters (SWHs) [18] may further assist in reducing energy demand and cost of hot water production [19]. Furthermore, these systems are a solution to mitigating the energy shortage, provide cleaner energy and further reduce the impact of the GHG emissions [20]. The ASHPWHs are amongst the most successful technologies in the South African's renewable energy market, assumably because the ambient weather conditions in South Africa and the capital cost duly favor the utilization of ASHP system and the relative ease of installation, compared to other energy saving water heaters. ASHPWHs operate at an efficiency of more than 200% year-round, in South Africa's weather condition [21]. Additionally, the country receives the highest insolation rates (approximately 2 500 hours of sunshine a year, over 300 days of sunshine per year in some provinces) [6].

ASHPWHs transfer heat from the ambient air into the water in the tank [22], by consuming relatively a small proportion (~30%) of the transferred energy [23], as compared to the ESTWHs. However, ASHPWHs are challenged in cases of high demand for hot water, as a results of slow heating process [3]. On the other hand, SWHs solely depend on thermal heat from the sun to heat water. The solar radiation is an indefinitely

renewable and free source of energy [24]. However, due to the solar radiation being available solely during the day, meeting the hot water demand, particularly during the night, may present a major challenge [25].

It is apparent that a single system is insufficient in supporting a continuous energy supply system and may still, at one point or another, depend on the grid electricity consumption as the main source of supply of the energy. Applying the hybrid systems, such as the solar-assisted HP (SAHP) system, could assist in reaching considerable savings of energy by using free resources of the ambient condition, or stored heat in the ground and sun [26]. The SAHP system may therefore, overcome the disadvantages of the HPWHs and SWHs. The system further promotes energy conservation and efficiency of the renewable energy system [27].

Furthermore, like the ESTWHs, the electricity driven HP units on the market use primary conventional ON/OFF control, known as the digital thermostat control systems. The main problem of these control systems is the dependency of the operation on temperature set-points solely and do not change the assumed operating states between the intervals. Digital thermostat actuation occurs upon hitting the lower/upper set-point, which prolongs the operation time and consumes a high amount of energy [28]. These control systems are not sufficiently accurate due to the simplicity of the method and the quality of the controllers are not up to standard due to their low cost [29]. The development of optimal control on systems, was a result of achieving energy savings and precise process control [30].

Eskom further presented the time-based pricing, known as time-of-use (TOU) tariff, as an energy management program [31]. The consumers may, therefore, shift part of their electricity use from the peak demand period to the off-peak demand period, so that the electricity load in the peak demand period may be reduced [32]. The pricing was meant to assist in alleviating the strain on the electricity grid supply, while reducing the consumers' electricity bills [31].

SAHPWHs are a possible solution to the escalating electricity charges faced by the South African community. Particularly to the continuous demand for sanitary hot water in the commercial sector, such as the University student residences. The solar system may provide a significant amount of thermal energy, to heat the water during the time when the

sun is available, and the heat pump consumes a minimal amount of energy to heat the water during the time when there is low to no solar energy available. The SAHPWH system may therefore operate 24 hours a day, with minimal to no use of the high-energy-consuming resistive element. With South Africa being said to have a favourable climate, making use of the SAHP water heating technologies may be a solution in assisting to reduce the high energy demand, which will further assist to alleviate the pressure on the electricity supply grid. Additionally, incorporating an optimal energy control scheme to shift the load to the TOU tariff plan, may help alleviate the demand strain on the supply grid, as well as maximize the energy savings, while maintaining the consumer's thermal comfort level.

## 1.2 PROBLEM STATEMENT

The Central University of Technology (CUT), Free State, has the base electrical load demand running from the Eskom's national grid and are primarily operating energy intensive devices, such as machines in the workshops, plug loads and lights, electric storage tank water heating systems (ESTWHs) (geysers and boilers) and air conditioners. The average monthly electricity cost, as per the Centlec (municipality) bills to the University, is over one million two hundred thousand Rand (> R 1120 000.00). However, a significant percentage of between 20 and 25%, were approximated to come from the contribution of electrical energy consumed by the ESTWHs that are inefficient.

The CUT campus has eight residences that use the ESTWHs for the water heating process. A survey of the resistive elements of the ESTWHs of these residences, was conducted and summed up to 494 kW, whereby the rough estimates indicate that approximately 30 to 60% of the total energy used in the residences may be allocated to water heating, as well as the total water storages of 33 580 litres. The data collected, is shown in Appendix A1 and A2. Based on the survey conducted, the following specific problems have been noticed:

- Thermostat systems, being the exception, no other energy management activities (or technologies) in terms of controlling the operation of these geysers have been applied; and the systems operate continuously throughout the day and night, whether they are being used or not. The energy is further wasted through the standby losses,

when there is no hot water demand for a certain period, as the temperature of the water decreases, the thermostat is automatically started to heat the water to the end user's set desired thermal level.

- The water heating process, in these residences further operates during the peak hours, where the electricity is more expensive than any other time of the day.
- ASHPWHs and SWHs are the most common systems used in South Africa to replace the ESTWHs, as an electric driven system. However, they display the following problems:
  - ✓ ASHPWHs have a slow rate of heating water and in cases of high demand for hot water, they are otherwise incapable of meeting the demand. In addition, they experience challenges associated with water and heat losses as storage tanks are mostly located inside with the heat pump unit outside the building [3].
  - ✓ SWHs is depended in the availability of the sun, which presents a major challenge in meeting the hot water demand during the night [7], [24].

It may therefore be acknowledged that energy costs for the two systems are high and that the society does not often make use of available technologies to form hybrid systems, as they are expensive to implement. Even though the hybrid systems improve the performance of the heat pump systems, few studies have been conducted to address this issue, particularly in the South African context.

In hindsight, the optimal energy management on a SAHP system has not been implemented in commercial buildings and, in particular, CUT students' residences. Moreover, limited studies for the system have been conducted, particularly in the South African context, with a time-based energy cost, such as TOU.

## 1.3 AIM AND OBJECTIVES

The aim of this study was to develop an optimal control strategy integrated with the load shifting of the TOU tariff for the SAHPWH system, to reduce the operation cost of the system, while maintaining the desired temperature level for the user.

The specific objectives of the project are as follows:

- Literature review on the various water heating systems and the methods of control applied.
- Sizing of a hybrid water heating system, consisting of a renewable energy source (solar) and a heat pump water heating system, based on the load profiles, solar irradiance availability and cost.
- Develop a mathematical model of a hybrid heat pump water heater system, using MATLAB, as well as formulating an energy management optimal control problem for the proposed system, under time-based pricing.
- Simulate the optimal operation of the hybrid heat pump water heating system, using the CUT residences as a case study,
- Conduct an economic analysis of the optimized hybrid heat pump system, which could be compared to the existing system (baseline), located at a case study.

## 1.4 RESEARCH METHODOLOGY & RESEARCH DESIGN

1.4.1 The literature: This focuses on studies conducted on the commonly used ESTWHs, standalone ASHPWHs and SWHs, as well as SAHP technologies and the methods of control applied to these systems in South Africa.

1.4.2 Data collection: The data collected during this study was used for the sizing and modelling of the SAHP system and for the optimal control to integrate the energy savings of the system.

- A walk-through survey was used to collect the data of the boilers at the CUT residences. The data collected is as follows:
  - ✓ Rated electrical power of the resistive elements;
  - ✓ Usage period of the element per day;
  - ✓ Volume of hot water storage tanks.
- Collection of real input (exogenous) data, using the appropriate sensors and weather station data are as follows:
  - ✓ Solar irradiance (Direct, Diffuse and Global irradiation);

- ✓ Ambient air temperature

- Hot water consumption i.e., hot water flow rates (to obtain the demand profile).
- Inlet water temperature data.
- Time-of-Use (TOU) tariffs applicable for the case study, were obtained from the Eskom Energy report.

1.4.3 Mathematical modelling. The model presents a demonstration of the hot water, heated in the storage tank to the thermal comfort level of the consumers, whenever needed for consumption. The variables of the model are the hot water temperature and the switching control status of the heat pump and the storage tank units.

- Developed a mathematical model of the main components and processes involved in a SAHP system using the real input data collected, as mentioned in Section 1.4.2. The main components of the system are as follows:
  - ✓ Solar thermal collector unit
  - ✓ Heat pump unit
  - ✓ Hot water storage tank unit
- Developed a mathematical model of the CUT boiler currently used (for comparison purposes with the proposed SAHP). The main components of the system are as follows:
  - ✓ Electric storage tank water heater unit
- Optimal control problem formulation – optimal control models were formulated and applied to the system, to minimize the operation cost and maximize the thermal comfort of the consumers subjected to the TOU plan.

1.4.5 Simulation of the optimally controlled SAHP system and baseline system in MATLAB, for the technical comparison.

1.4.6 As techno-economic analysis; the comparison of the optimally controlled system and baseline system, based on the cost of energy saved, the life cycle cost analysis and break-even cost, was conducted.

## 1.5 DELIMITATIONS

- The study solely focuses on commercial buildings, particularly students' residences and may be extended in the future to other types of buildings.
- Optimization, in terms of operation control, was conducted solely on the SAHPWH system, based on the TOU tariff applicable for the region.
- The study focuses on modelling the development and simulation use the real data, actual collected data and the interpolated data from the previous studies.
- The heat pump unit used is a liquid-source type, whereby the solar thermal collector is the heat source.
- The solar thermal collectors used are evacuated tube collectors.

## 1.6 PUBLICATIONS DURING THE STUDY

Conference papers:

- T. P. Gaonwe, K. Kusakana, and P. A. Hohne, "Prospect of Solar-assisted Heat Pump Water Heating Systems for Student Residences," *2019 Open Innovation Conference OI 2019*, pp. 199–205, 2019.
- T. P. Gaonwe, K. Kusakana, and P. A. Hohne, "Walk-through Energy Audit and Savings opportunities: Case of Water Heaters at CUT Residential Buildings." *2019 Open Innovation Conference OI 2019*.

Journal articles:

- T. P. Gaonwe, K. Kusakana, and P. A. Hohne, "A review of solar and air-source renewable water heating systems, under the energy management scheme" *Accepted in Energy Reports.*
- T. P. Gaonwe, K. Kusakana, and P. A. Hohne, "Optimal energy management of solar-assisted heat pump water heating systems" *submitted.*

## 1.7 DISERTAION LAYTOUT

This dissertation has been divided into six Chapters, with the main research results being presented in Chapter **4** and Chapter **5**.

**Chapter 1** comprises of the research background, the problem statement, objectives and methodology of the current study.

**Chapter 2** presents a literature review of the energy management and water heating systems, as well as previous studies conducted, relevant to the current study. Furthermore, key findings are discussed.

In **Chapter 3**, a mathematical model of the proposed SAHP system has been developed and presented. The optimal control problem formulation, applied to the SAHP system, has further been developed and presented.

**Chapter 4** presents the simulation results. The simulation figures of the ambient conditions and the water profiles have been presented. The proposed SAHP system modelled in Chapter **3**, has been simulated, using MATLAB and the results are presented. The baseline system was further developed from the components and parameters of the SAHP however, without the solar thermal system and the heat pump unit.

In **Chapter 5**, the Techno-economic analysis of the proposed SAHP was conducted and compared to that of the baseline. The energy cost profiles of the summer and winter seasons, for both the systems, were presented. The life cycle costs of the SAHP and baseline systems, where calculated and compared, to discover the possible savings at the end of the project lifetime.

**Chapter 6** presents a summary of the findings of the whole dissertation and the conclusions made. Finally, suggestions for the future research were given in this Chapter.

# CHAPTER 2: LITERATURE REVIEW

## 2.1 INTRODUCTION

This Chapter presents the background literature of energy management, on standard and renewable energy source water heating systems. A brief review on the demand-side management and the well-used control strategies, is presented. A brief review of the water heating systems and the background literature of the studies conducted, particularly in South Africa, is presented.

There are four sections following the introduction in this Chapter. Section 2.2 presents a summary of the energy management strategies; namely demand-side management and control and optimizations. In Section 2.3, a background literature of the studies conducted on the water heating systems is presented. Furthermore, in Section 2.4, the findings are briefly discussed, and the key results and findings are drawn from the previous Sections. Finally, Section 2.5 gives a summary of the whole Chapter.

## 2.2 ENERGY MANAGEMENT

Energy management may be defined as the strategies of shifting or optimizing the use of energy. The main purposes of energy management are: conservation of resources, climatic protection and energy cost saving [33]. The essential idea of energy management is the consistent, methodical and efficient review of energy use, focusing on energy cost optimization concerning user characteristics, financing ability, energy demands, funding opportunities and emission reductions accomplished [34].

### 2.2.1 Demand-Side Management

Demand-Side Management (DSM), is an instrument focused on changing the load profile, to optimize the entire power system from generation to end-use [35], [36]. DSM structures typically work on the condition that, either the demand side responds to price signals at peak times or other enablers allow load shifts, i.e. variations in supply frequency. DSM applications using low-carbon electricity sources, may bring about economic and

environmental benefits, in the form of improved demand-supply matching, reduced operating costs and lower carbon emissions [37].

End-users in the commercial sector, are required to reduce their consumption, particularly at defined peak-hour periods and further to be motivated to implement energy efficient systems and DSM structures [38]. A relevant DSM strategy is represented by demand response (DR) mechanisms, intended to achieve changes in electric usage by end-use customers from their normal consumption patterns, in response to changes in the price of electricity over time [36]. DR may participate in load management structures, to support the electrical power of the grid, to mitigate peak demand and prevent exposure of its infrastructure to critical strains [39]. There are two types of DR mechanisms, namely, price-based and incentive-based. The former is in response to changes in electricity prices, based on the time of the day, whereas, in the latter the customer is incentivized to reduce the load [40].

Time-of-use (TOU) tariff plan, that falls under the price-based type is one of the plans that are implemented in South Africa [31]. In this mechanism, the tariffs are charged, based on the time it is used. In a day, the time slots are divided as off-peak, standard and peak periods and the electricity rate changes in accordance with the time. Consumers are permitted to shift their activities to off-peak and standard periods, thereby achieving financial savings, TOU usually leads to changes in consumption patterns. These TOU rates, as well as the consumption patterns, vary with season (for summer and winter), leading to different rate charges and period time slots [41].

### 2.2.2 Control and Optimization strategies

In addition to demand-side management, optimization of water heating systems may be incorporated, to achieve high energy efficiency and more energy saving. [42]. The optimization-based energy management strategy regulates the control variables, based on numerical computation results, by minimizing a predefined cost function, within feasible constraints [43]. There are two main types of the control strategies, model-free (soft control) and model-based (hard control), mostly investigated for heating and cooling systems [29].

The term "model-free control", may refer to many different control techniques, ranging from classical proportional integral and derivative (PID) control to fuzzy logic (FL) control, to extremum seeking control (ESC) and to soft computing control approaches [44].

PID controllers, known to be lower level techniques [30], are feedback controllers, which work based on the errors of the system (differences between measured values and desired set point values) [29]. These controllers are well-known for their ability in correcting errors in control systems, stabilizing process, as well as controlling non-linear and time-variant systems. However, a PID controller is not always effective in producing a desired system performance, due to its simple structure and empirical tuning schemes [45]. These types of controllers have their limitations, in that the problem of multi-variable dynamic constrained processes cannot be handled. Application of lower level PID controllers to a process with uncertainty perturbations, may lead to system failure, as a result of inaccurate gain adjustment [30].

FL controllers are one of the intelligent controllers that may deal with uncertain dynamics and those with nonlinearities, as well as minimize the unnecessary consumption to maximize the energy saving [46]. Unlike classical logic that requires a deep understanding of a system, exact equations and precise numerical value, the FL controllers incorporate an alternative way of thinking, enabling the easy modelling of complex systems. They are based on the experience of the user. The FL control technique is based on rules describing the interrelations among the various inputs, to satisfy certain outputs. FL controllers are in the form of (if-then) rules and they should cover all the expected conditions in the system [47].

ESC is an adaptive algorithm, where the goal is to optimize an objective function in real-time, by driving inputs to value that minimize the cost. Although the goal is to minimize some function, it is assumed that the cost function and the plant dynamics are known [48].

Model-based control approaches, such as the model predictive controllers (MPC) and the optimal control (OC), generally employ different types of models to estimate system energy performance and dynamics to the changes of control settings [49], as well as provide significant cost savings. However, they require an accurate mathematical control model

[44]. The two strategies are known as higher level strategies, as they may effectively handle multi-variable dynamic constrained systems and an optimization problem that minimises the cost function[29], [30].

MPC is an optimization problem, which aims to uncover the optimal solution for the management of a system operation, over a certain time horizon and within certain constraints. MPC is a more complex strategy, relying on a model of the building to project its behaviour in the future [50]. A system model is used to generate an appropriate control vector. As a result, this controller is robust to both time-varying system parameters and disturbances and it is able to regulate the process within the given bounds [30]. Further known as a receding horizon control, MPC implements solely the first step of the obtained control strategy and repeats the entire process as the prediction horizon is shifted forward [22]. However, being a model-based controller is one of the main drawbacks of the MPC controller, due to its extensive online computational effort [51]

OC deals with the problem of calculus of variation and consists of differentiation equations depicting the control variables paths that minimise the cost functions. It finds an optimality criterion from set of control laws for the given process, which is usually a cost function of the control and state variables [30]. OC optimizes the system operation, by solving an OC problem (OCP) at each control time step. This yields a control input profile, which minimizes a given cost function, using a simplified dynamic system model, updated system information and disturbances predictions (e.g., weather forecast and occupancy prediction). The cost function is typically a weighted sum of the conflicting objectives of minimizing the energy cost and the thermal discomfort [52].

Direct methods for OC are further known as "first discretize then optimize" methods, as the OCP is transcribed into a nonlinear programming problem (NLP), by discretizing the continuous time system dynamics and the cost function. The NLP obtained after discretization, may further be seen as an OCP for the discrete time system, obtained by discretizing the original system on the selected sampling time. Another well-known approach for solving OCPs are (a) dynamic programming (DP) and the Hamilton–Jacobi–Bellman approach (HJB), as well as (b) indirect methods, further known as "first optimize then discretize" [53].

## 2.3 WATER HEATING TECHNOLOGIES

### 2.3.1 Electric storage tank-water heaters (ESTWHs)

ESTWH, as shown in Figure *2.1*, relies on the electrical energy from the grid to heat water, using an electric resistive element and stores hot water for when it is needed [54]. A temperature sensor detects the temperature level of the water and switches the electrical element on through a thermostat when the water temperature is below a certain pre-set threshold. The element increases the temperature of the hot water inside the storage tank, whenever the temperature falls. The temperature falls due to draw-offs, as the cold water is automatically poured in maintaining the constant volume [55], as well as due to the heat losses, when water is not drawn for a certain period [56].

These systems have higher service availability than any other energy source and at a low cost. Furthermore, they also usually have a longer lifetime than most water heating systems [54]. They may be located nearly anywhere within a building, particularly at or near the locations where hot water is required [57]. ESTWHs, however, consume excessive electrical energy, ensuring adequate hot water temperature at the fixtures. The reason is mainly due to the continuous mixing of the incoming cold water and the storage hot water, which results in a progressive decrease in the water temperature inside the storage tank [58]. The overall efficiency of converting fossil fuels to electrical energy and then to thermal energy, is notably low and participates in fossil fuels depletion [54].

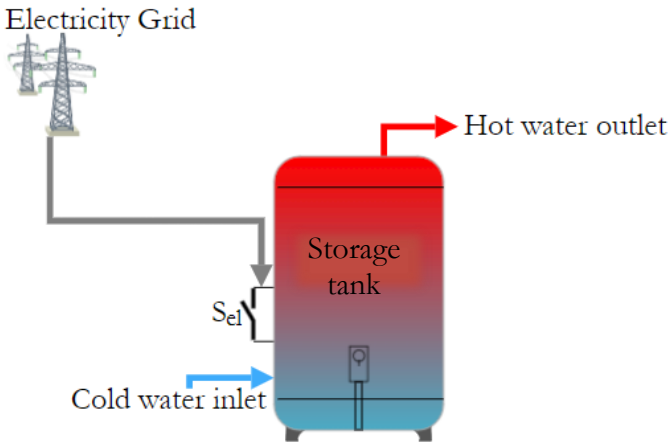


Figure 2.1: ESTWH with electricity supplied by the grid

A variety of studies, based on load shifting through scheduling and control methods on ESTWHs, have been performed, some of which are listed below:

Mabina and Mukoma [59] conducted an analysis study of direct load control of ESTWHs for strategic load conservation and load shifting for in a household. The aim of the study was to reduce energy consumption, by scheduling the ESTWH operations and, further shifting the load to off-peak periods. The study was conducted using the audit from the Energy Autonomous Campus from 100 ESTWHs. The results showed an energy consumption reduction of approximately 36% and a cost reduction of about 41%.

Shen et al. [60] formulated an optimization problem, to achieve a smart scheduling and control system, with forecast and robust model predictive control algorithms for ESTWH. The study was conducted using the data gathered from 77 electric water heaters, over 120 days in South Africa, divided into four seasons, with 30 days for each season. Simulations results showed electricity cost reductions of approximately 33.2% and 28%, as well as an average comfort fulfilment of approximately 98.7% and 98.3%, for a summer and winter day, respectively.

Khosa et al. [61], conducted a study of energy saving and cost saving on electricity consumption of an ESTWH, through the use of a smart controller for a household. The three test procedures, namely, manual mode, automatic mode and semi-automatic mode smart geyser controller. Based on the results achieved during the testing phase, savings of R3.02/kWh, when switched from manual mode to semi-automatic mode and R5.85/kWh for switching from manual to automatic mode, were obtained.

Booysen et al. [62], conducted a comparative study of energy savings through water heating using ESTWHs, by using a proposed novel optimal control of temperature and scheduling. The author examined 30 ESTWHs from the three South African provinces, namely, Western Cape, Gauteng and Mpumalanga, over a period of 20 days. Three strategies were compared. The three savings obtained are: 7.9% of temperature-matching, without adversely affecting the temperature at which water was delivered; 17.8% of the energy-matching method, with a reduction in energy lost to the environment, as well as a reduction in energy lost due to unintentional use; and 13.1% of the energy-matching method, with daily Legionella sterilisation.

Ritchie et al. [63], conducted an energy management study, by modelling the ESTWH as multi-nodal to achieve energy savings and providing it with optimal control, with perfect foreknowledge of the hot water usage profile. The impact of the number of nodes, by which the natural stratification, was evaluated. The simulation and optimization algorithm ESTWH were developed in the Jupyter Notebook and through using the Python programming. The average daily energy savings achieved for 77 households over one month, was 6.24% (0.44 kWh/day), for temperature-matched and 16.30% (1.05 kWh/day), for energy-matched optimal control of the heating element.

Roux and Booysen [64], conducted a comparative study of the ESTWHs performance with smart metering installed in two different locations, in South Africa, namely peri-rural Mkhondo and the urban Western Cape. The profiles of the water demand, energy demand and efficiency for the days of the week (including the weekend), were evaluated and compared between the two locations. The results showed that the urban Western Cape use approximately 20% more water on an average day, with 70.2% efficiency, as compared to 45.8% in Mkhondo.

### 2.3.2 Air-source heat pump water heaters (ASHPWHs)

The two types of the heat pump (HP) systems commonly used, are ground (geothermal) source HP (GSHP) and air-source HP (ASHP). GSHP has a superior performance than ASHP, both as a single or coupled system, as well as with an excellent payback-time. However, the capital cost of the design and construction of the GSHP system is significantly high and therefore limits its viability, as compared to the ASHP system in the field of sanitary hot water production [65]. ASHPWH produces low-pollutant heating energy, using the surrounding ambient air [66]. ASHPWH consists of four main components employed in a typical vapor compression refrigeration cycle, namely: an evaporator, a compressor, a condenser and an expansion valve [67].

Unlike ESTWHs that solely depend on the electrical energy to generate thermal heat [22], ASHPWHs consume a relatively small proportion (~30%) of energy to generate the same amount of thermal heat, as compared to ESTWHs [23]. They may increase energy savings in the order of 40-60% [68], [69]. ASHPWHs may be categorized into integrated and retrofit types, as shown in Figure *2.2*. In the integrated type, Figure *2.2*(a), both the

ASHP unit and the storage tank exist as a single system; the ASHP unit lies on top of the tank. Whereas, in the split type, Figure *2.2*(b), the ASHP unit is situated below the storage tank and connected by pipes [70].

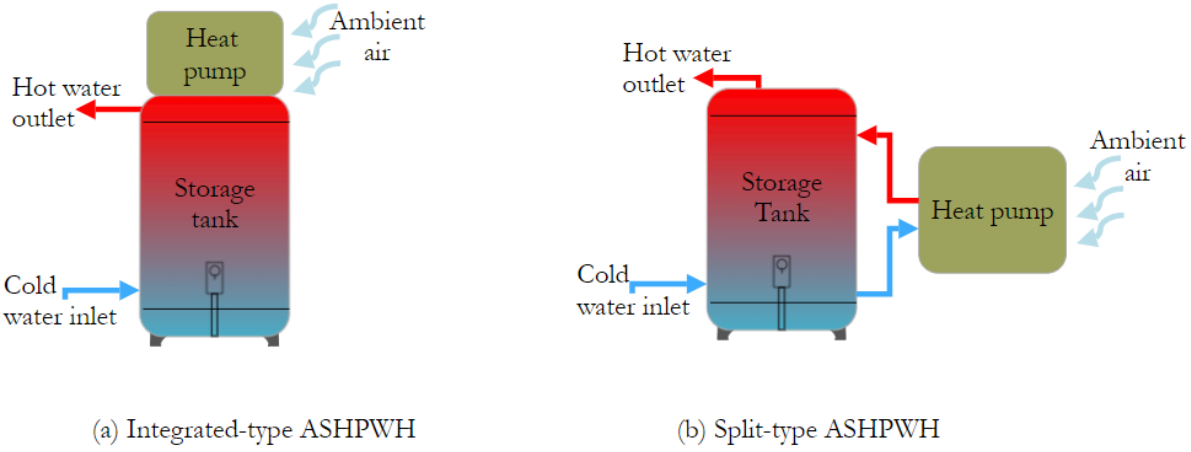


(a) Integrated-type ASHPWH (b) Split-type ASHPWH

Figure 2.2: ASHP retrofit types

The ASHPWHs is amongst the most successful technologies in the South African's renewable energy market [21]. This is, in all probability, due to the ambient weather conditions in South Africa and the capital cost duly favours the utilization of ASHP system as well as the relative ease of installation, compared to other energy saving water heaters. ASHPWHs operate at an efficiency of more than 200% year-round in South Africa's weather conditions [21]. However, there is solely 16% market penetration of the HPWH systems in South Africa [71]. The drawbacks of the HPWHs, include higher initial costs than those of conventional water heaters [54], slowing heating process, which poses a challenge in cases of high demand for hot water [71].

The results of research on HPWHs in South Africa, have revealed that the country's climate conditions favour these systems, as seen by the findings of the following studies:

Tangwe et al. [16] presented a study of data collection methods, based on the hot water profile data collected in one of the residences, at the University of Fort Hare, occupied by 75 students. The data collected was for the potential ASHP retrofit that could be installed in the residence. Two methods of data collection were experimental; using sensors and measuring devices, as well as questionnaires. The linear regression model was developed using the estimated volume of hot water, to accurately model the electrical

energy consumption from the calorifier. It was discovered that out of the 75 students, 94% used hot water during the morning peak and 61% during the evening peak. The average daily energy consumption of the 12 kW Calorifier, was 139.49 kWh, while the measured volume of hot water usage was 1950 L, which coincides with the hot water consumption from the questionnaires. The monthly energy consumption for the weekdays, were projected to be 2929.31 kWh. Furthermore, when retrofitting the Calorifier with an ASHP unit, the energy consumption was reduced to 976.43 kWh, based on its COP of 3. Finally, the payback period of the intended ASHP unit to retrofit the Calorifier, was approximated to be less than 2 years.

Tangwe et al. [65], developed and built multiple linear regression models of the COP and power consumption of an air-source heat pump retrofitted to a storage tank. The data was acquired through the installation of the relevant sensors and loggers in a middle-class home, in Fort Beaufort, South Africa. The aim of the study was to predict the performance of the ASHP water heater, with regards to the power consumption and COP under various weather conditions. The data analysis as well as the model simulation were done using SIMULINK in MATLAB software. The results show the average values of up to 1.51 per kW and 3.43 of the power consumption and COP, respectively.

Tangwe et al. [72], conducted a comparative study of the integrated and split types ASHP water heaters, to analyse the first hour heating rating and the heating cycle of the controlled volume of hot water drawn-off. Three different volumes of water storage were employed, namely, 50L, 100L and 150L. A data acquisition system was constructed and implemented, to monitor the performance of both systems for three volumes of storage tanks during the summer and winter seasons. The split type had a higher average COP values and lower power consumption values, as compared to the integrated type. Finally, the times of operation were 84 minutes and 138 minutes for the split type and integrated type, respectively.

Kukard and van Eldik [73], conducted a study on the scheduling optimization of HPWH systems, for commercial high-rise apartment buildings in South Africa. The consumption data was used as input for scheduling, to optimize the control of the predefined system and, further, to determine the required size of the HPWH equipment, along with an optimum control solution for the HP units. Simulated results showed a

possible storage capacity savings of up to 62.5%, which could substantially reduce approximately 55% of the initial capital cost of the water heating system, as well as an annual average cost saving of close to 54.87% as compared to the actual average energy costs.

### 2.3.3 Solar water heaters (SWHs)

Solar energy is recognized as one of the most promising alternative energy options. One of the simplest and most direct applications of this energy, is the conversion of solar radiation into heat. The solar radiation is an indefinitely renewable and free source of energy. Solar water heaters (SWHs), absorb thermal heat from the sun through solar radiation and transfers it to water [55]. Generally, SWHs consist of several basic components: the solar radiation collector panel, storage tank and heat transfer fluid. Furthermore, there are several additional components, such as the pump (solely necessary in active systems), auxiliary heating unit, piping units and heat exchanger [74].

SWH system recirculation of the water through the absorber panel, in the collector, may raise the temperature more than 80 °C on a favourable sunny day [75], [76]. Moreover, the solar collector placement plays a significant role in the amount of energy it may absorb. The solar collector, at any time of the day, should not be concealed from the sun [24]. Finally, the tilt angle of the collector, to be installed for the optimum performance, depends on specific coordinates of the location [77].

Furthermore, SWHs are widely used in South Africa, as the solar energy is said to be one of the renewable energy resources with the highest potential in the country [33]. South Africa receives significantly high insolation rates (approximately 2 500 hours of sunshine a year, over 300 days of sunshine per year, in some provinces) [6]. Compared to small-scale systems, these systems have the advantage that commercial clients can invest in high-quality systems, that may project high-cost savings, which may incur significant costs spent on planning and maintenance. Therefore, these may result in shorter payback periods and higher return on investment [78]. In South Africa, the optimal angle, has been found to be as approximately 30°, for maximum heat absorption during summer and winter seasons. Furthermore, these angles change significantly in the passing seasons [77].

Among others drawbacks, SWHs have disadvantages of comparatively high initial cost [54] , as well as the fact that solar radiation is solely available during the day and the chances of meeting the hot water demand, particularly, during the night, are minimal [25].

Solar radiation may be converted into either thermal energy and/or electricity, by using solar thermal collectors in thermal systems, such as SWHs, solar air heaters and photovoltaic (PV) panels, respectively [79]. There are two common types of solar thermal collectors commonly used for water heating: flat plate collectors (FPCs) and evacuated tubes collectors (ETCs) [54].

#### 2.3.3.1 Flat plate collector (FPC)

FPCs are more often selected due to the simple design, low price and the ability to produce heat up to 100 ℃ [75]. A few of the components of this FPC are shown in Figure *2.3*. The two basic functions of a collector may be described as, firstly, heating the fluid (water, water and refrigerant additive, air) and, second, collecting as much solar energy as possible, at the lowest possible total cost [24]. The two primary types are glazed (has a transparent cover) and unglazed flat plate collectors [76].

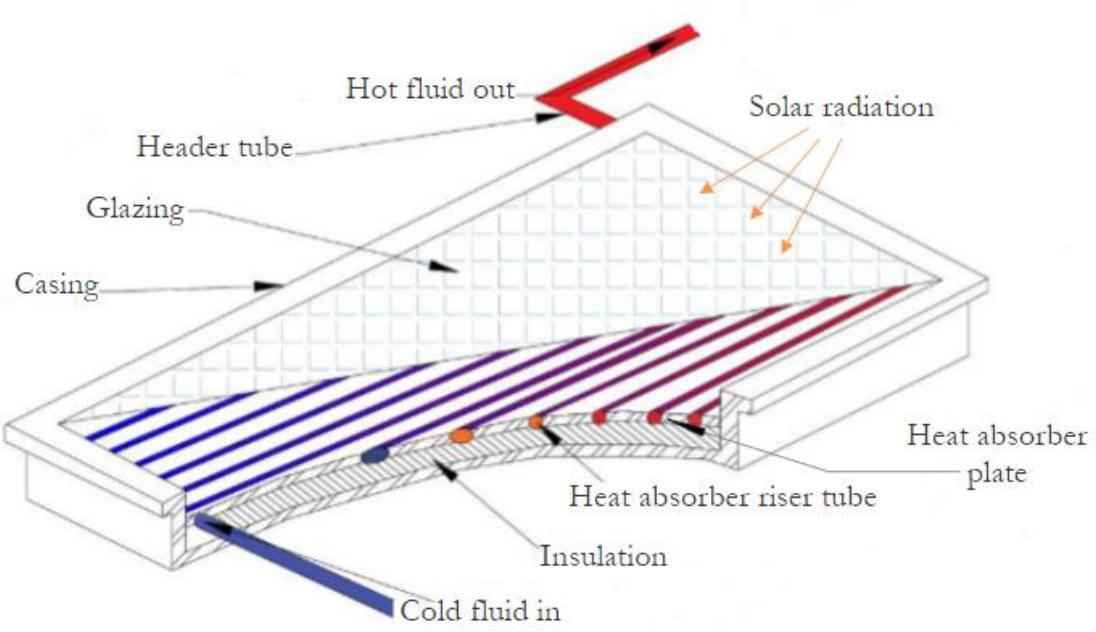


Figure 2.3: Flat plate collector

FPCs are inexpensive to manufacture, collect beam, as well as diffuse radiation and are permanently fixed, so tracking of the sun is not required [80]. The collectors should be oriented directly toward the equator, facing South in the Northern Hemisphere and North in the Southern Hemisphere. The optimum tilt angle of the collector is equal to the latitude of the location, with angle variations of 10° to 15°, more or less, depending on the application [81].

2.3.3.2 Evacuated tube collector (ETC)

On the other hand, ETCs are more efficient collectors, however, they are more expensive than FPCs [75]. ETCs have been commercially available for more than 20 years. Though they have better performance in producing high temperatures, when compared to FPCs, they are not competitive as a result of high initial costs [82]. The basic components of the ETC, are shown in Figure *2.4*. ETC consists of evacuated tubes (glass-glass seal) to minimize heat losses, copper heat pipes for rapid heat transfer and aluminium casing to provide durability and structural integrity to the system. ETC minimizes the heat losses due to convection and radiation [82].

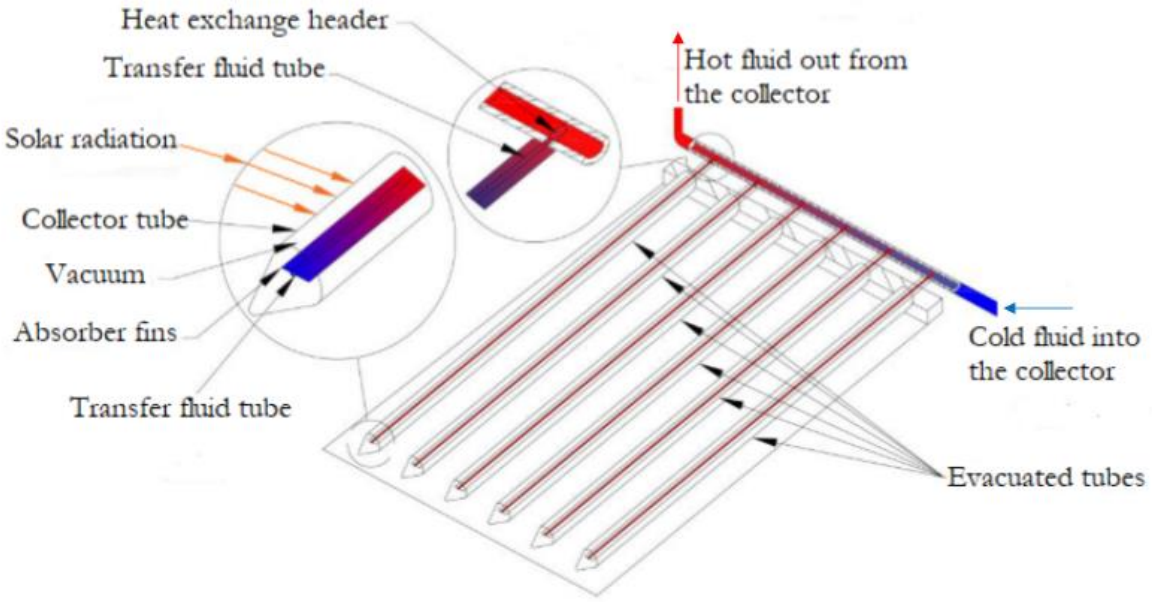


Figure 2.4: Evacuated tube collector

Alike to FPCs, ETCs collect both direct and diffuse radiation, however, their efficiency is higher at low incidence angles. This gives ETCs an advantage over FPCs, in terms of daylong performance [81]. ETCs are more likely to maintain their efficiency over a wide range of ambient temperatures and heating requirements. On the other hand, in constantly sunny climates, FPCs are more efficient, whereas, in more cloudy conditions, their energy output drops off rapidly in comparison to evacuated tubes [54].

ETCs may achieve temperatures above 200℃ [76], due to the combining effects of highly selective surface coating and vacuum insulation. However, many methods are available for heating of working fluid [83]. ETCs are more attractive than other heating, due to their high capability of heat extraction. These collectors are cost effective and the most reliable, with a reasonably longer life time [84].

The results of the study have demonstrated that the climate conditions in South Africa promote SHWs, as evidenced by the following studies:

Hohne et al. [15], conducted a study of optimal energy management and economic analysis, for a proposed hybrid SWH system, under TOU pricing. The system comprised of an electric storage tank and an indirect flat plate solar collector, for a case of a medium-density household, located in Bloemfontein, South Africa. The Solving Constraint Integer Programs (SCIP) solver, in MATLAB optimization toolbox, was used for simulation. The simulated results showed that the load shifting was successful, with the switching solely occurring during the off-peak periods, for both the winter and summer seasons. Additionally, the energy and life cycle cost saving potential of the system were evaluated. Therefore, the life cycle costs of the proposed system displayed a possible annual energy savings of up to 42.9% and the cost savings of R48 609.79, which is approximated to 44 %, over the project lifetime, as compared to the baseline. Finally, the system showed that a payback period of 3.3 years was achievable.

Gerber et al. [85], conducted the study on energy-saving strategies in school, to assess the use of a grid-tied PV solution, in combination with load shifting, through smart scheduling of energy storing electric water heaters. The aim of the study was to reduce both energy usage and the electricity bill of a school in South Africa, while maintaining the consumers' comfort level. The three incremental approaches were compared, based on total energy management and peak demand management. The solar system reduced the

school's yearly energy cost by 24%, without any intelligent water heater scheduling. For method one, a priority-base scheduler was configured using the water usage history, while diverting any excess solar energy to the water, heaters to exploit their energy storage capabilities and the school's energy bill savings was further increasing up to 26% per month. Secondly, the bi-thermal control method was added to the priority-based scheduler, employing a temperature delta to increase the amount of solar energy to be stored within the water heater tank, while minimising their grid reliance and improving the monthly savings to 28% per month. Finally, a demand-limiter control scheme was implemented, in conjunction with bi-thermal control, resulting in large demand-charge savings and an average energy bill reduction of 30% per month, producing the maximum savings, while maintaining suitable levels of user comfort.

Nshimyumuremyi and Junqi [86], conducted an investigative study, to determine thermal efficiency and cost analysis of a SWH, made in Rwanda and manufactured at Tumba College of Technology. The evacuated tube collectors were used for the system and the system was tested in three different locations. From the results obtained, the efficiencies of the systems ranged between 60% and 76% and the payback period obtained was 2 years.

Batidzirai et al. [87], investigated the potential of SWH in alleviating energy and economic problems, by carrying out a comparative evaluation of water heating practices, over a 25-year period, in the domestic, health and tourism sectors, in Zimbabwe. From the results obtained, SWH reduced coincident electricity winter peak demand by 13% and the final energy demand by 27%, assuming a 50% penetration rate of SWH potential demand. Additionally, up to $250 000 000.00 may be saved and CO2 emissions may further be reduced by 29%, over the 25-year period.

Jahangiri et al. [88], conducted an optimization study of SWHs across 22 major cities in Zambia, to determine the possibility of hot water generation and model the greenhouse gas (GHG) emission saving. TSOL Pro 5.5; a professional simulation program for the design and planning of solar thermal systems, was used. Results showed the high potential of GHG emission reduction, due to the nonconsumption of fossil fuels, owing to the deployment of SWHs and had the highest GHG mitigation of up to 1552.97 kg/y from one of the locations. On average, SWHs provided 62.47% of space heating and 96.05% of

the sanitary hot water requirement of consumers. The findings showed the potential for the deployment of SWHs, in Zambia.

Furthermore, as shown in the following comparison studies, renewable energy-saving technologies outperform ordinary ESTWHs, in terms of economic performance and ensure considerable energy and cost savings:

Zhang and Huan [27], presented a comparative study of HPWHs with SWHs and conventional ESTWHs, to analyse the energy consumption and economic performance of the residential sector, in South Africa. From the analysis, the electricity costs of HPWH and SWH were 73.33% and 80% less than an ESTWH system, with HPWH having a 30-45% shorter payback period than SWH.

Kakaza and Folly [89], conducted a comparative study of the SWHs and ASHPs technologies, based on the energy consumption, cost and payback period. For SWHs, the thermosyphon type was selected. The simulation results were based on actual data that collected from a Cape Town based company, that deals with HPs and SWHs. From the results, both the systems showed savings in energy consumption, as compared to the ESTWHs, with ASHPs being the most efficient. Simulation results showed energy savings of 78% and 42% of the ASHPs and SWHs, respectively. However, the initial cost of ASHPs was higher than that of SWHs. Results further revealed that HPs had a preferable payback period of 4.2 years, as compared to 7 years for SWHs.

### 2.3.4 Solar-assisted heat pump systems (SAHPWHs)

The combination of solar thermal collectors and a heat pump in a single system, which is known as a solar assisted heat pump (SAHP) [90], is a promising energy saving water heating technology and may significantly enhance system performance [13]. SAHP integrates the vapor compression heat pump and solar energy [91]. SAHPs are ideally suited for low-temperature thermal applications (≤70°C), such as sanitary hot water [92].

The efficiency of the SAHP systems immensely depends on environmental conditions, system and component size, as well as load characteristics. Therefore, there would not be any simple classification method to conform an easy communication to the public [66]. However, due to their easy accessibility of pollutant free ambient conditions,

these system could effectively cut the electricity consumption down and improve the renewable energy utilization for domestic heating supply [91].

Though SAHPWHs incur increased installation costs, due to additional equipment necessary for operations, SAHP have excellent potential in reducing carbon emissions, due to its high COP [92]. Furthermore, the SAHP system offers increased reliability and may be able to shave off significant energy costs, due to the ability of the two systems to operate independently, should one system fail [55].

SAHP systems can be configured in many ways. However, the configurations are characterised by the method the solar thermal and heat pump components interact. The configurations may generally be divided into direct, indirect (series and parallel mode) [26], [93] and regenerative systems [94].

A. Direct SAHP systems

For direct SAHP systems, the solar collector acts as the heat pump evaporator. As shown in Figure 2.5, the refrigerant evaporation processes occur simultaneously in the collector/evaporator panel [92]. The direct SAHP systems are known as direct-expansion solar-assisted heat pump (DX-SAHP) systems. The concept was first proposed by Sporn and Ambrose, in 1955 [95], [96].

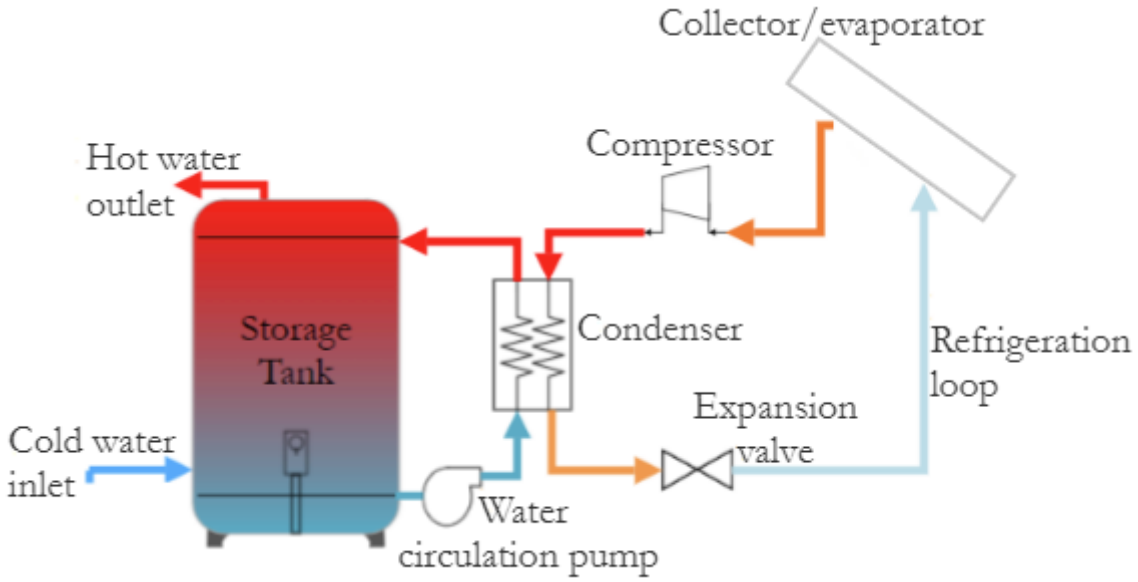


Figure 2.5: Schematic of a direct configuration of the SAHP

The performance of the DXSAHP systems is highly influenced by solar intensity, ambient temperature, wind velocity and relative humidity, due to the direct integration of solar collector with the heat pump [97]. The DXSAHP systems have minimum corrosion, due to the direct use of refrigerant in the solar collector, which should significantly increase the life of solar collectors, when compared to the water-based collectors. The freezing problem of the working fluid is further eliminated [98].

B. Indirect SAHP systems

In indirect SAHP systems, the solar thermal collectors do not act as evaporators for the heat pump. Rather, the heat pump is implemented as a closed unit in the system. The heat transfer medium is a refrigerant solution, such as water or air [26]. The indirect systems may further be divided into series and parallel modes. [13]. In a series mode, as shown in Figure 2.6, the solar thermal collector may act as a heat source of the heat pump unit [99]. The captured heat energy (solar energy) is fed into the evaporator of the heat pump by working fluid and the temperature of the working fluid is therefore reduced [66]. The performance of the heat pump is enhanced by solar energy. In this type of system, the heat pump is limited by the energy accessible from the collector, hence the fact that, if the solar energy is adequate for heating, the direct solar heating is made possible by passing the heat pump [26].

In the parallel mode, as shown in Figure *2.7*, useful energy is supplied independently by the solar thermal system and heat pump [99]. The solar thermal collector may generally feed energy to the thermal storage tanks. When there is insufficient solar energy (during the night or rainy/cloudy days), an auxiliary heat source may be worked in parallel with the solar thermal collector, to obtain the required amount of energy [13], [26]. The parallel mode has the advantage of a lower complexity compared to a series mode, in terms of hydraulic connections as well as system control and therefore they may be more robust and reliable [100].

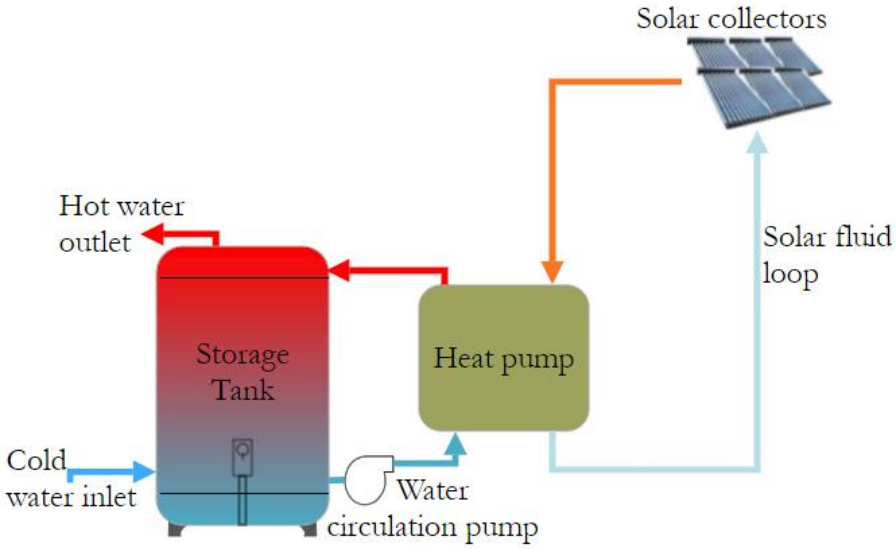


Figure 2.6: Schematic of an indirect series mode configuration of the SAHP

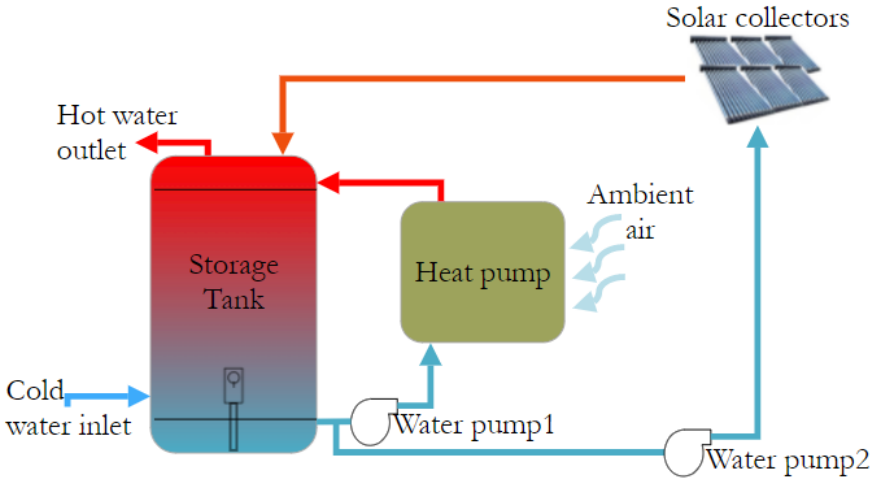


Figure 2.7: Schematic of an indirect parallel mode configuration of the SAHP

C. Regenerative systems

The SAHPWH is used for the regeneration of the interaction between the solar thermal system and the heat pump unit. An example of the regenerative system, is a dual-mode SAHP system [94], [99].

Studies of system performance and energy management methods conducted across the world, such as the ones mentioned below, indicate that SAHP systems are more efficient and cost-effective:

The GSHP combined solar ETC system configurations of DX- and IDX- (parallel and series), were simulated by use of TRNSYS. The simulations were assessed to meet the heating, cooling and hot water demands of a house in Tabriz City, a cold region of Iran. The optimum system was compared to the conventional system. The IDX- in parallel mode, was the optimal configuration with an overall COP of 3.96. A payback period of approximately 13 years, was obtained, compared to the conventional system. By adding these environmental and exporting incomes to the operating costs of the conventional system, the payback period was reduced down to 6 years, indicating that our proposed system is feasible in Tabriz City [26].

Wang et al. [101] proposed a novel control strategy for a IDX-SAHP (parallel mode) water heating system. The system comprised of an ASHP integrated with a solar unit and a cascade storage tanks. The ASHP had the standard thermostatic control connected to the heat storage tank, to compare the tank temperature to a set of reference temperature curves, that are functions of time. A TRNSYS model was developed to compare the proposed and the standard thermostatic control strategies, in three different climate conditions of China, namely, Changsha, Haikou and Beijing. The system obtained the annual total energy consumptions decrease of 35%, 36% and 47% under the proposed control strategy, as compared to the system under the thermostatic control strategy, in the abovementioned locations respectively. The proposed control strategy favoured the Beijing climate, where the consumptions in energy were reduced by 20% and 28% in transitioning and winter seasons, respectively.

Zanetti et al. [102], conducted an investigative study of the energy and cost savings, as well as the optimal control strategies of a PV-assisted system, based on the optimal control theory. The proposed system comprised of a radiant floor heating system, a gas boiler and a PV-assisted ASHP, as heat sources, with a water tank as thermal energy storage providing space heating to a school in Northern Italy, while minimizing the overall energy cost, ensuring thermal comfort and maximizing the photovoltaic self-consumption. The system was modelled using MATLAB, with a baseline rule-based controller (RBC). The

optimal control problem was formulated, using nonlinear programming (NLP), to define cost function, constraints, state and control variables. The simulation results show that the proposed system coupled, with optimal energy management strategy could potentially save up to 20% of the energy consumption cost, when compared to the state-of-the-art RBC and increased the photovoltaic self-consumption by 30%.

The studies undertaken in South Africa are listed below:

Sichilalu et al. [28] developed an optimal control (OC) model of a HPWH, supplied by a wind generator-PV-grid system, using a mixed integer linear program (MILP), to minimise energy cost, taking into account the time-of-use electricity tariff. The results showed a 70.7% cost reduction upon implementation of this intervention. The author concluded that the OC shows significant potential in both energy and cost saving, in comparison to the digital thermostat controller used in most of the HPWHs on the market.

Wanjiru et al. [3], created a mathematical model of the optimal control strategy for shifting the load of the HPWH, connected to an instant heater from, the peak period of the TOU structure, to the off-peak period, in order to meet the hot water demand in the kitchen faucet and bathroom sink. This system is powered by the solar energy from the PV system and the grid power, which may further receive power back through an appropriate feed-in-tariff. The aim of the study was to minimise the energy consumption of the grid, as well as the operation of the instant heater, essentially saving energy. A linear optimization problem was formulated and solved in MATLAB using the OPTI toolbox. The results obtained showed the savings of up to 35% of power-not-delivered from the grid, in a 24-h operating cycle, by the optimal controller and approximately 7.7 kWh of energy sold back to the grid, through an appropriate feed-in-tariff. When compared to the existing thermostatic control of the devices, the control strategy could save approximately 19% on energy costs. Once again, Wanjiru conducted a study on a closed-loop MPC strategy for the same system [71], with the same objectives. This control strategy could potentially save 32.24% and the energy sold back to the grid of up to 18.76 kWh in a day, with a revenue of R11.79 per day. The LCC was further analysed and resulted in the strategy payback period of approximately 9 years and 4 months.

Sichilalu et al. [103], developed an optimal scheduling strategy model for a grid-connected PV system, to power the HPWH. The aim of the study was to minimize energy

cost, while the PV power outputs to the HPWH and domestic appliances, are to be maximized, as well as the TOU pricing structure further incorporated in the optimal scheduling. The input from the PV system and the grid, was fed to the HPWH system and the loads. A case study was carried out, based on 3x16kW HPWH installed at a hotel in Pretoria, South Africa. The model therefore presented higher savings in the summer and autumn seasons, of 30.1% (December) and 41.5% (March), as compared to the savings of the winter and spring seasons, of 16.5% (June) and 22.3% (August), respectively. The PV payback period was said to be short with the feed-in tariff obtained.

## 2.4 DISCUSSION

### 2.4.1 Key findings

Energy management solutions, such as demand-side management and control optimization, have been examined in South Africa, according to the evaluated studies of the selected water heating systems. All studies demonstrate success in the methodologies utilized and larger savings are realized when a hybrid of demand-side response and optimization control is applied, with the shared aim of energy and cost reduction, during the process of heating water. Furthermore, renewable energy systems function optimally in Africa's environment, resulting in the highest overall performance of the systems.

The following points have been covered in prior African research, in relation to the current study:

- A variety of control-energy management systems, as well as the demand-side management approach of load shifting scheduling, have been deployed.
- The systems have seen considerable energy and cost reductions, as a result of the energy management measures.
- Load shifting may help save money by reducing costs and optimizing the system.
- The life cycle costs of renewable energy systems have been examined and energy management solutions have been found to reduce the systems' payback period, resulting in greater cost savings for the user.

It is commendable that South Africa has invested in renewable energy technology and energy management systems, to assist minimize energy and cost usage during the manufacturing of hot water. However, the following points have not been addressed in the wide range of research undertaken in South Africa:

- The ASHP unit is most utilized for SAHP water heating systems in South Africa, where the storage tank is heated by both solar thermal and ASHP units.
- PV systems are often employed as power supply hybrids with the grid, with merely a few studies employing heat collectors for SAHP systems.
- Even though these systems were tested in various climates across South Africa, most of the research concentrated on the residential sector, mostly for single-family homes.
- In South Africa, limited study has been carried out on the HP unit using solar thermal collectors as the heat source to the heat pump unit.
- The application of control techniques, such as optimal control, on these systems and its resultant performance, with respect to energy cost savings, have not yet been evaluated in detail.

## 2.5 SUMMARY

Even though traditional ESTWHs are the most frequently used water heating systems in the world, they are known to be among the highest energy consumers, due to their inefficiency in converting electrical energy to thermal energy. These systems have grown increasingly hostile to consumers, as power prices have risen and the solution to reduce energy consumption of the hot water production, while maintaining the users' thermal comfort level, has led to the development of more energy-efficient techniques and technologies.

This Chapter presents, analyses and compares a literature review of research on energy management techniques for energy-efficient water heating systems, that have been carried out in South Africa. Various water heating systems in South Africa have been extensively examined, in terms of system performance, load scheduling and various control strategies. The ESTHWs, SHWs, HPWHs and SAHPWHs have all been discussed in

relation to this study. In comparison to ESTWHs, the system performance of renewable energy technologies is more efficient and environmentally friendly, according to the studies presented. This is because renewable energy systems require less or no power to heat the same amount of water.

Different system types and components have been investigated in a wide variety of research carried out on various control systems under load scheduling, to lower consumption costs while preserving the user's comfort level, mainly for the residential sector. However, there have been minimal studies of the SAHP in the commercial sector, such as student residences and, particularly, with thermal collectors like the ETCs. Furthermore, in South Africa, the system in which the solar collector serves as an energy source for the heat pump unit, has not been examined.

Additionally, the application of control techniques on these systems and its resultant performance, with respect to energy cost savings, has not yet been evaluated in detail.

# CHAPTER 3: OPTIMAL ENERGY MANAGEMENT OF THE INDIRECT-EXPANSION SOLAR-ASSISTED HEAT PUMP WATER HEATER AND OPTIMAL CONTROL PROBLEM FORMULATION

## 3.1 INTRODUCTION

In this Chapter, a proposed indirect-expansion solar-assisted heat pump water heating (IDX-SAHPWH) system is described. The system consists of a closed loop solar thermal unit of the evacuated tube collectors, a heat pump unit, taken as a single unit component and the hot water storage tank. The solar thermal unit serves as an input source to the heat pump and the electric resistive element of the hot water storage tank, acts as a supplementary energy source to the system. The mathematical models are built on an existing solver and the optimal control problems are further formulated, under the TOU tariff structure, to optimize the proposed hybrid water heating system.

Section 3.2, describes the mathematical model formulation of the proposed system. In Section 3.3, the mathematical models built from an existing solver and the optimal control problems formulation, under the TOU tariff structure, are presented and Section 3.4 presents a summary of the Chapter.

## 3.2 MATHEMATICAL MODEL FORMULATION

The proposed water heating system, consists of the storage tank and an indirect-expansion solar-assisted heat pump (IDX-SAHP) system, as shown in Figure 3.1. The IDX-SAHP water heating system consists of two closed loop units of the solar thermal unit, using the evacuated tube collectors (ETCs) and the heat pump unit. The two circulation pumps are employed for circulation of the refrigerant within the solar thermal unit, as well as the water inside the storage tank. The mathematical models of the various components in the system, are presented in Section 3.2.1, in terms of heat and electrical energy. The Mathematical discrete formulation of the hot water temperature in the storage tank, is presented in Section 3.3.2.

### 3.2.1 Dynamic model of the IDX-SAHP water heating system

Figure 3.1, shows the schematic diagram of the proposed indirect-expansion solar-assisted heat pump (IDX-SAHP) water heating system. The solar thermal evacuated tube collectors (ETCs), serve as the heat source to the heat pump unit. The fluid circulation pump is used to transfer thermal heat to and from the solar thermal ETCs and the heat pump unit in a closed loop system, by circulating the solar fluid (e.i. anifreeze solution). Thermal heat from the solar thermal ETCs, is therefore exchanged to the refrigerant circulating in the heat pump unit. Subsequently, the hot refrigerant transfers thermal heat to the cold water, that is circulated fom the storage tank, using the water circulation pump. The heated water then returns to the thermal storage tank.

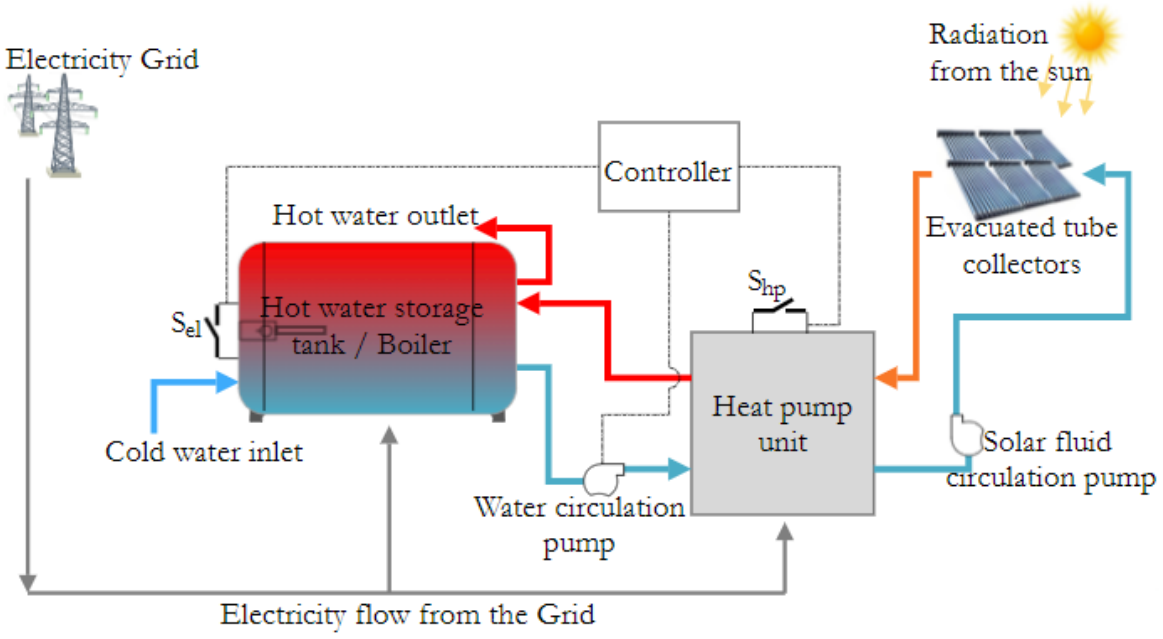


Figure 3.1: The IDX-SAHP system diagram

A heat pump consumes electrical energy of approximately a third, as compared to an ESTWH [27] and based on the previous studies and reviews, the coefficient of performance (COP) range is between 2 and 6, depending on the ambient temperature, the system design and the hot water heating loads [21], [68], [104]–[106]. Therefore, the input power and the COP of the heat pump unit are assumed in this study.

For modelling simplicity of the system, the following assumptions have been made:

- The hot water temperature distribution inside the tank is treated as uniform.
- The power demand rating of the heat pump unit, is further assumed to be fixed and operating at full capacity when switched on.
- The COP of the heat pump is assumed to be constant.
- The energy losses of the solar thermal collectors, heat pump unit and the water during the circulation and exchanging of heat, are assumed to be negligible and the flow of the fluids is assumed to be steady.

Therefore, solely energy losses due to convectional (standby) loss $Q_L(t)$ and hot water drawn $Q_D(t)$ are modelled.

The performance of ETC may be analysed by Eq. (3.1). The total absorbed solar radiation may be estimated, by multiplying each term by the appropriate transmittance absorptance product [107]. Transmittance absorptance product is assumed to be the same for all the radiations. Then the basic equation of the absorbed solar radiation, utilizing the isotropic diffuse model, is given by [13], [107], [108]:

$$G_\beta(t) = (\tau\alpha)\left( G_b(t)\cos\theta_\beta + G_d(t)\left[\frac{1+\cos\beta}{2}\right] + \rho G_g(t)\left[\frac{1-\cos\beta}{2}\right]\right) \quad (3.1)$$

Where:

$G_b$ is the horizontal beam radiation ($\mathrm{W/m^2}$);

$G_d$ is the horizontal diffuse radiation ($\mathrm{W/m^2}$);

$G_\mathrm{g}$ is the horizontal reflected radiation ($\mathrm{W/m^2}$);

$\tau$ is the transmittance of the glass;

$\alpha$ is the absorptance of the glass;

$\theta_\beta$ incidence angle of beam radiation (°);

$\beta$ is the tilt angle (°);

$\rho$ is the foreground's albedo;

$A_{ap}$ is the aperture area of a collector ($\mathrm{m^2}$).

To calculate the thermal performance of the evacuated tubes, Eq. (3.1) has been integrated over the whole absorber area of the collector. The aperture area is assumed to

be the same throughout the thermal collector. The performance equations may be described in Eqs. (3.2) and (3.4), adapted from [107]:

The performance equation for the total incidence radiation by the solar collector tubes:

$$I_{\beta}(t)A_{abs} = A_{ap}\left(G_b\cos\theta_{\beta} + G_d(t)\left[\frac{1+\cos\beta}{2}\right] + \rho G_g(t)\left[\frac{1-\cos\beta}{2}\right]\right) \tag{3.2}$$

Where:

$A_{ap}$ is the aperture area of a collector.

The performance equation for the total absorbed radiation by the solar collector tubes:

$$G_{\beta}(t)A_{abs} = (\tau\alpha)G_{\beta}(t)A_{ap} \tag{3.3}$$

$$\therefore G_{\beta}(t)A_{abs} = (\tau\alpha)A_{ap}\left(G_b(t)\cos\theta_{\beta} + G_d(t)\left[\frac{1+\cos\beta}{2}\right] + \rho G_g(t)\left[\frac{1-\cos\beta}{2}\right]\right) \tag{3.4}$$

The useful heat transfer of the collector ($Q_{coll}(t)$), may be calculated using the energy balance of the fluid volume, with regards to the temperature change of the refrigerant solution circulated through the collector unit, as given below [109]:

$$\dot{Q}_{coll}(t) = \dot{m}_c(t)C_{p,c}\Delta T_{af}(t) = \dot{m}_c(t)C_{p,c}\left(T_{af,o}(t) - T_{af,i}(t)\right) \tag{3.5}$$

Where:

$\dot{m}_c(t)$ is the mass flow of the of the refrigerant solution (kg/s);

$C_{p.c}$ is the specific heat capacity of refrigerant solution (J/kg °C);

$T_{af.o}(t)$ is the outlet temperature of the refrigerant solution (°C);

$T_{af.i}(t)$ is inlet temperature of the refrigerant solution (°C).

The energy balance of the collector may further be obtained as the net power output of the total incidence solar irradiation, as shown in Eq. (3.6)[107]:

$$\dot{Q}_{coll}(t) = G_{\beta}(t)A_{abs} - \dot{Q}_{man\_Loss}(t) \tag{3.6}$$

$Q_{man\_Loss}(t)$ being the manifold heat loss to the environment, which is calculated by [110]:

$$Q_{man\_Loss} = U_{man\_Loss}A_{man}\left(T_{mean}(t) - T_{amb}(t)\right) \tag{3.7}$$

Further, $T_{mean}(t)$ is the mean temperature of the refrigerant solution calculated as:

$$T_{mean}(t) = \frac{\left(T_{af,o}(t) + T_{af,i}(t)\right)}{2} \tag{3.8}$$

Eq. (3.6) is therefore given as follows:

$$\dot{Q}_{coll}(t) = G_{\beta}(t)A_{abs} - U_{man\_Loss}A_{man}\left(\frac{T_{af,o}(t) + T_{af,i}(t)}{2} - T_{amb}(t)\right) \tag{3.9}$$

Where:

$A_{abs}$ is the area for energy absorption ($\mathrm{m}^2$);

$G_{\beta}(t)$ is the variable total absorbed hourly solar radiation on a tilted collector ($\mathrm{W/m}^2$);

$U_{man\_Loss}$ is the manifold heat loss coefficient provided by the manufacturer data ($\mathrm{W/m}^2\,°\mathrm{C}$);

$A_{man}$ is the internal area of the manifold ($\mathrm{m}^2$);

$T_{amb}(t)$ is the ambient temperature (°C).

The inlet temperature of the refrigerant solution is assumed in relation to the ambient temperature. The mass flowrate and the outlet temperature of the refrigerant solution are unknown and may therefore be determined by the tube efficiency (η), defined as the ratio of the net power output and the input power of the total incidence solar irradiation, as shown in Eq.(3.10) [107]:

$$\eta = \frac{G_{\beta}(t)A_{abs} - \dot{Q}_{man\_Loss}(t)}{I_{\beta}(t)A_{abs}} \tag{3.10}$$

Where:

η is the tube efficiency of the collector.

By substituting Eq. (3.9) into Eq. (3.10), to give the following expression:

$$\eta = \frac{1}{I_{\beta}(t)A_{abs}}\left(G_{\beta}(t)A_{abs} - U_{man\_Loss}A_{man}\left[\frac{T_{af,o}(t) + T_{af,i}(t)}{2} - T_{amb}(t)\right]\right) \tag{3.11}$$

Firstly, to determine the outlet temperature of the refrigerant solution, Eq. (3.11) is simplified to Eq. (3.12):

$$T_{af,o}(t) = 2\left(\frac{G_\beta(t)A_{abs} - \eta I_\beta(t)A_{abs}}{U_{man\_Loss}A_{man}} + T_{amb}(t)\right) - T_{af,i}(t) \quad (3.12)$$

To minimize the complexity of the hybrid water heating system, the coefficient of performance ($COP$) is assumed to be constant. The rated power input of the heat pump at the compressor unit, is given as:

$$\dot{W}_{comp} = P_{hp}t_{(h)} \quad (3.13)$$

$$\dot{W}_{comp} = P_{hp}t_{(h)}$$

The required electric power to the heat pump is controlled by the switch ($S_{hp}(t)$) and is given as [71]:

$$\dot{W}_{hp} = COP \times P_{hp}t_{(h)}S_{hp}(t) \quad (3.14)$$

Where:

$P_{hp}(t)$ is the input power to the heat pump (kW);

$S_{hp}(t)$ is the control switch of the heat pump.

Therefore, the heating capacity of the SAHP system measured at the condenser, expressed as the energy balance, given as:

$$\dot{Q}_{SAHP} = \dot{Q}_{coll} + \dot{W}_{hp} \quad (3.15)$$

By substituting Eqs. (3.9) and (3.14) into (3.15), the energy balance of the SAHP becomes:

$$\dot{Q}_{SAHP}(t) = G_\beta(t)A_{abs} - U_{coll\_Loss}A_{man}\left(\frac{T_{af,o}(t) + T_{af,i}(t)}{2} - T_{amb}(t)\right) + COP \times P_{hp}t_{(h)}S_{hp}(t) \quad (3.16)$$

Where:

$P_{hp}$ is the input power to the heat pump (kW);

$S_{hp}$ is the control switch of the heat pump.

The electric resistive element of the storage tank serves as an auxiliary energy supply to increase hot water availability. Therefore, if the solar-assisted heat pump energy supply is insufficient to increase the thermal level of the water to the desired temperature level,

electrical energy $Q_{EL}(t)$ will be supplied to the electric resistive element, which is controlled by the switch $S_e(t)$, to maintain the desired temperature, as presented [15]:

$$\dot{Q}_{EL}(t) = P_{EL} t_{(h)} S_e(t) \tag{3.17}$$

Where:

$P_{EL}$ is the input power to the electric resistive element of the storage tank (kW);

$S_e(t)$ is the control switch of the electric resistive element of the storage tank.

The standby losses, $Q_L(t)$, represent power losses owing to the surface conduction o the casing material and is given as in Eq. (3.18) [15]:

$$\dot{Q}_L(t) = U_s t_{(h)} A_s \left(T_s(t) - T_a(t)\right) \tag{3.18}$$

Where:

$U_s$ is the heat loss coefficient of a storage tank in (W/m² °C);

$A_s$ is the surface area of the storage tank (m²);

$T_s(t)$ is the variable temperature of the water inside the storage tank (°C);

$T_a(t)$ is the variable ambient temperature of the surrounding air (°C).

The other loss is due to the hot water demand $Q_D(t)$, allowing inlet cold water. Consequently, every time a demand occurs, $T_s$ drops, due to cold water flowing into the tank to keep a constant volume. Losses, due to the hot water demand, are given in Eq. (3.19) [15]:

$$\dot{Q}_D(t) = \dot{W}_D(t) C_{p,w} \left(T_s(t) - T_w(t)\right) \tag{3.19}$$

Where:

$c_{p.w}$ is the specific heat capacity of the water (4184 J/kg °C);

$\dot{W}_D$ is the variable hot water demand flow rate (kg/h);

$T_w(t)$ is the variable temperature of the inlet water (°C).

The energy balance ($Q_S(t)$), is a first derivative differential function, representing the heat energy in the storage tank and is equal to the following [15]:

$$\dot{Q}_s(t) = M_w C_{p,w} \dot{T}_s \tag{3.20}$$

Where:

$M_w$ is the water mass inside the storage tank (kg);

$C_{p.w}$ is the heat capacity of water (4184J/kg/°C);

$\dot{T}_s$ is the temperature derivative variation of the water inside the storage tank (°C).

The energy gains from the IDX-SAHP system, $Q_{hp}(t)$ and the energy supplied by the electric resistive element, $Q_{EL}(t)$, are energies supplied for water heating in the system. The energy losses in the system are due to hot water demand, $Q_D(t)$ and standby losses, $Q_L(t)$, representing power losses owing to the casing material surface conduction. The resulting energy balance $Q_S(t)$ equation, with the heat gains and losses in the system, are given in Eq. (3.21) [15]:

$$\dot{Q}_s(t) = \dot{Q}_{SAHP}(t) + \dot{Q}_{EL}(t) - \dot{Q}_L(t) - \dot{Q}_D(t) \tag{3.21}$$

Substituting all variables and coefficients (parameters) from Eqs. (3.16) – (3.20), into the energy balance, Eq. (3.21), result in Eq. (3.22):

$$\begin{aligned} M_w C_{p,w} \dot{T}_s &= G_\beta(t) A_{abs} - U_{man\_Loss} A_{man} \left( \frac{T_{wf,o}(t) + T_{wf,i}(t)}{2} - T_{amb}(t) \right) \\ &+ COP \times P_{hp} t_{(h)} S_{hp}(t) + P_{EL} t_{(h)} S_e(t) - U_s t_{(h)} A_s \left( T_s(t) - T_a(t) \right) \\ &- \dot{W}_D(t) C_{p,w} \left( T_s(t) - T_a(t) \right) \end{aligned} \tag{3.22}$$

Further simplification yields Eq. (3.23):

$$Y(t) = G_\beta(t) A_{abs} - U_{man\_Loss} A_{man} \left( \frac{T_{wf,o}(t) + T_{wf,i}(t)}{2} - T_{amb}(t) \right) \tag{3.23}$$

Therefore:

$$\begin{aligned} M_w C_{p,w} \dot{T}_s &= Y(t) + COP \times P_{hp} t_{(h)} S_{hp}(t) + P_{EL} t_{(h)} S_e(t) - U_s t_{(h)} A_s \left( T_s(t) - T_a(t) \right) \\ &- \dot{W}_D(t) C_{p,w} \left( T_s(t) - T_w(t) \right) \end{aligned} \tag{3.24}$$

The temperature of the water inside the storage tank $\dot{T}_s$ is isolated as the state variable and made the subject of the formula:

$$\begin{aligned} \dot{T}_s &= \frac{Y(t)}{M_w C_{p,w}} + \frac{COP \times P_{hp} t_{(h)} S_{hp}(t)}{M_w C_{p,w}} + \frac{P_{EL} t_{(h)} S_e(t)}{M_w C_{p,w}} - \frac{U_s t_{(h)} A_s \left( T_s(t) - T_a(t) \right)}{M_w C_{p,w}} \\ &- \frac{\dot{W}_D(t) C_{p,w} \left( T_s(t) - T_w(t) \right)}{M_w C_{p,w}} \end{aligned} \tag{3.25}$$

And simplified once more, to get Eq. (3.26):

$$\dot{T}_s = \frac{Y(t)}{M_w C_{p,w}} + \frac{COP \times P_{hp} t_{(h)} S_{hp}(t)}{M_w C_{p,w}} + \frac{P_{EL} t_{(h)} S_e(t)}{M_w C_{p,w}} - \frac{U_s t_{(h)} A_s \left(T_s(t) - T_{amb}(t)\right)}{M_w C_{p,w}} - \frac{\dot{W}_D(t) C_{p,w} \left(T_s(t) - T_m(t)\right)}{M_w C_{p,w}} \tag{3.26}$$

$$\dot{T}_s(t) = \frac{Y(t)}{M_w C_{p,w}} + \frac{COP \times P_{hp} t_{(h)} S_{hp}(t)}{M_w C_{p,w}} + \frac{P_{EL} t_{(h)} S_e(t)}{M_w C_{p,w}} - \frac{U_s t_{(h)} A_s + \dot{W}_D(t) C_{p,w}}{M_w C_{p,w}} \left(T_s(t)\right) + \frac{U_s t_{(h)} A_s T_a(t) + \dot{W}_D(t) C_{p,w} T_m(t)}{M_w C_{p,w}} \tag{3.27}$$

Eq. (3.27), is separated into the following components, as shown in Eqs. (3.28)–(3.31), so that a state space equation is formulated [15]:

$$A(t) = \frac{U_s t_{(h)} A_s + \dot{W}_D(t) C_{p,w}}{M_w C_{p,w}} \tag{3.28}$$

$$B_1 = \frac{COP \times P_{hp} t_{(h)}}{M_w C_{p,w}} \tag{3.29}$$

$$B_2 = \frac{P_{EL} t_{(h)}}{M_w C_{p,w}} \tag{3.30}$$

$$\gamma(t) = \frac{Y(t)}{M_w C_{p,w}} + \frac{U_s t_{(h)} A_s T_a(t) + W_D(t) C_{p,w} T_m(t)}{M_w C_{p,w}} \tag{3.31}$$

In the state space equation, given by Eq.(3.32), the state variable is $\dot{T}_s$, while the control or decision variables are $S_{hp}(t)$ and $S_e(t)$ and the disturbance variable in the system, is $\gamma$ [15]:

$$\dot{T}_s = -A(t) T_s(t) + B_1 S_{hp}(t) + B_2 S_e(t) + \gamma(t) \tag{3.32}$$

### 3.2.2 Discretized Hot Water Temperature

Eq. (3.33), is a continuous function, which has an infinite number of degrees of freedom and should be transferred into a general discrete formulation, in terms of the k$^{th}$ hot water function. This inevitably limits the degrees of freedom. The limitation is required, due to the finite nature of the subsequent calculation processes. Function spaces, necessary to produce all solutions possible for given initial and boundary conditions, have an infinite dimension. Therefore, discretization is required to obtain a function space, where a realistic

finite number of base functions containing suitable approximations of the analytical solution may be calculated [15].

$$T_{k+1} = T_k(1-t_sA_k) + t_sB_1S_{hp_k} + t_sB_2S_{e_k} + t_s\gamma_k \tag{3.33}$$

Where: $k$ denotes the temperature variation inside the hot water storage tank.

Since the state variable, $T_{k+1}$ should be expressed in terms of its initial value, $T_0$ and the control variable, $S_e(t)$, of the initial, $T_{k+1}$ at each interval, is first derived as [15]:

When substituting $k = 0$, the expression of Eq. (3.33) is simplified to $T_1$ in Eq. (3.34) :

$$T_1 = T_0(1-A_0) + t_sB_1S_{hp_0} + t_sB_2S_{e_0} + t_s\gamma_0 \tag{3.34}$$

Similarly, when $k = 1, T_2$ is given in Eq. (3.35):

$$T_2 = T_1(1-t_sA_1) + t_sB_1S_{hp_1} + t_sB_2S_{e_1} + t_s\gamma_1 \tag{3.35}$$

Substitute $T_1$ in Eq. (3.34) into Eq. (3.35), to achieve Eq. (3.36):

$$T_2 = \left[T_0(1-t_sA_0) + t_sB_1S_{hp_0} + t_sB_2S_{e_0} + t_s\gamma_0\right](1-t_sA_1) + t_sB_1S_{hp_1} + t_sB_2S_{e_1} + t_s\gamma_1 \tag{3.36}$$

$$\begin{aligned} T_2 = {} & T_0(1-t_sA_0)(1-t_sA_1) + \left[(1-t_sA_1)S_{hp_0} + S_{hp_1}\right]B_1t_s + \left[(1-t_sA_1)S_{e_0} + S_{e_1}\right]B_2t_s \\ & + \left[(1-t_sA_1)\gamma_0 + \gamma_1\right]t_s \end{aligned} \tag{3.37}$$

Following the same steps from Eq. (3.34) - (3.37) after $k = 2, T_3$ will be denoted in Eq. (3.38):

$$\begin{aligned} T_3 = {} & T_0(1-t_sA_0)(1-t_sA_1)(1-t_sA_2) + [(1-t_sA_1)(1-t_sA_2)S_{hp_0} + (1-t_sA_2)S_{hp_1} + S_{hp_2}]B_1t_s \\ & + \left[(1-t_sA_1)(1-t_sA_2)S_{e_0} + (1-t_sA_2)S_{e_1} + S_{e_2}\right]B_2t_s + [(1-t_sA_1)(1-t_sA_2)\gamma_0 \\ & + (1-t_sA_2)\gamma_1 + \gamma_2]t_s \end{aligned} \tag{3.38}$$

A state space equation is formulated, using the energy balance in Eq. (3.38), after isolating the control and state variables in the system. In order to visualize the variation in temperature of the water inside the storage tank, the continuous temperature function ($\dot{T}_s$) should be transferred into a general discrete formulation, resulting in Eq. (3.39) [15]:

$$\begin{aligned} T_{k+1} = {} & T_0\prod_{j=0}^{k}(1-t_sA_j) + t_sB_1\sum_{j=0}^{k}S_{hp_j}\prod_{i=j+1}^{k}(1-t_sA_i) + t_sB_2\sum_{j=0}^{k}S_{e_j}\prod_{i=j+1}^{k}(1-t_sA_i) \\ & + t_s\sum_{j=0}^{k}\gamma_j\prod_{i=j+1}^{k}(1-t_sA_i) \end{aligned} \tag{3.39}$$

## 3.3 CONTROL OPTIMIZATION PROBLEM

### 3.3.1 Optimal control problems formulation

- Operation cost minimisation

To minimize the cost of energy supplied to the compressor input power and the electric resistive element, the TOU tariff structure, shown in Figure 3.2, should be taken as the core consideration, when formulating the objective function. This is accomplished, by changing the state of the control variables to represent the ON states in regions where it is the least expensive [15].

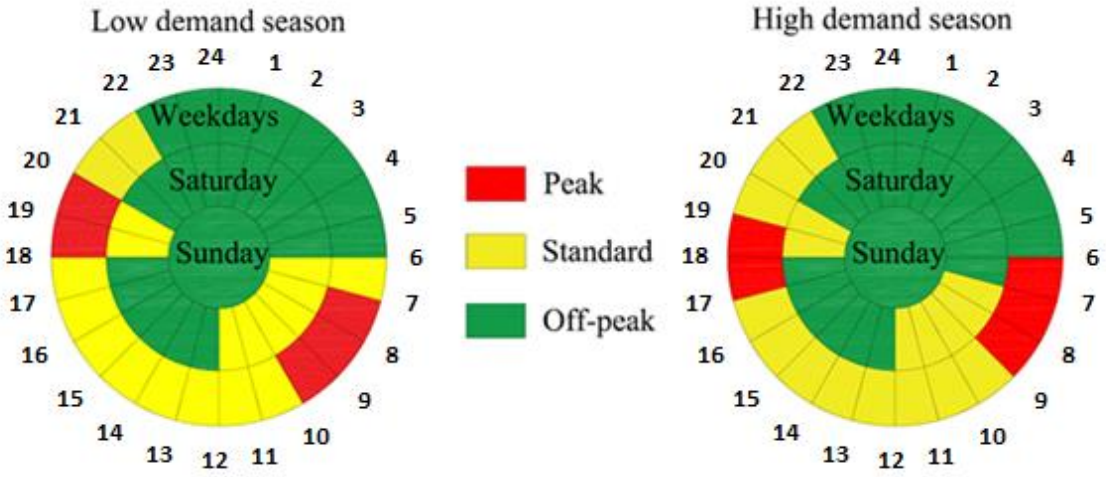


Figure 3.2: Time-of-Use Periods

From the TOU structure, shown in Figure 3.2, the tariff circle chart on the left represents the TOU tariff periods of the low demand season, whereas the circle chart on the right, denotes the periods of the high demand season. The low demand season is from September to May, whilst the high demand season begins in June and ends in August. The winter season peak period starts an hour earlier than the summer season. This may be accredited to increased energy requirement to heat water to the desired temperature and the usage of other high energy consumption appliances, such as space heaters [15].

As a result, the TOU tariff structure forms a substantial part of the objective function and is derived in Eq. (3.40), which is the electricity cost $J_P$ minimization. The switching functions, $S_{hp_k}$ and $S_{e_k}$, are therefore highly dependent on the TOU tariff. The cost minimization function may be seen as the primary objective function: [15].

$$\min J_p = t_s \int_{t_0}^{N} \left( P_{hp,k} S_{hp,k} + P_{EL,k} S_{e,k} \right) p_k \tag{3.40}$$

Where:

$t_s$ is the sampling time (hours);

$P_{hp.k}$ is power of the heat pump compressor (kW);

$S_{hp_k}$ is the switching status function of the heat pump;

$P_{EL.k}$ is the rated power of the electric resistive element (kW);

$S_{e_k}$ is the switching status function of the electric resistive element;

$p_k$ is the TOU tariff function (R/kWh).

- Thermal discomfort level minimisation

The degree to which discomfort is experienced, once the temperature levels of the water supplied to the user are above or below the desired temperature, may be defined as the thermal discomfort level. When the desired hot water temperature is reached at the thermal level, this degree of discomfort is reduced. In hindsight, the secondary objective therefore becomes the minimization of thermal discomfort experienced by the user. To determine the exact time that the desired temperature should be reached, the consumer's specific hot water consumption profile is consulted. The consumption profile is a continuous function of time represented by $F(t)$ and denotes the times at which the desired hot water temperature of the user should be attained. $T_s(t)$ is the temperature of the water inside the storage tank and should be close or equal to the desired temperature, when hot water is usually drawn by the consumer. In other words, $F(t)$ and $T_s(t)$ should be as close to equal as possible, at the exact instant when hot water is usually drawn. Thus, the difference in temperature $\left(T_s(t) - F(t)\right)^2$, should be minimized. The secondary objective function, therefore, becomes $J_s$ and is shown in Eq. (3.41) [15]:

$$\min J_s = \int_{t_0}^{t_f} \left(T_s(t) - F(t)\right)^2 dt \tag{3.41}$$

Where:

$t_0$ is the initial sampling interval at $T_s(t) = T_s(t_0)$;

$t_f$ is the final sampling interval at $T_s(t) = T_s(t_f)$.

- Fixed-final state condition

To simulate the repeated implementation and continuous operation of the optimal energy control scheme for the hybrid system, the thermal energy stored in the storage tank at the final time step of the control horizon, should be equal to the thermal energy at the initial interval of the control horizon. Therefore, the sum of the energy gains, should be equal to all the energy lost in the system, for the considered control horizon. This is presented in Eq. (3.42). The final temperature ($T(t_f)$) in the last sampling interval should, therefore, be as close to equal as possible to the initial temperature ($T(t_0)$) of the water inside the storage tank, at the initial sampling interval of the control horizon [15].

$$\sum_{k+1}^{N} (Q_{s_k}) = 0 \tag{3.42}$$

This may be achieved by minimizing the difference between the initial temperature of the water inside the storage tank and the desired final temperature. The same method used to minimize the discomfort level of the user, may be adjusted for this instance, so that Eq. (3.43), presents the tertiary objective function [15].

$$\min J_t = \int_{t_0}^{t_f} \left(T_s(t_f) - T_s(t_0)\right)^2 dt \tag{3.43}$$

- Operation cost and discomfort level minimization

In order to minimize the energy cost of the IDX-SAHP water heater, while maintaining the desired temperature of the user, the primary, secondary and tertiary objective functions, should be combined to form the combined objective function, as in Eq.(3.44). [15]

$$\min J = w_1\left(t_s\sum_{k+1}^{N}(P_{hp,k}S_{hp,k}+P_{EL,k}S_{e,k})p_k\right)+w_2\left(t_s\sum_{k+1}^{N}(T_k-F_k)^2+t_s\sum_{k+1}^{N}(T_N-T_0)^2\right) \quad (3.44)$$

Where:

$w_1$ is the weighting factor to adjust the priority given to energy cost minimization;

$w_2$ is the weighting factor to adjust the priority given to discomfort level minimization;

J is the aggregate objective function that is to be minimized.

The aggregate objective function, shown in Eq. (3.44), is a non-linear mixed integer function with a binary control variable, that should be solved, in order to obtain the optimal switching status function of the heat pump compressor switch and the electric resistive element [15].

- Constraints on the state of temperature inside the storage tank

For the constraint on the state of temperature inside the storage tank, the desired temperature, taking the hot water consumption profile into consideration, is approximately 65 °C at 06:30 and at 20:00 in the evening, while from 07:00 to 20:00, the temperature may vary without constraint. Fixed final sate conditions dictate that the final storage tank water temperature in the control horizon should be equal to the initial temperature. Eq. (3.45) shows the temperature constraints throughout the 24-hour control horizon [15]:

$$F(t)=\begin{cases}T_s(t), t\in[00h00,06h00)\cup[20h30,24h00)\\65, t\in[06h30]\cup[20h00]\\T_0(t_0), t\in[24h00]\end{cases} \quad (3.45)$$

Where: F (t) is the desired temperature function; and,

$$T_{k+1}=T_0\prod_{j=0}^{k}(1-t_sA_j)+t_sB_1\sum_{j=0}^{k}S_{hp_j}\prod_{i=j+1}^{k}(1-t_sA_i)+t_sB_2\sum_{j=0}^{k}S_{e_j}\prod_{i=j+1}^{k}(1-t_sA_i)$$
$$+t_s\sum_{j=0}^{k}\gamma_j\prod_{i=j+1}^{k}(1-t_sA_i) \quad (3.46)$$

The switching status of a function is a single binary value indicating the switching ON or OFF, to deliver either full rated power or no power, respectively, to the electrical unit, whenever required. The switching functions of the heat pump and the storage tanks, are presented in Eq.(3.47), respectively [15]:

$$S_{hp,k} \in \{0,1\}$$
$$S_{e,k} \in \{0,1\} \tag{3.47}$$

$$T_k^{\min} \le T_k \le T_k^{\max} \tag{3.48}$$

### 3.3.2 Proposed optimization solver and mathematical programming models

With the aim to obtain the optimal switching status of the heat pump unit and the electric resistive element, the objective function, as shown in Eq. (3.44), is a non-linear function with an integer binary control variable, that should be solved. This type of problem may be solved by the universal Solving Constraint Integer Programs (SCIP) solver, in the MATLAB optimization toolbox [15].

The mixed integer nonlinear programming (MINLP) form should be satisfied, to successfully run SCIP. The MINLP form, is shown in Eq. (3.49). The objective function is minimized by default and is subjected to the constraints shown in the equation. The mathematical model should be adapted and converted for suitable SCIP constraints implementation. The optimized output variable, is the control variable in the system [15].

$$\begin{gathered}
\min_x f(x) \\
Subject\,to: Ax \le b \\
A_{eq}x = b_{eq} \\
lb \le x \le ub \\
c(x) \le d \\
c_{eq}(x) = d_{eq} \\
x_i \in \mathbb{Z} \\
x_j \in \{0,1\}
\end{gathered} \tag{3.49}$$

Where:

$f(x)$ is the objective function;

$Ax \le b$ is the linear inequality constraint;

$A_{eq}x = b_{eq}$ is the linear equality constraint;

$lb \le x \le ub$ is the decision variable bounds;

$c(x) \le d$ is the nonlinear inequality constraint;

$c_{eq}(x) = d_{eq}$ is the nonlinear equality constraints;

$x_i$ is an integer number decision variable;

$x_j$ is a binary number decision variable.

The objective function is consequently replaced with f(x); no linear inequality or equality constraints exist. The decision variable, as shown in Eq.(3.49), is a binary value, meaning that solely a 1 or 0 may be obtained as the switching status. The lower and upper boundaries are, therefore, shown in Eqs. (3.50) and (3.51), respectively [15]:

$$lb^T = [0 \ldots 0_N] \tag{3.50}$$

$$ub^T = [1 \ldots 1_N] \tag{3.51}$$

The control variable that should be optimized, is therefore constrained, as shown in Eq. (3.52):

$$lb \leq x \leq ub \tag{3.52}$$

## 3.4 SUMMARY

In this Chapter, a description of the dynamic model of the proposed IDX-SAHPWH system is given and the mathematical formulation of the energy balance of the storage tank is described for the energy gains of the solar thermal collector unit, as well as the heat pump unit. The objective function, control, state variables and disturbances were identified and, then, formulated the desired temperature function in the storage tank. The models were built to solve decision variables of the proposed system using SCIP solver in the MATLAB interface optimization toolbox.

The constraints used on the operation of the proposed system have been set, according to the thermal comfort level of the consumers and the possible savings in energy and cost. This was achieved by shifting the load of the hot water production to the cheaper TOU tariff pricing.

# CHAPTER 4: SIMULATION RESULTS AND DISCUSSION

## 4.1 INTRODUCTION

In this Chapter, simulation results of the optimal operation of the proposed system, simulated using the SCIP solver in MATLAB OPTI-Toolbox, are given. The objective of the simulation, is to present the performance of the optimal control methods applied to the hybrid water heating system, aiming to minimize the energy costs of hot water production and maximize the cost savings. This system consists of the solar thermal unit, heat pump unit and electric storage tank unit.

A load profile and all other relevant data for summer and winter seasons, were obtained. The component size and parameters of the hybrid systems are given, as well as the TOU pricing and the simulation parameters.

This Chapter consists of Section 4.2, which presents the description of the data acquired and component sizing. Section 4.3 presents the simulation profile results of the storage tank temperature, as well as the switching controls of the baseline system and the proposed system is obtained. Lastly, the summary of the Chapter is given in Section 4.4.

## 4.2 DATA DESCRIPTION

In this Section, a case study from which the environmental data, hot water consumption profile and system component sizes, are presented. The data is used as input to develop the model of the proposed system, as well as the baseline and the optimal control approach, which are later compared.

Section 4.2.1, illustrates the data at 1-minute averaged intervals. The sampling time is taken to be 20 minutes, with the resulting total sampling interval and control horizon, as well as other relevant parameters, discussed in Section 4.2.2.

### 4.2.1 Case study and data acquisition

The research is based on student residences at the Bloemfontein campus of the Central University of Technology in Free State, South Africa. The data climate conditions

were collected from the Southern African Universities Radiometric Network (SAURAN) devices, located at the Central University of Technology (Latitude: -29.121337; Longitude: 26.215909 and Elevation: 1397 m), in Bloemfontein [111], as shown in Figure *4.1*. The data profiles of the average solar irradiances and ambient air temperature collected from SAURAN, as well as the inlet water temperature, are presented in Figures 4.2 - 4.5.


Figure 4.1: SAURAN located at the Central University of Technology

This data is for the annual seasonal extremes of a typical winter day in July and a typical summer day in January, to highlight the variation throughout each typical day. The Köppen climate classification for the case study area, is necessary to quantify the climate variation in the region. The Bloemfontein area, with an elevation of 1 395 m and coordinates: 29.0852° S, 26.1596° E, has a Tropical and Subtropical Steppe Climate classification, subtype "BSk". The average temperature for the year is 16.7 °C, with the warmest month in January, at an average of 23.9 °C. The coldest month is typically June, with an average temperature of 8.3 °C [112], [113].

The numerical data of winter and summer seasons are tabulated in Appendices B1 and B2. The diffuse horizontal irradiance, diffuse normal irradiance and global horizontal irradiance are shown in Figures *4.2* and *4.3* for the winter and summer seasons, respectively. The data was obtained directly from the excel sheet, extracted through the SAURAN devices.

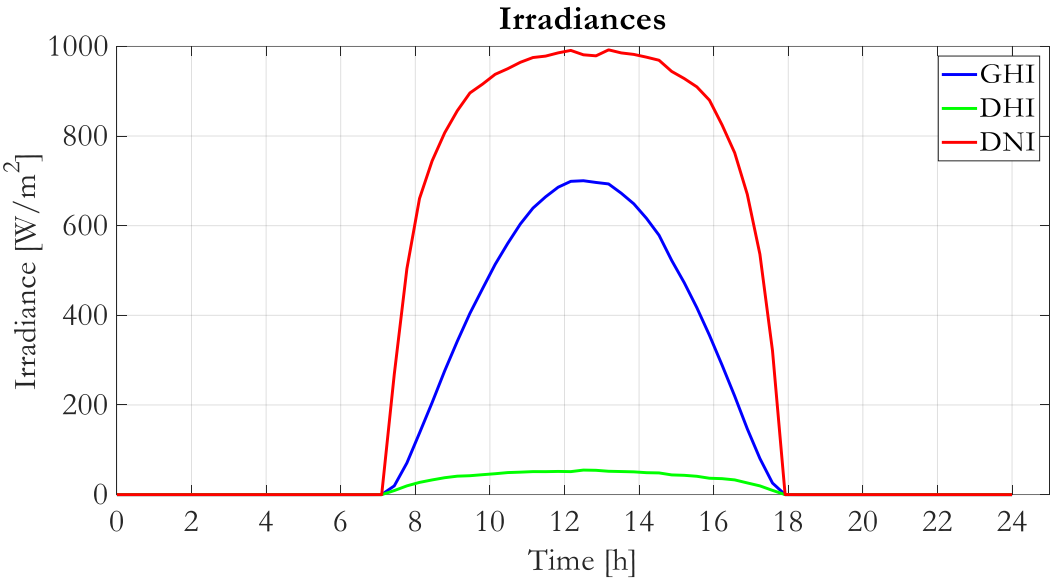


Figure 4.2: Winter solar irradiance (July 2020).

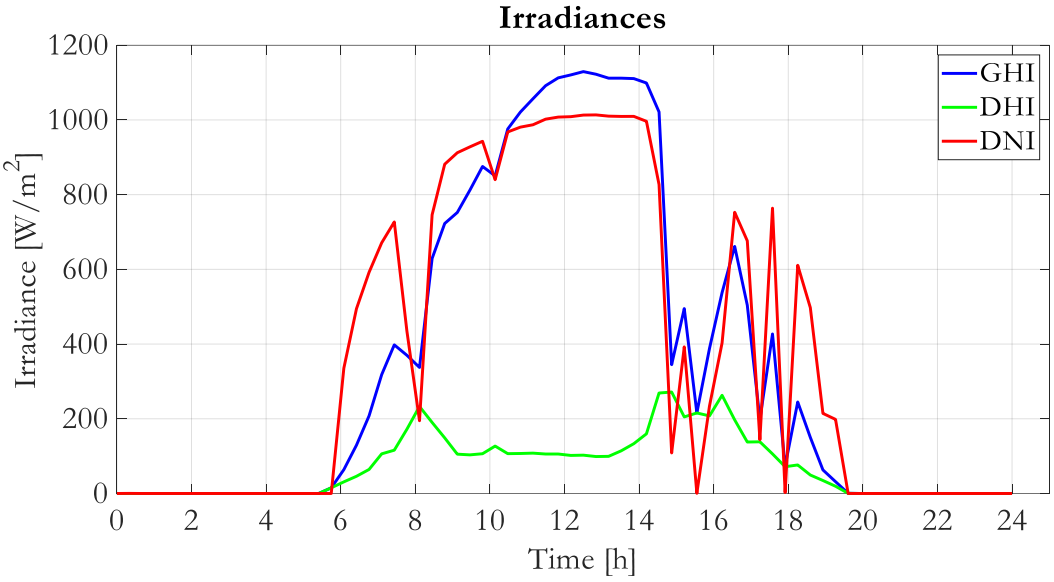


Figure 4.3: Summer solar irradiance (January 2020).

The temperatures of the ambient air and inlet water, are further shown in Figures 4.4 and 4.5, for the winter and summer season, respectively. The data of the ambient air temperature was further obtained directly from the database of the SAURAN network of measuring equipment.

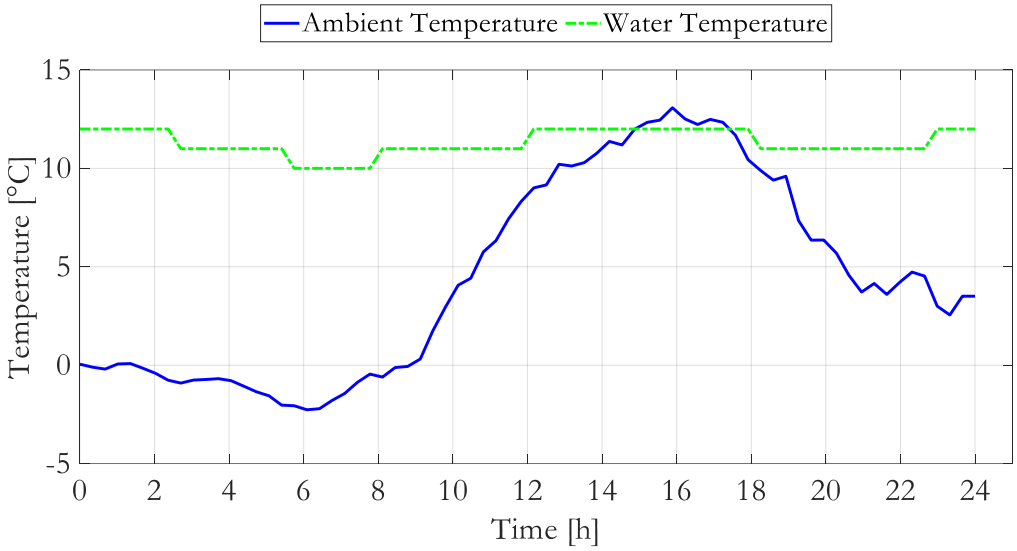


Figure 4.4: Winter ambient and inlet water temperature (July 2020).

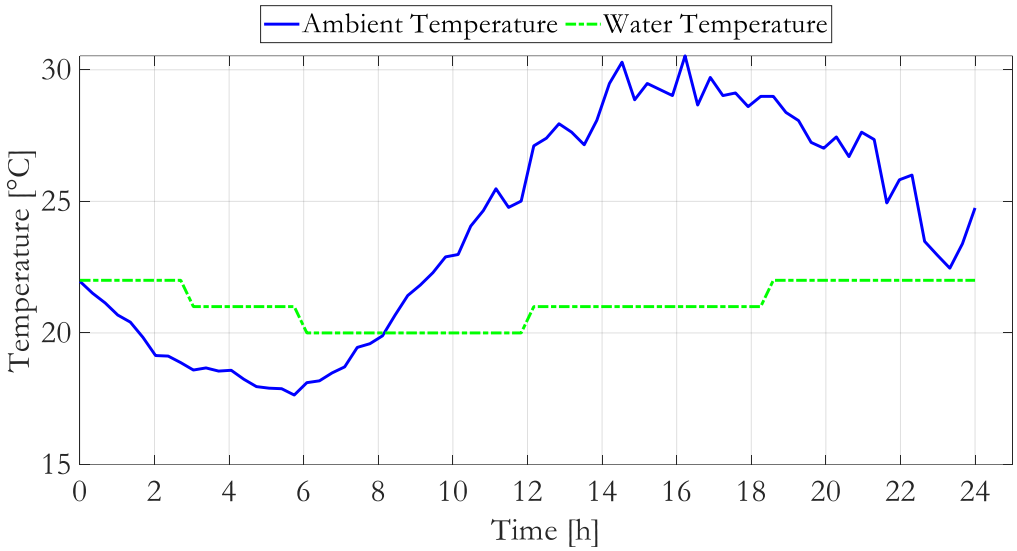


Figure 4.5: Summer ambient and inlet water temperature (January 2020).

The CUT campus accesses water through a borehole, situated around the premises [114]. However, there is no recorded data found for the water temperature, hence, in this case study, the inlet water temperature was based on assumptions. As a result, the winter and summer median inflow water temperatures were set at 11 °C and 21 °C, respectively [115]. When compared to the inlet water temperature, the ambient air temperature varies significantly over time. Considering that fluctuations in ground temperature are

substantially lower than those in ambient air temperature, solely minor temperature changes may be expected for the intake water. As a result, the influence of ambient air temperature on the inlet water temperature, is reduced [15].

Due to the COVID-19 lockdown, that started in March of 2020, universities and residences in South Africa were subsequently closed. This has led to the process of data collection changing for certain input data, i.e. the hot water consumption and the inlet water temperature. As mentioned in the previous paragraph, the inlet water temperature data was approximated based on assumptions. The hot water consumption profile was approximated, with reference to [8], [116], [117]. The average hot water drawn was calculated from the extrapolated data obtained from [8]; and the weekday hot water consumed per student from the same study, was 25 litres. The average energy usage profile and daily energy consumption per student, were adapted from [116]. The energy usage data was further extrapolated from the profile and used to calculate the average of the energy usage per student. The averages of hot water volume drawn for the winter and summer seasons, were obtained from [117] for the seasonal change in consumption.

From the above-mentioned data, the ratios of electricity consumed per student (for male and for female), to the average of the two (male and female), was calculated. The ratio of the hot water drawn, from the extrapolated profile to the average weekday hot water consumed per student, was further calculated. Therefore, the water consumption factor was calculated, by multiplying together the ratio of the electricity consumed (first for the males and then for the males), the ratio of the hot water drawn, the average energy usage, the load factor and the number of students consuming the hot water (75 in this study). The seasonal consumption factor is further calculated, by dividing the hot water volume drawn per season from [117]. The hot water consumption at a given point of time, from the extrapolated hot water drawn profile from [8], is multiplied by the hot water consumption factor. This is carried out for every 20-minute time point, for the 24-hour control horizon, for the male and the female students.

The averages of the 24-hour detailed winter and summer hot water consumption profiles obtained, are shown in Figures *4.6* and *4.7*.

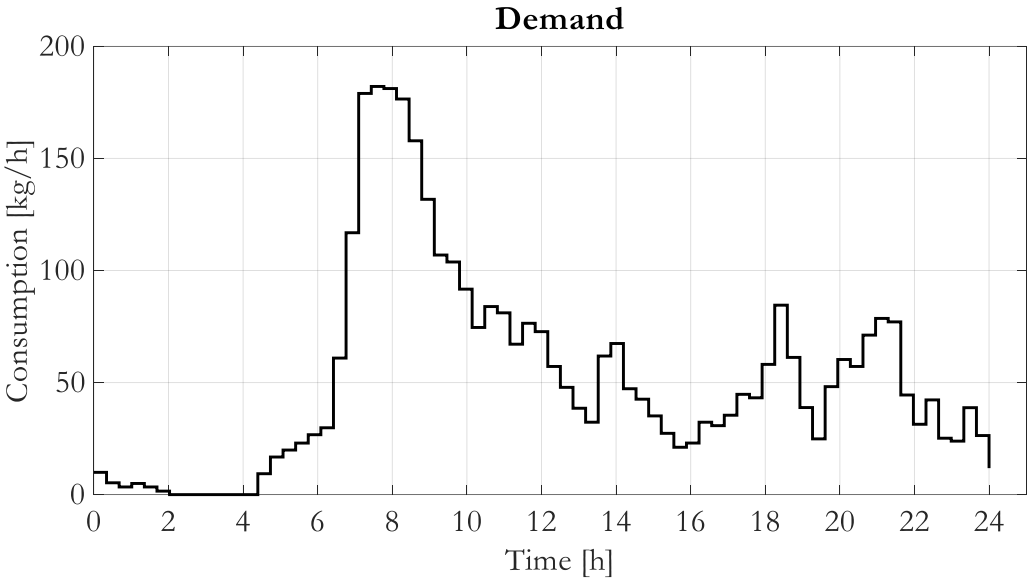


Figure 4.6: Winter hot water demand i.e. flow rate (July 2020).

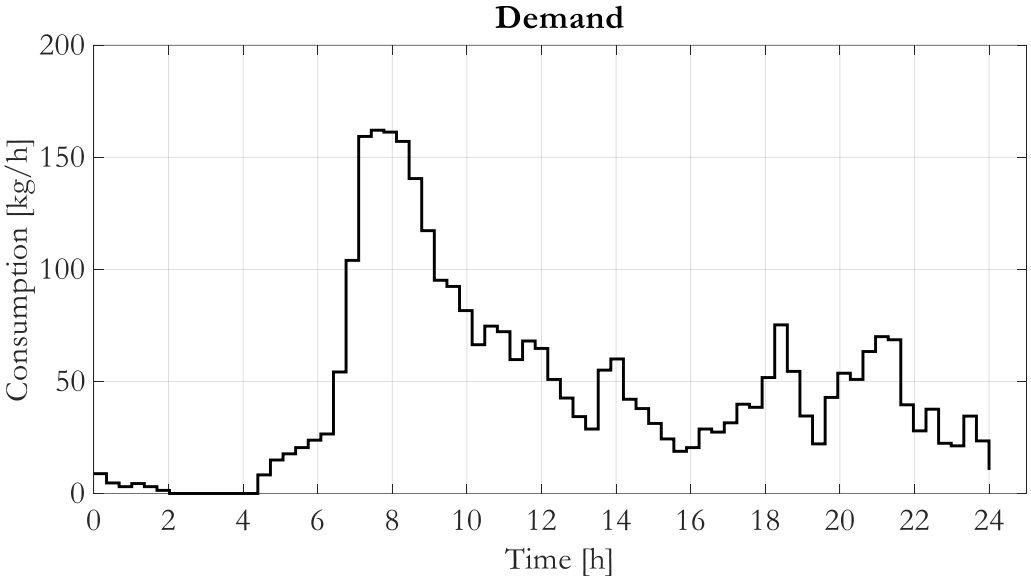


Figure 4.7: Summer hot water demand i.e. flow rate (January 2020).

For variation over the course of a typical seasonal day, the hot water consumption was multiplied by the seasonal factor, to obtain the hot water profiles of the winter and summer seasons. The calculations showed that the male student had consumed more hot water compared to the female and therefore the male student profiles was used. According to the profiles, there is a substantial amount of hot water drawn during the Eskom morning and evening peaks; a result of most, if not all, students have classes in the mornings that they

should prepare for may be assumed that a few students bathe at night, when they return from their daily activities.

### 4.2.2 Component sizes and simulation parameters

The aim of the current study is to apply an optimal energy management scheme to the hybrid water heating system. The baseline model is developed using the hybrid system model to simulate thermostat operation. In the baseline system, solely the electric resistive element is used to supply the required thermal energy to the system.

The collector type used in the study, is the evacuated tube collector (ETC), with the specification of 20 tube borosilicate glass tube with copper internal heat pipe, using the water-glycol solution as a heat transfer fluid. The specifications were sourced from previous literature and datasheets from local suppliers [118]–[121]. The ETCs were selected for this case study, due to their higher temperature range and the fact that their efficiency does not drop as quickly when the outside air temperatures drops, meaning they outperform flat plate collectors (FPCs) in colder climates [75]. The tilt angle of the collector is taken as 30° for winter and summer, which is the average angle of optimal angles of radiation for maximum solar thermal absorption throughout the year in Bloemfontein [15].

Since there are limited studies conducted on liquid-source heat pump systems, the parameters used for the heat pump unit are based on the average of the ASHP unit, commonly used in South Africa. On average, the COP range of a ASHP water heater is between 2 and 4 [106], [122], [123]. Therefore, the input power and average COP of the heat pump unit are assumed as 7.2-kW and 3, respectively.

The baseline model is simulated using the storage tank and the electric resistive elements with same sizes of the components and input data as the hybrid water heating system. For the baseline case, the electric resistive element of the 2000 L storage tank is 24-kW (as indicated by the supplier or manufacturer) [124]. The electric resistive element will solely be employed as a supplementary heat supply to the proposed system whenever required. Therefore, the electric resistive element for the storage tank is reduced by half (which is 12-kW). This decision on the size (capacity) was made, based on the needs of the 75 occupants (students) in the case study.

Table 4.1 shows the component sizes and parameters of the baseline and proposed water heating systems, which were approximated for the South African case from [118]–[121], [124].

Table 4.1. Component sizes and parameters of the proposed water system

| Description | Parameter | Value |
|---|---|---|
| **Collector** | | |
| Specific heat capacity of the transfer fluid (J/kg℃) | $C_{p.c}$ | 3550 |
| Collector tube efficiency factor (-) | $\eta$ | 0.79 |
| Manifold area (m²) – [diameter = 60mm] | $A_{man}$ | 0.0007069 |
| Aperture area (m²) | $A_{ap}$ | 1.86 |
| Absorber area (m²) | $A_{abs}$ | 1.62 |
| Heat loss coefficient (W/m²℃) | $U_{coll\_Loss}$ | ≤ 0.60 |
| Tilt angle (°) | $\beta$ | 30 |
| Angle of incidence for winter season (°) | $\theta$ | 0 |
| Angle of incidence for summer season (°) | $\theta$ | 0 |
| Absorptive Coefficient (-) | $\tau$ | 0.94 |
| Transmittance (-) | $\alpha$ | 0.92 |
| Foreground's albedo (-) | $\rho$ | 0.2 |
| Number of collectors used | | 6 |
| **Heat Pump** | | |
| Heat pump input power (kW) | $P_{hp}$ | 7.2 |
| Coefficient of performance (-) | $COP$ | 3 |
| **Storage Tank** | | |
| Storage capacity (L) | $M_w$ | 2000 |
| Area of the storage tank (mm)- [diameter=1170mm] | $A_s$ | 1.0751 |
| Specific capacity of water (J/kg ℃) | $c_{p.w}$ | 4184 |
| Overall heat loss capacity of the storage tank (W/ m² ℃) | $U_s$ | 0.3 |

| | | |
|---|---|---|
| Electric resistive element for baseline system (kW) | $P_{EL}$ | 18 |
| Electric resistive element for the proposed system (kW) | $P_{EL}$ | 9 |
| Storage tank desired temperature (°C) | $T_s$ | 55 |
| Storage tank minimum temperature (°C) | $T_{min}$ | 50 |
| Storage tank maximum temperature (°C) | $T_{max}$ | 80 |

The baseline model is simulated using the storage tank and the electric resistive elements with same component sizes and input data as the hybrid water heating system. For the baseline case, the electric resistive element of the 2000 L storage tank is 24-kW (as indicated by the supplier or manufacturer) [124]. The electric resistive element will solely be employed as a supplementary heat supply to the proposed system, whenever required. Therefore, the electric resistive element for the storage tank is reduced by half (which is 12-kW). This decision on the size (capacity) was made, based on the needs of the 75 occupants (students), in the case study. CUT is charged at the Industrial TOU, where the energy cost is high during peak pricing periods (morning and evening) and low in standard and off-peak pricing periods (daytime and night) [125]. The peak, off-peak and standard periods of the low and high demand seasons start and end at different times throughout the day and differ by seasons. The high demand season occurs throughout the winter months of June to August, whereas the period between September and May, low demand season is incurred [41].

The TOU tariff structure and pricing layout, imposed by Centlec (electricity distribution and managing company for Bloemfontein and the nearby area), is shown in Table 4.2. The conversion rate, at the time of writing, of the 1.00 ZAR, is 0.068 USD, which will be used to present the costs analyses results in the next Chapter.

The sample time refers to the rate at which a discrete system samples its inputs. Smaller sampling intervals are typically required for state variables that change rapidly when disturbances are introduced into the system [15]. In this study, water temperature is the state variable, which, in comparison to other processes, tends to react slowly. The computational constraints of a 20-minute sampling interval over a control horizon of 72, is used. The simulation parameters are presented in Table 4.3.

Table 4.2. Megaflex single phase TOU tariff structure and pricing.

| Season | Months | Period | Time | Rate (ZAR) |
|---|---|---|---|---|
| High Demand (Winter) | June - August | Off-peak | 00h00–06h00, 22h00–24h00 | 70.76 |
| | | Standard | 09h00–17h00, 19h00–22h00 | 130.32 |
| | | Peak | 06h00–09h00, 17h00–19h00 | 430.19 |
| Low Demand (Summer) | September - May | Off-peak | 00h00–06h00, 22h00–24h00 | 61.28 |
| | | Standard | 06h00–07h00, 10h00–18h00, 20h00–22h00 | 96.61 |
| | | Peak | 07h00–10h00, 18h00–20h00 | 140.33 |

Table 4.3. Simulation parameters.

| Parameter | Description | Value |
|---|---|---|
| ts | Sampling time (min) | 20 |
| N | Control horizon (-) | 72 |
| Hours | Total hours in control horizon (hour) | 24 |

## 4.3 SYSTEMS SIMULATIONS

To compare the performance of the proposed optimally controlled system, the simulation approach was performed against a previously established (baseline) system and the results of the two systems are presented and analysed in this Section. The results are based on the extremes of the typical day in the winter and summer seasons. The simulations were conducted in association with the winter and summer hot water demand profiles (Figures 4.6 and 4.7), respectively, presented under Section 4.2.1.

For simulation purposes, (1) the acquired input data listed in Table 4.1 was used to simulate the operation of the baseline (without the optimal control) and the hybrid system with the optimal control scheme; (2) the pricing of the costs during energy consumption is based on the TOU tariff structure, as presented in Table 4.2, where the cost of energy

consumed during the peak periods is significantly high during the peak periods and equally low during the off-peak periods. The highest and lowest TOU tariff pricing occur during the winter season peak periods and the summer season off-peak periods, respectively; and (3) the switching profile and storage tank temperature profile sampling times were determined using the parameters listed in Table 4.3, all of which are listed in Section 4.2.1.

Whenever the hot water inside the storage tank reaches the low set-point, the electric resistive element automatically switches ON. The electric resistive element switches OFF when this temperature reaches the highest temperature to sustain the hot water demand of the consumers throughout the day. The cold water supplied to the storage tank, is from the mains and, enters the thermal storage tank whenever there are hot water draw-offs to maintain a constant volume.

The simulation results of a baseline water heating system and the optimally controlled SAHP water heating system are discussed in Sections 4.3.1 and 4.3.2, respectively. Section 4.3.3 compares these two systems, with the aim to draw a conclusion.

### 4.3.1 Baseline (without the optimal scheduling)

A baseline system is simulated with solely a standard electric storage tank and an electric resistive element, from the components and parameters listed in Table 4.1, under Section 4.2.2.

A thermostat regulates the temperature, using a controller, which controls the electric resistive element of the storage tank. The thermostatic temperature is set to 60 °C by default and has a temperature range of approximately 5 °C. Cold water is supplied to the tank from the mains and enters the thermal storage tank whenever there are hot water draw-offs [15]. The two separate baseline cases, for winter and summer seasons, are simulated and illustrated under the winter case and summer case sections, below. Figures 4.8 - 4.11 present the switching function of the thermostat and the correlated change in water temperature inside the storage tank.

4.3.1.1 Baseline: Winter case

- Switching profile and water temperature during the off-peak period [00h00,06h00)

In the winter case, there is a small amount of hot water consumed, as shown in Figure 4.6, presented in Section 4.2.1, in the first few hours of the day (00h00-02h00). There is no switching of the electric resistive element (illustrated in Figure 4.8) during the off-peak period and the water temperature starts to decrease from 05h00. The temperature in the storage tank, shown in Figure 4.9, remains at 60 °C until the hot water consumption reoccurs at 04h15.

- Switching profile and water temperature during the peak period [06h00,09h00)

During this period, there is a higher electricity cost for energy consumption, as shown in Table 4.2. Furthermore, here is a rapid increase in the hot water demand, as illustrated in Figure 4.6, until the highest, approximately 184 L/h, is reached. The hot water demand then starts to decrease. As the temperature in the storage tank (Figure 4.9) drops to the lowest set temperature of 55 °C, the electric resistive element, in Figure 4.8, turns on from 07h40, for an hour and 20 minutes, until the temperature reaches 60 °C again.

- Switching profile and water temperature during the standard period [09h00,17h00)

The hot water demand profile (Figure 4.6) fluctuates during this period and the storage tank temperature (Figure 4.9) starts to decrease again, until it reaches the lowest set temperature. The electric resistive element (Figure 4.8) switches ON again at 12h00, for another hour and the storage tank water temperature continues to gradually decrease. There is a moderate electricity price for the energy consumption during this period.

- Switching profile and water temperature during the peak period [17h00,19h00)

The storage tank temperature (Figure 4.9) continues to slowly decrease as the hot water demand (Figure 4.6) continues to fluctuate. There is no switching taking place during this period (as shown in Figure 4.8).

- Switching profile and water temperature during the standard period [19h00,22h00)

As the hot water demand (Figure 4.6) continues to fluctuate and the hot water temperature (in Figure 4.9) reaches the low set temperature point. The switching (Figure 4.8) starts at the beginning of the standard period for 1 hour and 20 minutes. The hot water temperature in the storage tank starts to increase, until it reaches the high set temperature point and, then, decreases again, due to the continuing consumption of the hot water.

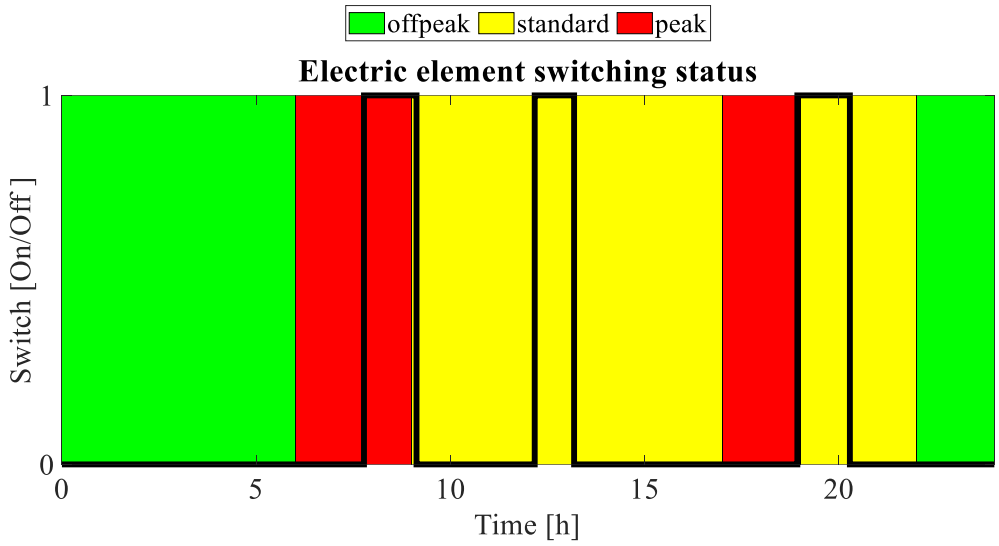


Figure 4.8: Switching function of the ESTWH during winter season.

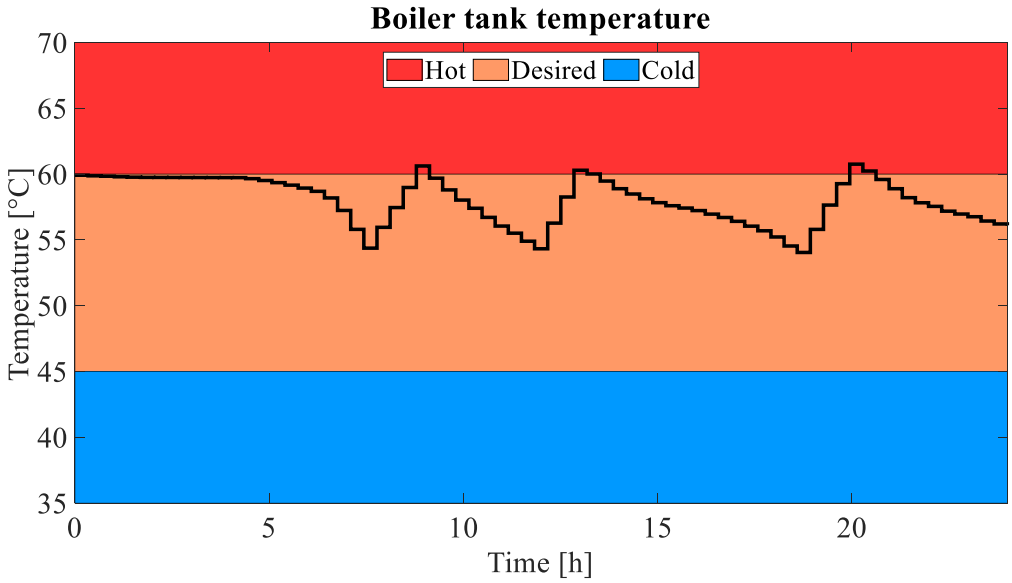


Figure 4.9: Storage tank water temperature of ESTWH for winter season.

- Switching profile and water temperature during the off-peak period [22h00,24h00)

The hot water temperature (Figure 4.9) continues to decrease. There is a reduced amount of hot water consumed and the demand (Figure 4.6) continues to fluctuate to the end of the day. The hot heater temperature at the end of the control horizon is above the low temperature set point and no switching (Figure 4.8) occurs.

4.3.1.2 Baseline: Summer case

- Switching profile and water temperature during the off-peak period [00h00,06h00)

For the summer case, there is a trivial amount of hot water consumed, as shown in Figure 4.7 from the first few hours of the day (00h00-02h00) and then again, starting from 04h15. The temperature in the storage tank, shown in Figure 4.11, remains at 60 °C and starts to decrease at 05h00. No switching occurs (Figure 4.10) during the off-peak period, as the hot water temperature remains above the lowest set point temperature of 55 °C.

- Switching profile and water temperature during the standard period [06h00,07h00)

No switching occurs, as shown in Figure 4.10, occurring during this period, however, there is a rapid increase of the hot water demand (Figure 4.7) and a steady drop of hot water temperature in the storage tank (Figure 4.11). No electricity consumption occurs during this period.

- Switching profile and water temperature during the peak period [07h00,10h00)

The hot water temperature continues to decrease with sharp increasing of the hot water consumption (Figure 4.7). The consumption increases until it reaches its peak, at approximately 164 L/h and then, starts to decrease. The storage tank temperature (Figure 4.11), continues to decrease, until it drops to the low set temperature point. The electric resistive element switching (Figure 4.10), occurs at 08h20 for an hour, until the hot water temperature reaches the high set temperature point. The water starts to decrease again, due to the continued hot water consumption. The electricity cost during this period is high for

the peak period in the summer season, however, lower, as compared to the price of the peak period during winter season.

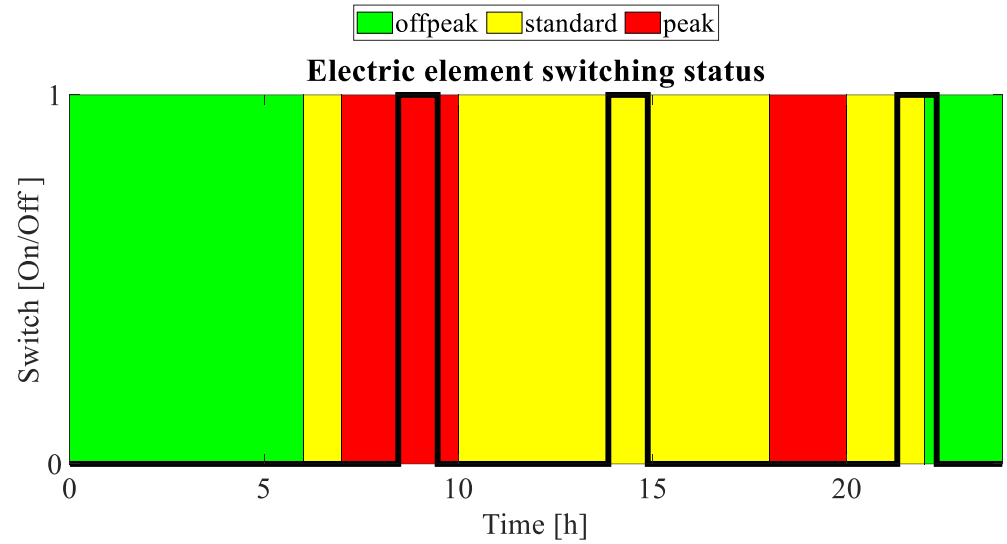


Figure 4.10: Switching function of the ESTWH during summer season.

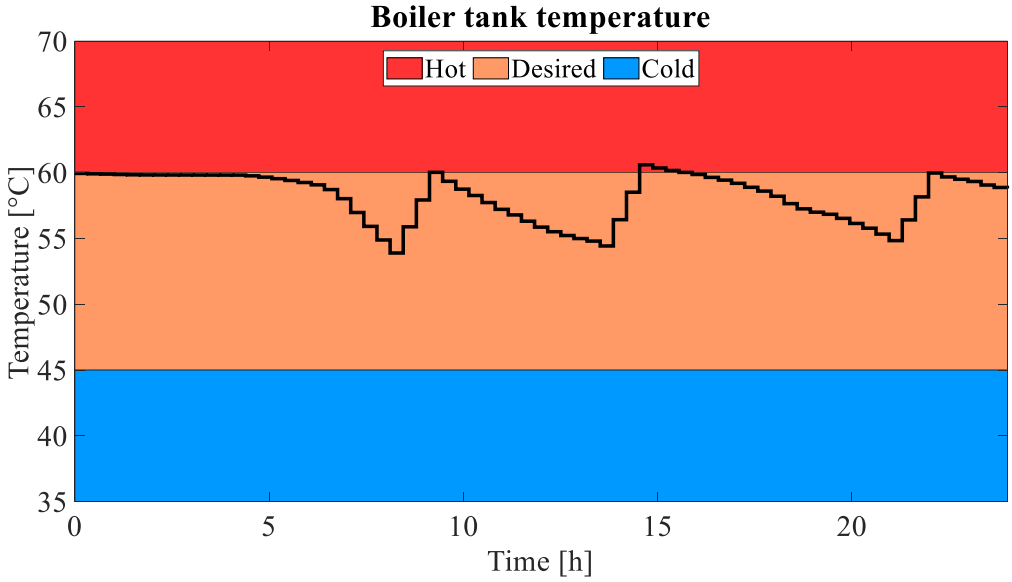


Figure 4.11: Storage tank water temperature of ESTWH for summer season.

- Switching profile and water temperature during the standard period [10h00,18h00)

The hot water demand profile (Figure 4.7), fluctuates in during this period. The storage tank temperature (Figure 4.11) starts to decrease again, until it reaches the lowest

set temperature. The electric resistive element (Figure 4.10) switching again occurs from 13h40 for an hour and the storage tank water temperature continues to gradually decrease. There is a moderate electricity price for the cost consumption during this period, which is less compared to the winter season prices.

- Switching profile and water temperature during the peak period [18h00,20h00)

The storage tank temperature (Figure 4.11), continues to slowly decrease as the hot water demand (Figure 4.7) continues to fluctuate. There is no switching (Figure 4.10) occurring during this period, as the hot water temperature in the storage tank remains above the low set temperature point.

- Switching profile and water temperature during the standard period [20h00,22h00)

The hot water demand (Figure 4.7), continues to fluctuate. The storage tank temperature (Figure 4.11) continues to slowly decrease, until it reaches the lowest set temperature point. The switching (Figure 4.10) occurs for the remaining 40 minutes, before the end of the standard period.

- Switching profile and water temperature during the off-peak period [22h00,24h00)

The switching (Figure 4.10) continues to the off-peak period for the first 20 minutes and increases the hot water temperature (Figure 4.11) to 60 °C. The hot water demand (Figure 4.7) continues upon the control horizon.

### 4.3.2 Optimal scheduling of the proposed IDX-SAHP water heater

The operation of the proposed system was simulated, based on the optimal cost saving with the optimal scheduling. The optimal scheduling was achieved by load shifting of the hot water production, from high electricity price periods to the low electricity cost periods, to achieve possible cost savings, based on the TOU pricing, presented in Table 4.2. The following sections provide a brief breakdown of the results, presented in Figures 4.12-4.17.

4.3.2.1 Optimal control of the IDX-SAHP: Winter case

- Switching profile and water temperature during the off-peak period [00h00,06h00)

From Figure 4.6, due to the hot water consumed from the first few hours of the day (00h00-02h00), the temperature of the hot water inside the storage tank (illustrated in Figure 4.14) is below 60 °C, at the beginning of the control horizon. The heat pump unit switching (Figure 4.12), occurs at the start of the control horizon for 40 minutes, to maintain the temperature just above 60 °C. The switching of the heat pump occurs from 03h20 and switches ON several times, until it switches OFF at 06h00, at the end of the off-peak period. The temperature reached in the storage tank is approximately 79 °C, as illustrated in Figure 4.14. The temperature then starts to gradually decrease. The electric resistive element, illustrated in Figure 4.13, remains at zero throughout the off-peak period and for the rest of the 24 hours, as the heat pump unit supplies sufficient energy during this period.

- Switching profile and water temperature during the peak period [06h00,09h00)

No switching occurs for both the heat pump unit (Figure 4.12) and the electric resistive element (Figure 4.13) during this period. This is to avoid the high-cost consumption, due to the higher electricity prices. The quick rise of the hot water demand (Figure 4.6) occurs during this period, until it reaches approximately 184 L/h and then starts to decrease. The hot water temperature (Figure 4.14), continues to decrease to a temperature below 70 °C.

- Switching profile and water temperature during the standard period [09h00,17h00)

No switching occurs for both the heat pump unit (Figure 4.12) and the electric resistive element (Figure 4.13) during this period. There is a moderate electricity price for the cost consumption during this period. The hot water demand (Figure 4.6) fluctuates during this period. The hot water temperature (Figure 4.14), continues to gradually decrease to a temperature below 60 °C.

- Switching profile and water temperature during the peak period [17h00,19h00)

No switching occurs for both the heat pump unit (Figure 4.12) and the electric resistive element (Figure 4.13) during this period. The hot water demand (Figure 4.6) fluctuates during this period. The hot water temperature (Figure 4.14) continues to gradually decrease to a temperature below 60 °C and remains above 50 °C.

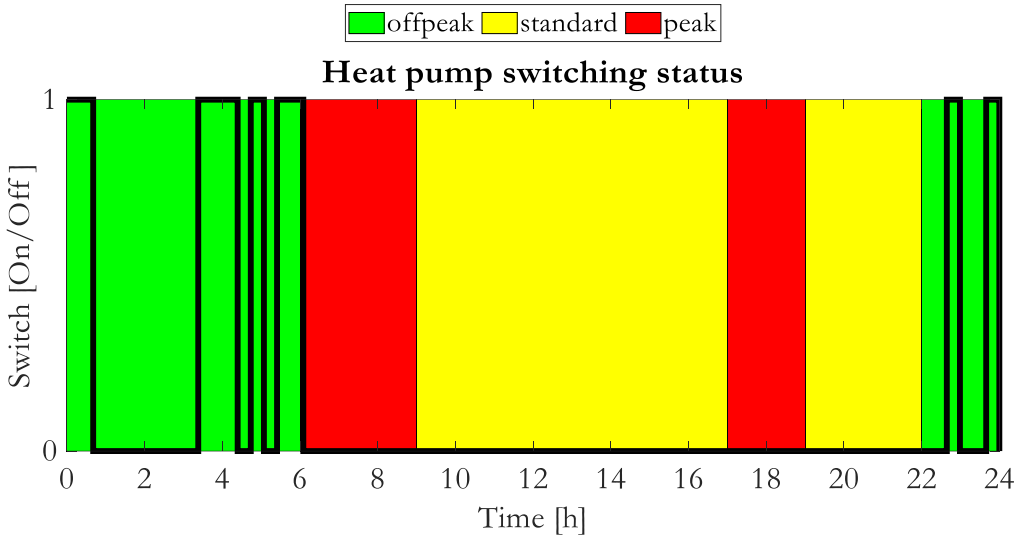


Figure 4.12: Heat pump switching for the winter season.

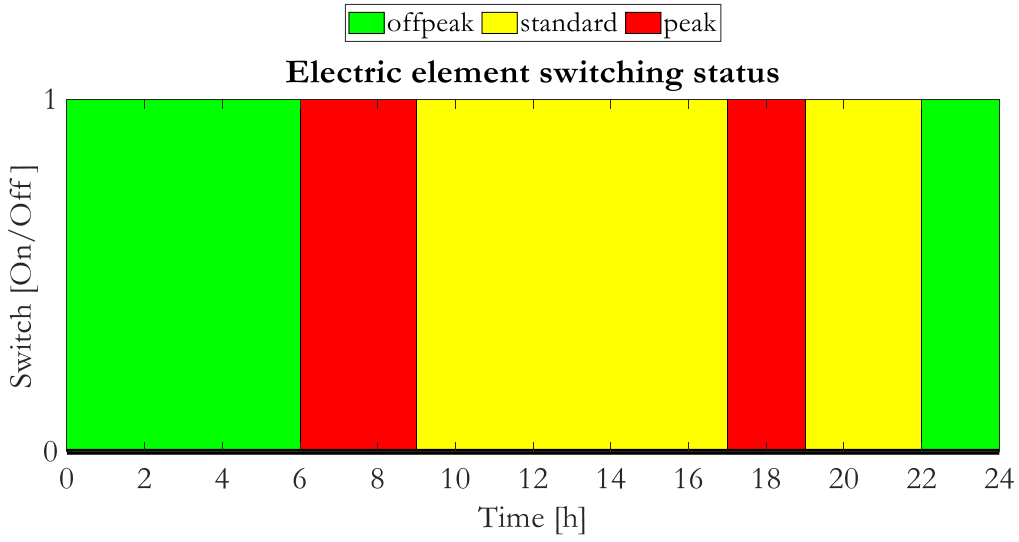


Figure 4.13: Electric resistive element switching for the winter season.

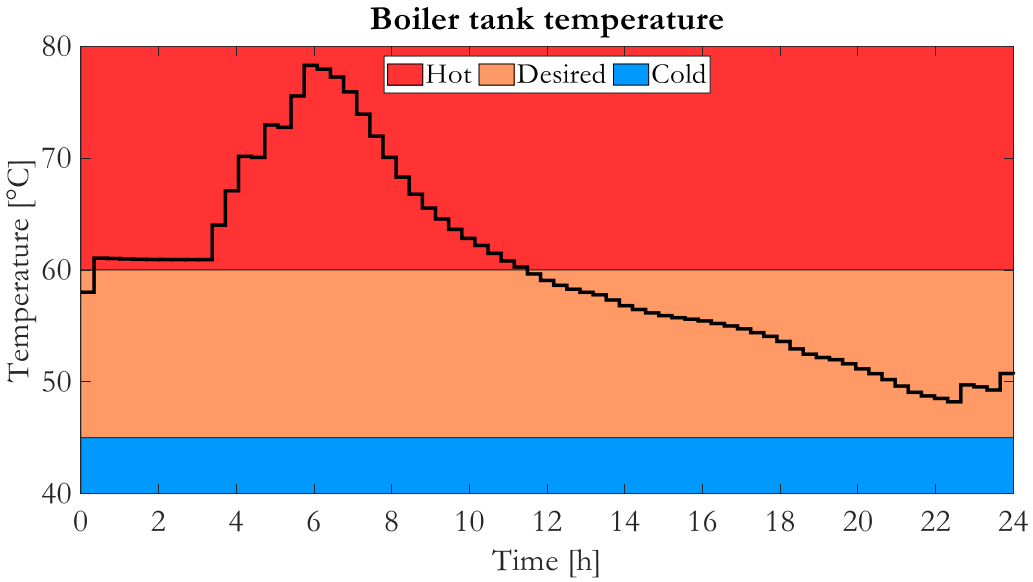


Figure 4.14: Storage tank temperature of IDX-SAHPWH for winter season.

- Switching profile and water temperature during the standard period [19h00,22h00)

No switching occurs for both the heat pump unit (Figure 4.12) and the electric resistive element (Figure 4.13) during this period. The hot water demand (Figure 4.6) fluctuates during this period. The hot water temperature (Figure 4.14) continues to gradually decrease to a temperature below 50 °C. The system does not switch ON to heat water during this period, due to the cost minimisation.

- Switching profile and water temperature during the off-peak period [22h00,24h00)

The hot water demand (Figure 4.6), fluctuates during this period. The hot water temperature (Figure 4.14) continues to gradually decrease to approximately 48 °C. The heat pump unit (Figure 4.12), then switches ON at 22h40, for 20 minutes and again at 23h40, for a further 20 minutes and then, switches OFF at the end of the control horizon. There is still no switching occurring for the electric resistive element (Figure 4.13) during this period, to the end of the control horizon.

4.3.2.2 Optimal control of the IDX-SAHP: Summer case

- Switching profile and water temperature during the off-peak period [00h00,06h00)

Users consume a minimal amount of hot water between 00h00-02h00, as shown in Figure 4.7. The hot water consumption resumed at 04h20 and the demand gradually increased. To prepare hot water for the consumption, the switching, as shown in Figure 4.15, occurs during the off-peak period at 03h00, for 20 minutes, again at 04h40 for 40 minutes and lastly at 04h40, for another 20 minutes. No switching occurs on the electric resistive element for the whole control horizon, as illustrated in Figure 4.16. The hot water temperature in the storage tank, as illustrated in Figure 4.17, is heated from 55 °C, up to approximately 66 °C. The hot water starts to decrease, as there is water consumption and cold water pours inside the tank, while the hot water is consumed.

- Switching profile and water temperature during the standard period [06h00,07h00)

There is a rapid increase in hot water consumption (Figure 4.7) during the standard period and hot water temperature (Figure 4.17), further continues to decrease. There is no switching for both the switching controls (Figures 4.15 and 4.16) and, therefore, no cost of electricity consumed, during this period.

- Switching profile and water temperature during the peak period [07h00,10h00)

There is a rapid increase of hot water consumption (Figure 4.7), which continues until it reaches a maximum of 164 L/h and starts to decrease. The temperature drops of the hot water in the storage tank (Figure 4.17), are increased compared to the last period, due to the high hot water consumption, until the temperature goes below 60 °C. The hot water temperature continues to decrease gradually. There is no switching for both the switching controls (Figures 4.15 and 4.16) and, therefore, no cost of electricity consumed during this period.

- Switching profile and water temperature during the standard period [10h00,18h00)

The hot water consumption (Figure 4.7) is below 90 L/h and the demand fluctuates. The hot water temperature (Figure 4.17), further continues to decrease steadily. There is

still no switching for both the switching controls (Figures 4.15 and 4.16) and, therefore, no cost of electricity consumed during this period.

- Switching profile and water temperature during the peak period [18h00,20h00)

The hot water consumption (Figure 4.7), continues to fluctuate below the 90 L/h demand. The hot water temperature (Figure 4.17), further continues to decrease steadily. No switching occurs for both the switching controls (Figures 4.15 and 4.16) and, therefore, no cost of electricity is consumed during this period.

- Switching profile and water temperature during the standard period [20h00,22h00)

The hot water consumption (Figure 4.7), continues to fluctuate below the 90 L/h demand. The hot water temperature (Figure 4.17), further continues to decrease steadily. No switching occurs for both the switching controls (Figures 4.15 and 4.16) and, therefore, no cost of electricity is consumed during this period.

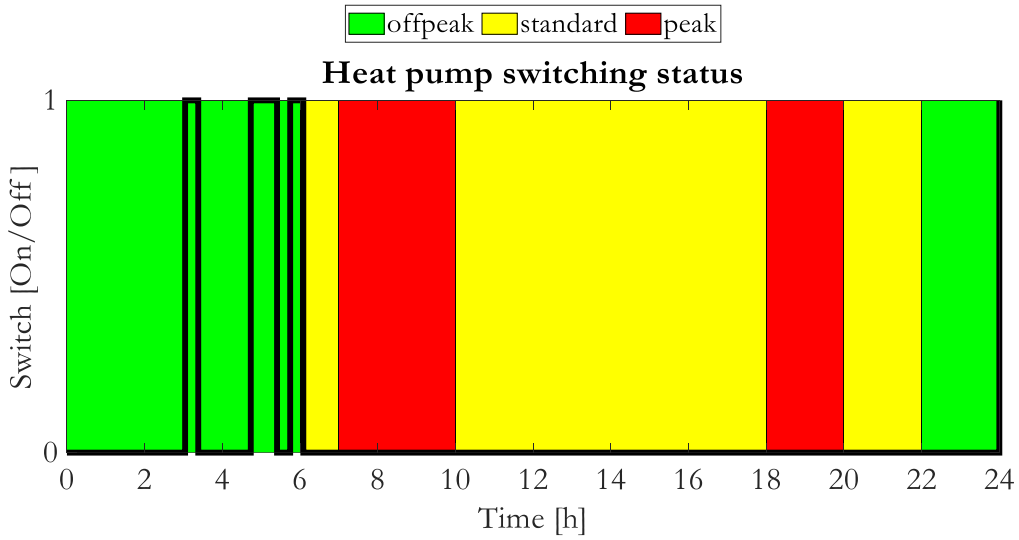


Figure 4.15: Heat pump switching for the summer season.

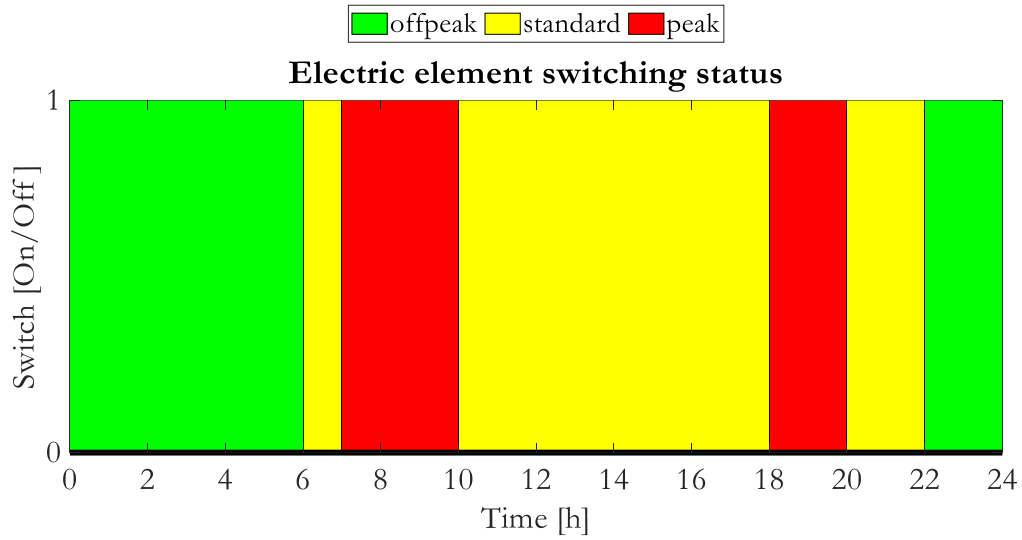


Figure 4.16: Electric resistive element switching for the summer season.

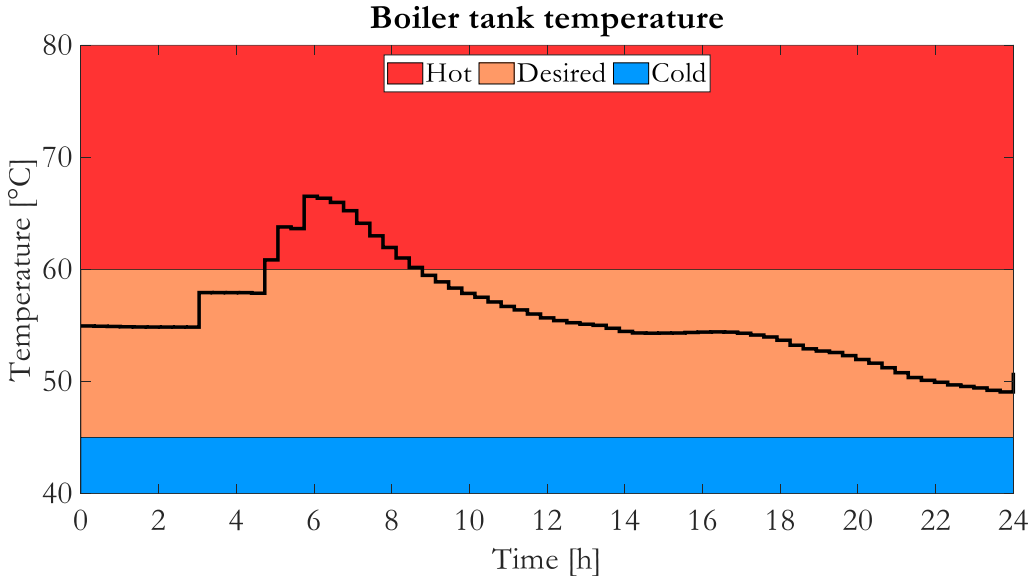


Figure 4.17: Storage tank temperature of IDX-SAHPWH for summer season.

- Switching profile and water temperature during the off-peak period [22h00,24h00)

The hot water consumption (Figure 4.7) is below 90 L/h and the demand fluctuates until the end of the control horizon. The hot water temperature (Figure 4.17) continues to further decrease steadily, until it drops to a temperature of 50 °C, by 1 °C at the end of the control horizon. There is still no switching for both the switching controls (Figures 4.15 and 4.16) and, therefore, no cost of electricity consumed during this period.

### 4.3.3 Comparison between the baseline and optimal control of the IDX-SAHP

Both the baseline and the hybrid water heating systems, raise the thermal level of the water to 60 °C and above, to eliminate the legionella pathogenic bacterium and the simulation of the thermostat operation, is within the 3 °C range of the operation, meaning that the accuracy of the operation was maintained. The systems further achieved the general aim of maintaining the comfort level of the consumers.

The baseline system contributes to the high consumption of electricity, whereby the switching of the electric resistive element of the baseline system occurs whenever the temperature of the water is at or below the set temperature. This includes the switching that occurs even during the peak periods of the TOU tariff pricing structure. Therefore, the customer is billed a significant amount at the end of the day, for the process of heating water.

The hybrid water heating system, with the optimal energy control scheme, selected the most affordable time periods of the TOU tariff structure to heat the water. The electric resistive element is used as a supplementary input energy, solely when the IDX-SAHP unit is unable to produce sufficient energy to heat the water. From the results of the switching profiles, solely the heat pump switches ON to heat the water, whereas the electric resistive element remains at zero throughout the horizon. The switching of the IDX-SAHP system starts in the early hours of the morning, to heat up the water to the highest temperature maintaining the thermal consumption of the consumers. Therefore, the consumers will save on energy costs, since the hybrid water heating system will merely use a minimal portion of energy to heat water to a significantly high temperature, at a notable low cost

## 4.4 SUMMARY

In this Chapter, the optimal operation control model of the hybrid system has been simulated, using SCIP solver in the MATLAB OPTI-Toolbox. The seasonal extremes of the winter and summer seasons were collected from the historic weather data of Bloemfontein weather conditions and the water and ambient temperatures approximated from the previous literature, were collected and presented. The collected data was therefore

utilized, to successfully develop models used to represent the operation of a baseline, as well as an optimal control strategy applied to the proposed system. The daily non-linear load, non-linear renewable resources, and the storage tank temperature dynamic, were evaluated, in terms of the impact on the daily operation cost of the hybrid system, compared to the baseline. The profiles of the control switching of the baseline system and of the optimally controlled model of the hybrid system, were analysed and compared.

The optimal energy management model has further been used to:

- Attain minimised operation costs, by using the optimally controlled proposed IDX-SAHP system,
- Analyse the impact of the solar irradiance of the solar system coupled, with the heat pump on the storage tank temperature dynamic during the two seasons, represented by the TOU tariff, implemented by the electricity supplier,
- Reveal the importance of considering the differences in seasonal load profiles and variations in the renewable energy technology, water inlet temperature, as well as ambient temperatures, while calculating the daily and annual operation cost of the hybrid system.

From the simulated Figures, it may be seen that, the proposed optimally controlled system heats the water using the power input from the heat pump unit alone. Furthermore, the system switches during the morning and evening off-peak period. This may result in further cost savings, since the heat pump solely uses a third of the power input, as compared to the electric resistive element. In addition, the charges during the off-peak periods are exceedingly low, as compared to the standards and peak periods. Whereas, the baseline system uses the electric resistive element to heat water and the switching occurs, mostly, during the standard and peak periods, being the high consuming regions of the TOU pricing structure.

Knowing that the proposed system has different components as the baseline, further analyses are required to assess the techno-economic performance of the former, as compared to the latter. This is carried out in the next Chapter, analysing the cumulative energy costs and the life cycle costs at the end of the 20 years project period.

# CHAPTER 5: ECONOMIC ANALYSIS

## 5.1 INTRODUCTION

In this Chapter, techno economic of the simulated optimally controlled system and the baseline systems are presented and analysed. The analysis includes the costs incurred through the energy consumed during the hot water production for the proposed system and baseline, compared for the winter and summer cases, as well as the life cycle costs incurred throughout the project span, to determine the possible cost savings at the end of the project span of 20 years. The results from the simulation and cost calculations are presented.

This Chapter consists of four sections that analyse and compare the costs of the optimally proposed system and baseline. Section 5.2, presents the cost of purchase from the manufacturer or suppliers in the South African market. Section 5.3. compares the cost cumulated by the energy consumed during the hot water production. Whereas Section 5.4 presents the comparison of the life cycle cost of the two systems to further assess the savings over the life span of the project (20 years). Finally, Section 5.5 provides a summary of the Chapter as a whole.

## 5.2 INITIAL IMPLEMENTATION COST OF THE INDIRECT-EXPANSION SOLAR-ASSISTED HEAT PUMP WATER HEATING SYSTEM

The initial investment cost of a proposed optimal water heating system is presented. The specifications of the products from the manufacturers, ultimately conform with Eskom the and South African Bureau of Standards (SABS) criteria [126].

Since there is currently a lack of liquid-to-liquid heat pump units on the market, the heat pump unit price is assumed to be equal to the air-source heat pump unit, which is available on the market. The average component prices for the year 2021, obtained from a price check website [127] that presents a comparison of the prices of the products in the South African market, shown in Table 5.1. The estimated billing of the baseline system and

the proposed systems are 108 375.00 ZAR (7 402.46 USD) and 215 554.00 ZAR (14 723.23 USD), respectively.

Table 5.1: Bill of quantity of the IDX-SHAP.

| System | Description | Qty | Unit price (ZAR) | Net price (ZAR) |
|---|---|---|---|---|
| Baseline (ESTWH) | 2000L Hot Water Storage Tank | 1 | 96 795.00 | 96 795.00 |
| | 6kW Electric Screw Element | 4 | 2 895.00 | 11 580.00 |
| | Total initial investment costs | | | 108 375.00 |
| Proposed (IDX-SAHP) | ITS 20 Tube ETC Collector | 6 | 9 495.00 | 56 970.00 |
| | 22kW Commercial Heat Pump | 1 | 45 995.00 | 45 995.00 |
| | 2000L Hot Water Storage Tank | 1 | 96 795.00 | 96 795.00 |
| | 6kW Electric Screw Element | 2 | 2 895.00 | 5 790.00 |
| | Geyser Temperature Controller 3000W | 1 | 1 195.00 | 1 195.00 |
| | Fluid Pumps (solar and water circulation) | 2 | 2 555.00 | 5 110.00 |
| | 110℃ Air Release Valve | 1 | 199.00 | 199.00 |
| | Labour | - | 3 500.00 | 3 500.00 |
| | Total initial investment costs | | | 215 554.00 |

## 5.3 CUMULATIVE COST COMPARISON

The total cumulative costs of the projects are incurred from different aspects throughout the project's lifetime, which, in this case, is 20 years. These costs incurred include, firstly, the initial implementation cost ($C_{initial}$), as described is Section 5.2, followed by the replacement cost ($C_{rep}$), operation and maintenance (O&M) cost ($C_{OM}$), annual energy cost ($C_{annual-EC}$) and the salvage cost ($C_{salvage}$). These costs occur at various time-periods during the project's lifetime, from the first year of the project's commencement, through to the end of the project's lifetime.

The initial implementation and salvage costs are incurred once, where the former is incurred at the beginning of the project and the latter may solely be observed once, at the end of the project's period. Additionally, the salvage cost may be subtracted from the entire life cycle cost. The replacement cost depends on the lifespan of each component within the project lifetime and the operation, as well as maintenance costs, are incurred whenever there is a need for component replacement, as well as during the maintenance and operation of the system. Lastly, the energy cost is incurred throughout the project lifetime, as soon as the system starts to operate, to the end of the period set for the project lifetime.

### 5.3.1 Cumulative energy cost

To calculate the daily cumulative energy cost ($C_{d-EC}$), the primary objective function in Eq. (3.40), may be adapted from Chapter 3 into Eq. (5.1). For the annual cumulative energy cost ($\mathbf{C_{annual-EC}}$), the days of the year are divided into the Eskom defined high and low demand season, which consists of 92 days for the winter (high demand) season and 273 days for the summer (low demand) season, per annum. The total annual energy cost may, therefore, be calculated for each season, with the number of days multiplied with the energy cost in each respective season, as shown in Eq. (5.2) [128]:

$$C_{d-EC} = t_s \sum_{k+1}^{N} (P_{hp,k} S_{hp,k} + P_{EL,k} S_{e,k}) C_{TOU,k} \tag{5.1}$$

$$c_{annual-EC} = C_{dw-EC} \cdot 92 + C_{ds-EC} \cdot 273 \tag{5.2}$$

Where:

$t_s$ is the sampling time;

$P_{hp.k}$ is the rated power of the heat pump (kW);

$P_{EL.k}$ is the rated power of the electric resistive element (kW);

$S_{hp_k}$ the switching status of the heat pump;

$S_{e_k}$ the switching status of the electric resistive element;

$C_{TOU_k}$ is the time-based cost of electricity at each kth interval (ZAR/kWh);

$C_{dw-EC}$ is the daily cumulative energy cost for the winter season (ZAR);

$C_{ds-EC}$ is the daily cumulative energy cost for the summer season (ZAR).

With this, the cumulative daily cost values (ZAR), of a typical winter and summer day, were obtained and illustrated in Sections 5.3.1.1 - 5.3.1.2. In Section 5.3.1.3, the seasonal cumulative costs, for the winter and summer cases, respectively, as well as the annual cumulative costs, are calculated and compared, using the total daily energy cost values obtained in terms of the low and high demand seasons, defined by Eskom.

5.3.1.1 Winter daily cumulative energy cost comparison

The cumulative costs of the baseline and optimal systems, as shown in Figure 5.1, in correspondence to the switching profiles of the two systems, show that, when the switching occurs, cumulated energy costs incur throughout the control horizon. As the switching changes to the ON state occur, the energy cost increases at a charge of the specific time-based pricing, which, at the end of the day, shows how much energy cost has accumulated throughout the day.

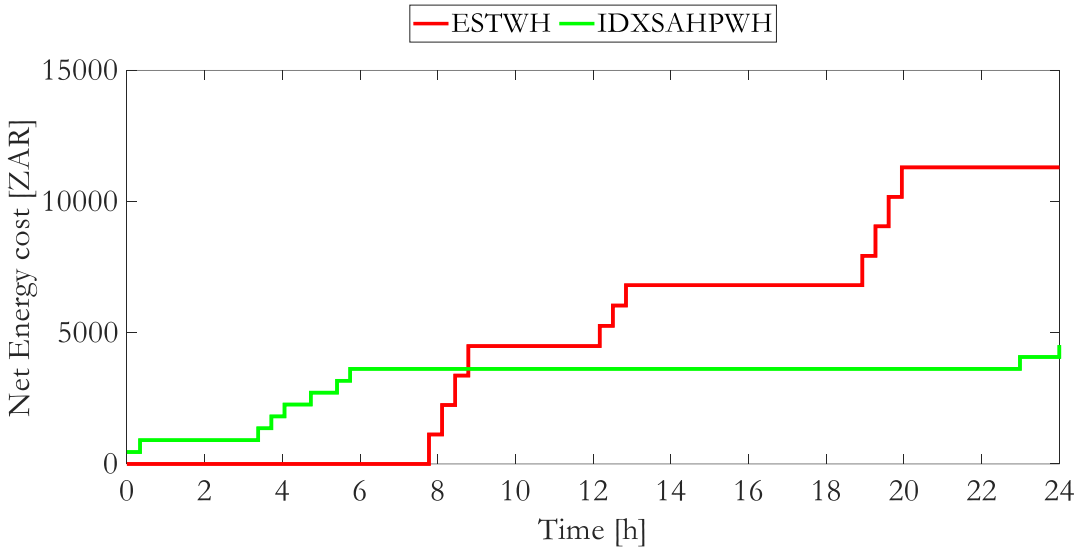


Figure 5.1: Winter cumulative energy cost.

For the winter season, the TOU pricing is the most expensive, compared to the low demand season and has the highest demand incurred. The cumulative cost of the baseline is too high, as the system operates during the peak hours of the TOU tariff structure and, due to the high amount of TOU pricing during the season, particularly during the peak

periods. The baseline switching of the day, starts during the morning peak period, as the water temperature drops to the low set point during the draw-offs and the costs incurred during this time, are significantly high. The next switch is during the afternoon standard period of the TOU tariff, and the costs are moderate during this period. The final switch occurs during the evening peak period. The graph shows a rapid increase in energy costs during the peak period, as compared to the standard period.

The optimal hybrid system switches on exclusively during the morning and evening off-peak TOU tariff periods of the day, aiming to save the cost accumulated when heating the water. The optimal hybrid system prepares the hot water early in the morning and heats the water up to a notably high temperature, enough to maintain the consumers' thermal level, throughout the day, ensuring that the water will not require to be heated during the peak periods.

Compared to the cumulative costs of the baseline and optimally controlled hybrid system at the end of the control horizon (end of the day), the cumulative cost of the baseline is greater than the optimally controlled hybrid water heating system, by a factor of 2.5.

#### 5.3.1.2 Summer daily cumulative energy cost comparison

From the cumulative cost of the summer period curve, presented in Figure 5.2, the baseline system switches ON and OFF three times throughout the day, to heat the water up. The first switch occurs during the morning peak, the second switch occurs during the afternoon standard period and the last switch occurs during the night off-peak period, during the last hours of the day. The TOU tariff pricing for the summer season, is not as high as that of the winter season, where, for the peak period, the summer season charges approximately a third of the amount charged for the winter season, as may be observed in Figure 5.2. The cost during the peak period increases rapidly for the peak period, moderately for the standard period and, furthermore, significantly less for the off-peak period.

The optimal hybrid system switching occurs exclusively during the morning off-peak period and the curve remains constant for the rest of the control horizon. The demand during the summer season, is much lower and, therefore, requires less energy, as compared

to the winter case. The difference in cumulative energy cost at the end of the control horizon, shows that the baseline energy cost is higher, by a factor of 5.11.

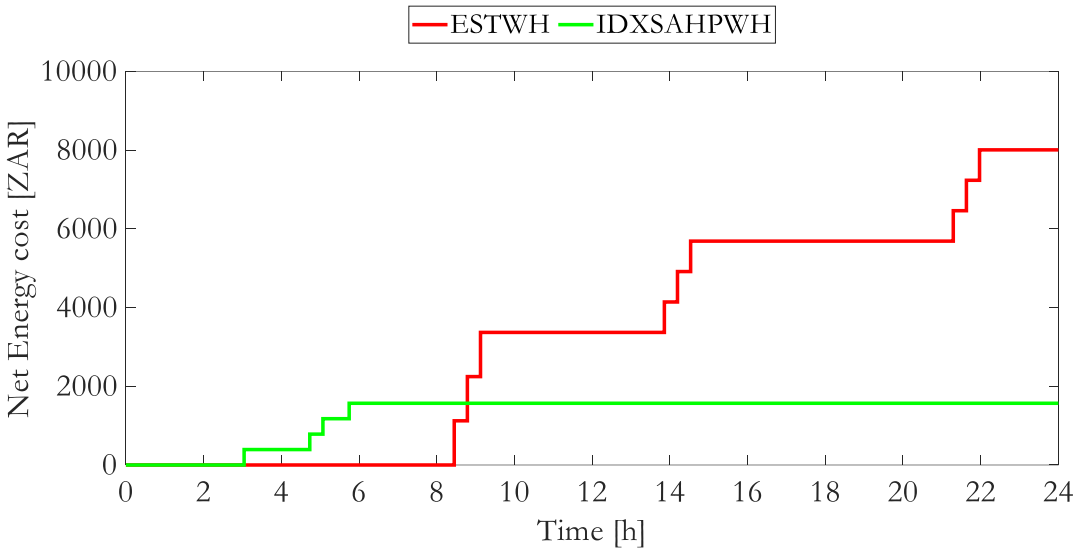


Figure 5.2: Summer cumulative cost.

5.3.1.3 Annual energy consumption and savings

The average daily energy and cost usage of the baseline and hybrid water heating systems, for a typical summer and winter day, are calculated. The difference between each is subsequently calculated, to obtain the daily savings for each month and is presented in Table 5.2.

Table 5.2: Daily energy consumption and savings.

| Season | Baseline (ESTWH) | | Optimally controlled (IDX-SAHP) | | Daily Savings | |
|---|---|---|---|---|---|---|
| | Energy (kWh) | Cost (ZAR) | Energy (kWh) | Cost (ZAR) | Energy (kWh) | Cost (ZAR) |
| Winter | 88.1 | 979.06 | 24.0 | 235.10 | 64.1 | 743.96 |
| Summer | 72.0 | 333.55 | 9.6 | 81.50 | 62.4 | 252.05 |

To obtain the annual energy and cost usage, as well as the savings, the daily energy and cost consumption are multiplied by the number of days for each season (winter: 92 and summer: 273); the annual savings obtained, are presented in Table 5.3.

Table 5.3: Seasonal energy consumption and savings.

| | Baseline (ESTWH) | | Optimally controlled (IDX-SAHP) | | Annual Savings | Annual Savings (%) | |
|---|---|---|---|---|---|---|---|
| Season | Energy (kWh) | Cost (ZAR) | Energy (kWh) | Cost (ZAR) | Cost (ZAR) | Energy | Cost |
| Winter | 8 103.4 | 90 073.27 | 2 205.8 | 21 629.02 | 68 444.26 | 72.8 | 76.0 |
| Summer | 19 656.0 | 91 059.15 | 2 614.2 | 22 250.16 | 68 808.99 | 86.7 | 75.6 |
| Total | 27 759.4 | 181 132.42 | 4 820.04 | 43 879.17 | 137 253.25 | 82.6 | 75.8 |

The optimal hybrid system shows a significant savings in energy consumption, as well as in costs. This is since the optimal system operates at the notably low-cost pricing of the TOU tariff structure, as compared to the baseline and, therefore, a high amount of costs may be shaved off, resulting in the consumer gaining a large cost return. The optimal hybrid water heating system shows possible cost savings of approximately 68 444.26 ZAR (4 675.03 USD) for the winter case and 68 808.99 ZAR (4 699.94 USD) for the summer season, which is approximately 76.0% and 75.6%, respectively, as compared to the baseline. For the entire year, the system shows a possible cost savings of approximately 137 253.25 ZAR (9 374.97 USD), amounting to 75.8 %, compared to the baseline. The results of this comparison highlight the importance of avoiding the use of electricity during high demand periods.

## 5.4 LIFE CYCLE COST ANALYSIS

A project lifetime of 20 years was determined for the proposed water heating system, to reduce the margin of error. The lifetime was chosen, based on the manufacturers' specifications of the collector's lifespan being more than 20 years and that of the storage

tank heat pump unit, being more than 15 years. This means that, there is a possibility that the whole system may not require replacement until the end of the project lifetime. As a result, the average number of years between the guaranteed and reported lifespans was selected. In addition, u sing the average inflation rate, the future cost of the components may be predicted, presented in Figure 5.3 (adapted from [129]), by assuming the average inflation rate equals the interest rate [15]:

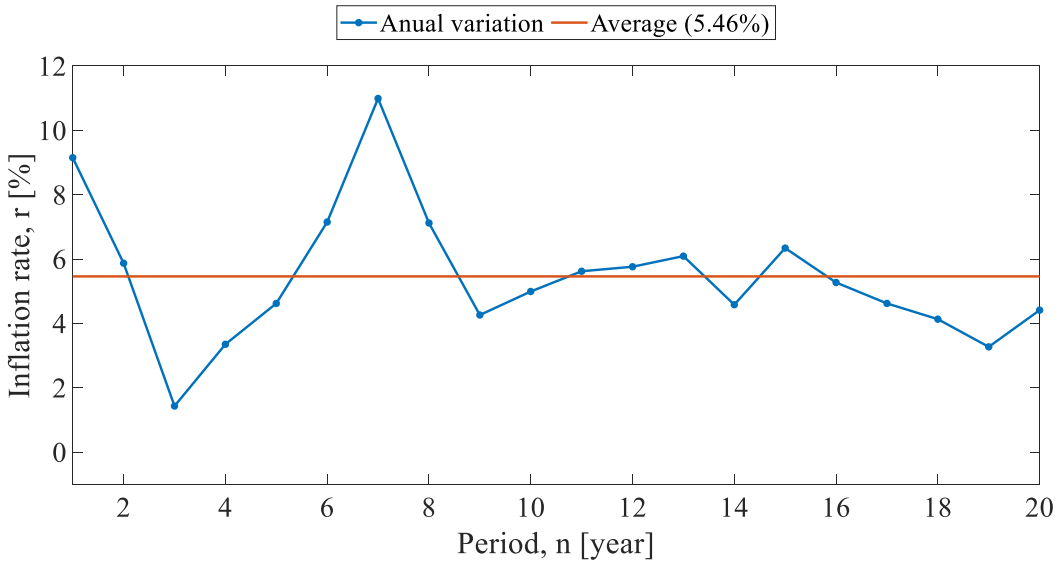


Figure 5.3: Inflation rate of South Africa (from 2000 to 2021)

The cumulative replacement costs ($C_{rep}$) of the system components at the end of the project lifetime, may be calculated, using Eq. (5.3) [15].

$$C_{rep} = t_s \sum_{k=1}^{N_{rep}} C_{cap} \cdot k(1+n \cdot r) \tag{5.3}$$

Where:

$C_{cap}$ is the initial capital cost for each component;

$N_{rep}$ is the number of component replacements of the project lifetime;

$n$ is the lifespan for a specific component (years);

$r$ is the historic average inflation rate shown as 5.46% in Figure 5.3;

$k$ represents each year in the project lifetime.

### 5.4.1 Baseline (ESTWH) life cycle cost analysis

The ESTWH consists of the storage tank and the electric resistive elements. These two components form a unit and are replaced at the simultaneously, and the amount of the two components make up the total cost of the ESTWH, for the baseline case. The total lifecycle replacement costs ($C_{repBTC}$) are, therefore, equal to the replacement costs of the ESTWH ($C_{repESTWH}$), throughout the 20 year lifespan of the baseline [130], as shown in Eq. (5.4).

$$C_{repBTC} = C_{repESTWH} \tag{5.4}$$

The cumulative replacement cost of the ESTWH ($C_{repESTWH}$), obtained over a 20-year project lifetime, was calculated using Eq. (5.3) and presented in Table 5.4.

Table 5.4: Total replacement cost for the ESTWH.

| Parameters | Value |
|---|---|
| Baseline system study lifetime. n (years) | 20 |
| 2000L Hot Water Storage Tank lifetime (years) | 15 |
| $N_{rep2000L}$ (-) | 1 |
| $N_{rep2000L}$ (ZAR) | 176 070.11 |
| 6kW Electric Screw Element lifetime (years) | 15 |
| $N_{repEL}$ (-) | 1 |
| $N_{rep2000L}$ (ZAR) | 21 064.02 |
| $C_{repETSWH}$ | 197 134.13 |
| $C_{repBTC}$ | 197 134.13 |

The cumulative electricity costs incurred over a 20-year lifespan for the baseline system, is shown in Appendix B. The cumulative cost of energy for the first year, was taken from Table 5.3 and the cost at the end of year 20, equates to the total cumulative electricity cost, with an increase of 10% annually considered, shown in Eq.(5.5).

$$C_{EC} = \sum_{K=1}^{20} c_{initial=EC} \cdot k(1+a) \tag{5.5}$$

Where:

$C_{initial-EC}$ is the cumulative cost of energy at the end of year one (ZAR);

$k$ represents the year at which the cumulative cost should be calculated (years);

$\alpha$ is the annual increase of 10%.

The operation and maintenance costs at the end of year one of the system, may be taken as 1% of the initial implementation cost. The total operation and maintenance cost, throughout the project lifetime, may be obtained, using Eq. (5.6) [15]:

$$C_{OM} = t_s \sum_{k=1}^{N} C_{OM-initial} \cdot k(1+n \cdot r) \tag{5.6}$$

Where:

$C_{OM-initial}$ is the operation and maintenance cost for the first year.

The salvage costs ($C_{salvage}$), were taken as 20% of the initial cost of implementation ($C_{ini-imp}$) for both the baseline and hybrid water heating system, as shown in Eq. (5.7). This accounts for replacement upgrades, to more efficient systems in the future [15]:

$$C_{salvage} = 0.2 \cdot C_{ini-imp} \tag{5.7}$$

The total life cycle costs (LCC) of the baseline system are obtained, by adding the cumulative costs, described in Eqs. (5.3) - (5.7), as shown in Eq. (5.8).

$$LCC_{ESTWH} = C_{initial} + C_{rep-BTC} + C_{EC} + C_{OM} - C_{salvage} \tag{5.8}$$

The total LCC of the ESTWH ($LCC_{ESTWH}$), that will be incurred during the project lifespan, as presented in Table 5.5, shows the estimated total $LCC_{ESTWH}$ amount of approximately 10 695 941.76 ZAR (730 577.21 USD).

Table 5.5: Total life cycle cost for the ESTWH.

| Cumulative Costs | Value (ZAR) |
|---|---|
| $C_{initial}$ | 108 375.00 |
| $C_{repBTC}$ | 197 134.13 |
| $C_{OM}$ | 37 748.28 |
| $C_{EC}$ | 10 374 359.36 |
| $C_{salvage}$ | 21 675.00 |
| $LCC_{ESTWH}$ | 10 695 941.76 |

### 5.4.2 Hybrid system with optimal scheduling life cycle cost analysis

For the hybrid water heating system, further components were added to the ESTWH system with various lifespans, as presented in Table 5.1. The replacement cost ($C_{rep}$), for each component, was calculated using Eq. (5.3) for a 20-year lifespan of the project, as presented in Table 5.6.

The calculated replacement costs for all the components, were summed up to obtain the total replacement cost ($C_{repTC}$), as shown in Eq. (5.9), for the hybrid water heating system.

$$C_{rep-TC} = C_{rep-ETC} + C_{rep-HP} + C_{rep-ESTWH} + C_{rep-CONT} + C_{rep-PMP} + C_{rep-VLV} \quad (5.9)$$

The same method of calculating the costs to be incurred during the project lifespan, was conducted for the IDX-SAHP, for a 20-year project lifetime. The total LCC of the IDX-SAHP system ($LCC_{IDX-SAHP}$), was obtained by summing up all the cumulative costs, as shown in Eq. (5.10). The total $LCC_{IDX-SAHP}$ amount of approximately 3 052 012.60 ZAR (208 465.13 USD), as presented in Table 5.7, will be spent, with an optimal energy management scheme implemented to the IDX-SAHP.

$$LCC_{IDX-SAHP} = C_{initial} + C_{rep-TC} + C_{OM} + C_{EC} - C_{salvage} \quad (5.10)$$

Table 5.6: Total replacement cost for the IDX-SAHP.

| Parameters | Value |
|---|---|
| Hybrid system lifetime. n (years) | 20 |
| 20 Tube ETC solar collectors | 25 |
| $N_{repETC}$ (-) | 0 |
| $C_{repETC}$ (ZAR) | 0 |
| 22kW Commercial Heat Pump | 15 |
| $N_{repHP}$ (-) | 1 |
| $C_{repHP}$ (ZAR) | 83 664.91 |
| 2000L Hot Water Storage Tank lifetime (years) | 15 |
| $N_{rep2000L}$ (-) | 1 |
| $C_{rep2000L}$ (ZAR) | 176 070.11 |
| 6kW Electric Screw Element lifetime (years) | 15 |
| $N_{repEL}$ (-) | 1 |
| $C_{repEL}$ (ZAR) | 10 532.01 |
| Geyser Temperature Controller 3000 W lifetime (years) | 15 |
| $N_{repCONT}$ (-) | 1 |
| $C_{repCONT}$ (ZAR) | 2 173.71 |
| Fluid Pump lifetime (years) | 8 |
| $N_{repPMP}$ (-) | 2 |
| $C_{repMPM}$ (ZAR) | 18 869.19 |
| 110℃ Air Release Valve lifetime (years) | 20 |
| $N_{repVLV}$ (-) | 0 |
| $C_{repVLV}$ (ZAR) | 0 |
| $C_{repTC}$ (ZAR) | 291 309.91 |

Table 5.7: Total life cycle cost for the IDX-SAHP with optimal scheduling.

| Cumulative Costs | Value (ZAR) |
|---|---|
| $C_{initial}$ | 215 554.00 |
| $C_{repTC}$ | 281 875.32 |
| $C_{OM}$ | 74 190.04 |
| $C_{EC}$ | 2 513 179.51 |
| $C_{salvage}$ | 42 599.80 |
| $LCC_{DX-SAHP}$ | 3 052 012.60 |

### 5.4.3 Break-even point (BEP)

The break-even point is the point in time at which the implementation and operational costs of two systems are equal. The cumulative cost curves for the two systems, which comprise of the initial investment cost and total annual costs incurred over a project lifetime of 20 years on the same axis, are shown in Figure 5.4. The intersection points of these two curves, shows the point in time (years) at which the two systems break even over this period.

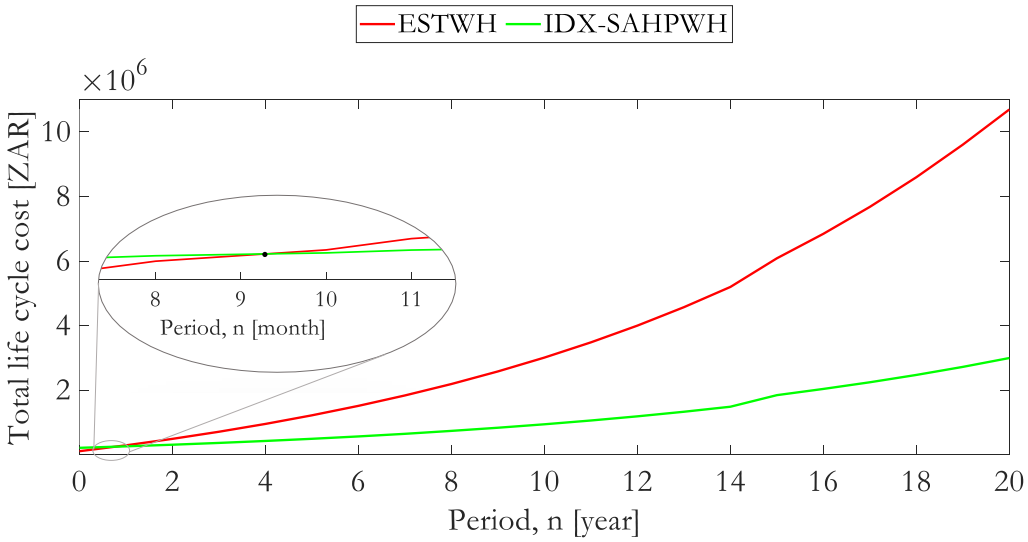


Figure 5.4: Break-even point.

From Table 5.5 and Table 5.7, the initial total cost of implementation of the hybrid water heating system, as well as the standalone ESTWH, are 212 999.00 ZAR (14 548.72 USD) and 108 375.00 ZAR (7 402.46 USD), respectively. These costs are at the starting points of the two curves. After the first year has passed, the total annual cost of energy is added to the initial investment cost, which is the total present cost of energy, shown in Table 5.3. This equates to the total cumulative cost for the first year after implementation. For the second year, a 10% increase in the price of electricity is considered to calculate the annual energy costs. This amount is once again added to the previous total cumulative cost of the first year. The above-mentioned method is followed every year, through to the end of the project's lifetime.

For this curve, the replacement costs, and lifetimes of all the components, are considered, for increased accuracy in cumulative cost representation. When calculating the replacement cost of each component, the average inflation of the last 20 years, was considered. The costs are, therefore, summed up, to make up the total replacement cost of the whole system for the baseline and for the hybrid water heating system. From Figure 5.4, a possible affirmation clearly shows that the break-even point occurs notably earlier in the project lifetime.

The break-even point of this project occurs during the 9$^{th}$ month of the first year, at a cost of 246 271.50 ZAR (16 821.37 USD). The variances in total money spent at the end of the project lifetime also serve as a vital economic performance measure and are discussed in Section 5.4.4.

### 5.4.4 Life cycle cost comparison

The break-even point analysis provides the estimate of the cumulative cost that the baseline ESTWH system and the hybrid water heating system, with an optimal energy management control scheme, equalize at the point in time (year) during the project lifetime. The life cycle cost (LCC) assesses the cost savings to be obtained at the end of the project lifetime when the former system is replaced with the later. After following the method explained in the Section 5.4.3, for the two systems from beginning to the end of the project, the LCC costs of each system were calculated and shown, in Tables 5.5 and 5.7, under Sections 5.4.1 and 5.4.2.

The LCC costs of the two systems are, therefore, compared in Table 5.8 and it could be concluded that, there may be an approximate saving of 7 643 929.16 ZAR (522 112.08 USD), at the end of the project lifetime, when the optimal energy management system is implemented, making a possible saving of up to 71.5 %.

Table 5.8: Life cycle cost comparison.

| LCC | Value (ZAR) |
|---|---|
| $LCC_{ESTWH}$ | 10 695 941.76 |
| $LCC_{DX-SAHP}$ | 3 052 012.60 |
| Total savings over 20 years (ZAR) | 7 643 929.16 |

The detailed life cycle cost breakdown, is shown in Appendix C, illustrating the cumulative costs after each year.

## 5.5 SUMMARY

The techno-economic analysis of the optimally controlled proposed system and the baseline systems, for a project lifespan of 20 years, is provided, as well as analysed in this Chapter. With all cost aspects considered, the optimally controlled proposed system was shown to be the most cost-effective. For the winter and summer seasons, the daily energy cost for the proposed system and the baseline system, were provided and compared. For the winter and summer cases, the proposed system saved approximately 68 444.26 ZAR (4 675.03 USD) and 68 808.99 ZAR (4 699.94 USD), respectively. Furthermore, the annual cost reductions are approximately 137 253.25 ZAR (9 374.97 USD). The results show that the costs for the winter season are significantly high, particularly in the baseline case. Since it operates solely during the off-peak time, when electricity costs are minimal, the proposed system may save costs in both seasons. As a result, the system may save costs by up to 76.0 %, 75.6 % and 75.8 % for the winter season, summer season and the entire year, respectively.

The life cycle costs of the two systems, were further evaluated for the duration of the project's 20-year lifetime. The optimally controlled proposed system, had an initial cost of 291 309.91 ZAR (1998.68 USD), at the start of the project, which was higher than the baseline system's initial cost of 197 134.13 ZAR (135 465.08 USD). The proposed system has shown to be considerably efficient for use in the commercial sector, as it ensures high-cost savings, with a short payback period. The proposed system has life cycle costs of approximately 3 052 012.60 ZAR (208 465.13 USD), at the end of the project's lifetime, compared to a baseline of approximately 10 695 941.76 ZAR (730 577.21 USD). This amounts to a possible 71.5 % savings. Finally, at a cost of 246 271.50 ZAR, this project will break even during the ninth month of the first year (16 821.37 USD).

# CHAPTER 6: CONCLUSION

## 6.1 FINAL CONCLUSIONS

South African Universities, akin to any other organisations in the commercial sector, are faced with increasing costs of electricity charges, due to the inefficient and energy intensive devices used. A great deal of hot water production for sanitation purposes in the student residences, using the inefficient, energy intensive electric resistive water heating systems, is one of the contributors to the high costs incurred by the institutions. In addition to that, the hot water demand occurs mostly during the peak demand, incurring significant pressure in the electricity supply grid.

A wide range of research on the energy management of water heating systems, has been performed in South Africa. Several studies have been presented, all of which are based on a variety of system performance, control-energy management approaches and the demand-side management methodology of load shifting via scheduling. According to the research, energy management strategies resulted in significant cost and energy savings, as well as system optimization. Furthermore, energy management technologies have been found to shorten the payback period of systems, resulting in higher cost savings for the user.

However, limited studies have been carried out on the SAHP system, in which the solar thermal system provides energy to the heat pump, which subsequently heats the water indirectly. In addition, relatively few experiments using ETCs were conducted for the SAHP, as most systems in South Africa were studied with PV panels. Another factor is that most of the study is focused on the residential sector, mostly single-family homes, with merely a few studies focusing on the commercial sector, such as student residences.

The aim of this project was to develop a proposed IDX-SAHP water heating system with an optimal energy control scheme for the commercial sector, such as student residences, to ensure maximum energy savings, while maintaining the consumer's comfortable thermal level. A mathematical model of the IDX-SAHP water heating system and an optimal energy management scheme, to minimize the electricity cost based on the TOU tariff, while maximizing the thermal comfort of the hot water users, was developed. The proposed optimal energy management model, considered computational variables,

taken at 20-minute intervals, in the case study. The optimal control models were built to solve decision variables of the proposed system, using the Solving Constraint Integer Programs (SCIP) solver, in the MATLAB interface optimization toolbox.

The simulation results of the proposed hybrid water heating system with the optimal energy control scheme show that the system selects the most affordable TOU tariff pricing period, to generate hot water and save electricity. The system ensures that the water in the storage tank is heated to the highest possible temperature, that will be able to maintain the thermal level of the consumers during the standard and peak periods of the TOU tariff. The winter case heats up to above 75 °C, while the summer case heats up to 65 °C, as there is more demand during the winter season, as compared to the summer season. Compared to the baseline ESTWH, the proposed system operates optimally, as it avoids the peak and standard periods of the TOU tariffs, which guarantees savings in energy and costs.

From the economic analysis, the IDX-SAHP water heating system shows significant savings in energy and costs, particularly during the winter season; because the optimally controlled IDX-SAHP water heating system solely operates during the off-peak period of the TOU tariff, while the baseline ESTWH mostly operates during the peak and standard periods of the TOU pricing. The cost savings acquired by the proposed system for the winter and summer seasons, as well as annually, are 76.0 %, 75.6 % and 75.8 %, respectively, as compared to the baseline. The results further indicate that there is a possible life cycle cost saving of approximately 71.5 %. Finally, this project will break even during the ninth month of the first year, at a cost of 246 271.50 ZAR (16 821.37 USD).

The IDX-SAHP water system, when operated with the developed optimal energy control scheme, shows a significant savings in costs, while maintaining the comfort level of the consumers. Furthermore, with the significant savings in energy, the system may contribute to the load reduction during peak energy usage periods on the electricity grid supply. As a result, this system may further be used in alternative commercial enterprises, that have a high demand for sanitary water heating, such as hotels.

## 6.2 SUGGESTIONS FOR FURTHER RESEARCH

This dissertation is part of the ongoing studies of the solar assisted heat pump water heating systems, in the commercial sector. With the university student residence being used as a case study, under the weather conditions of Bloemfontein, further studies may be conducted on the following aspects:

- For other commercial enterprises that do a great deal of water heating and, furthermore, for other sectors, such as residential.
- Further research on the components of the liquid-source heat pump (i.e. evaporator heat exchanger) developed and tested under the weather conditions of South Africa, or Africa, with different input variables.
- This system should, additionally, be developed and tested with other forms of solar collectors, as well as different system configurations.

## REFERENCES

[1] S. Guo, Q. Liu, J. Sun, and H. Jin, "A review on the utilization of hybrid renewable energy," *Renew. Sustain. Energy Rev.*, vol. 91, pp. 1121–1147, 2018, doi: 10.1016/j.rser.2018.04.105.

[2] K. J. Lomas *et al.*, "Do domestic heating controls save energy? A review of the evidence," *Renew. Sustain. Energy Rev.*, vol. 93, pp. 52–75, 2018, doi: 10.1016/j.rser.2018.05.002.

[3] E. M. Wanjiru, S. M. Sichilalu, and X. Xia, "Optimal control of heat pump water heater-instantaneous shower using integrated renewable-grid energy systems," *Appl. Energy*, vol. 201, pp. 332–342, 2017, doi: 10.1016/j.apenergy.2016.10.041.

[4] X. Zhao, E. Long, Y. Zhang, Q. Liu, Z. Jin, and F. Liang, "Experimental Study on Heating Performance of Air - Source Heat Pump with Water Tank for Thermal Energy Storage," *Procedia Eng.*, vol. 205, pp. 2055–2062, 2017, doi: 10.1016/j.proeng.2017.10.087.

[5] K. Chang, W. Lin, and G. Ross, "Dissemination of solar water heaters in South Africa," vol. 22, no. 3, pp. 2–7, 2011, doi: http://dx.doi.org/10.17159/2413-3051/2011/v22i3a3216.

[6] J. Krupa and S. Burch, "A new energy future for South Africa: The political ecology of South African renewable energy," *Energy Policy*, vol. 39, no. 10, pp. 6254–6261, 2011, doi: 10.1016/j.enpol.2011.07.024.

[7] P. A. Hohne, K. Kusakana, and B. P. Numbi, "A review of water heating technologies: An application to the South African context," *Energy Reports*, vol. 5, pp. 1–19, 2019, doi: 10.1016/j.egyr.2018.10.013.

[8] S. Tangwe, N. Mzolo, M. Simon, and E. Meyer, "Modeling the demand of a calorifier to establish the baseline before retrofitting it with a commercial air source heat pump," in *2014 International Conference on the Eleventh Industrial and Commercial Use of Energy*, 2014, pp. 1–8.

[9] A. P. Rogers and B. P. Rasmussen, "Opportunities for consumer-driven load shifting in commercial and industrial buildings," *Sustain. Energy, Grids Networks*, vol. 16, pp. 243–258, 2018, doi: 10.1016/j.segan.2018.08.004.

[10] N. Maistry and M. Mckay, "Promoting energy efficiency in a South African University," *J. Energy South. Africa*, vol. 27, no. 3, pp. 1–10, 2006.

[11] M. Michael, S. B. K. Ntsaluba, and L. Zhang, "A Comparative Study on Electrical Energy Usage of University Residences in South Africa ( 2017 )," in *2019 International Conference on the 27th Domestic Use of Energy (DUE)*, 2019, no. 27, pp. 201–205.

[12] O. M. Popoola and C. Burnier, "Solar water heater contribution to energy savings in higher education institutions: Impact analysis," *J. Energy South. Africa*, vol. 25, no. 1, pp. 51–58, 2014.

[13] T. Kim, B. Choi, Y. Han, and K. Hyung, "A comparative investigation of solar-assisted heat pumps with solar thermal collectors for a hot water supply system," *Energy Convers. Manag.*, vol. 172, pp. 472–484, 2018, doi: 10.1016/j.enconman.2018.07.035.

[14] R. Rankin and P. G. Rousseau, "Sanitary hot water consumption patterns in commercial and industrial sectors in South Africa: Impact on heating system design," *Energy Convers. Manag.*, vol. 47, no. 6, pp. 687–701, 2006, doi: 10.1016/j.enconman.2005.06.002.

[15] P. A. Hohne, K. Kusakana, and B. P. Numbi, "Optimal energy management and economic analysis of a grid-connected hybrid solar water heating system: A case of Bloemfontein, South Africa," *Sustain. Energy Technol. Assessments*, vol. 31, pp. 273–291, 2019, doi: 10.1016/j.seta.2018.12.027.

[16] S. Tangwe, N. Mzolo, M. Simon, and E. Meyer, "Qualitative and quantitative methods for the prediction of sanitary hot water consumption of a Calorifier and the justification of proposal of an air source heat pump unit as a retrofit: A case study, University of Fort Hare residence," in *Proceedings of the Conference on the Industrial and Commercial Use of Energy, ICUE*, 2016, pp. 170–177.

[17] W. Stone, T. M. Louw, G. K. Gakingo, M. J. Nieuwoudt, and M. J. Booysen, "A potential source of undiagnosed Legionellosis: Legionella growth in domestic water heating systems in South Africa," *Energy Sustain. Dev.*, vol. 48, pp. 130–138, 2019, doi: 10.1016/j.esd.2018.12.001.

[18] M. Lei, H. Zhang, F. Wang, and X. You, "Experimental study of an instantaneous-

heating air source heat pump water heater with a temperature stratified water tank," *Adv. Mech. Eng.*, vol. 8, no. 9, pp. 1–9, 2016, doi: 10.1177/1687814016671248.

[19] M. S. Buker and S. B. Riffat, "Build-up and performance test of a novel solar thermal roof for heat pump operation," *Int. J. Ambient Energy*, vol. 38, no. 4, pp. 365–379, 2017, doi: 10.1080/01430750.2015.1121920.

[20] I. Dincer, "Renewable energy and sustainable development: A crucial review," *Renew. Sustain. energy Rev.*, vol. 4, no. 2, pp. 157–175, 2000, doi: 10.1016/S1364-0321(99)00011-8.

[21] J. Yongoua, S. Tangwe, and M. Simon, "A review on the performance assessment and optimization techniques of air source heat pump water heaters used in South Africa," in *Proceedings of the 24th Conference on the Domestic Use of Energy, DUE 2016*, 2016, no. April 2018, doi: 10.1109/DUE.2016.7466725.

[22] X. Jin, N. Renewable, J. Maguire, N. Renewable, D. Christensen, and N. Renewable, "Model Predictive Control of Heat Pump Water Heaters for Energy Efficiency," in *2014 ACEEE Summer Study on Energy Efficiency in Buildings*, 2014, no. October, pp. 133–145, doi: 10.13140/2.1.1295.6167.

[23] O. Ibrahim, F. Fardoun, R. Younes, and H. Louahlia-Gualous, "Air source heat pump water heater: Dynamic modeling, optimal energy management and mini-tubes condensers," *Energy*, vol. 64, pp. 1102–1116, 2014, doi: 10.1016/j.energy.2013.11.017.

[24] A. Jamar, Z. A. A. Majid, W. H. Azmi, M. Norhafana, and A. A. Razak, "A review of water heating system for solar energy applications," *Int. Commun. Heat Mass Transf.*, vol. 76, pp. 178–187, 2016, doi: 10.1016/j.icheatmasstransfer.2016.05.028.

[25] Z. Wang, F. Wang, X. Wang, Z. Ma, X. Wu, and M. Song, "Dynamic character investigation and optimization of a novel air-source heat pump system," *Appl. Therm. Eng.*, vol. 111, pp. 122–133, 2017, doi: 10.1016/j.applthermaleng.2016.09.076.

[26] G. Nouri, Y. Noorollahi, and H. Yousefi, "Designing and optimization of solar assisted ground source heat pump system to supply heating, cooling and hot water demands," *Geothermics*, vol. 82, pp. 212–231, 2019, doi: 10.1016/j.geothermics.2019.06.011.

[27] M. Zhang and Z. Huan, "Study on performance on heat pump water heaters in

South Africa," in *21st Conference on the Domestic Use of Energy, DUE 2013*, 2013, pp. 1–6.

[28] S. Sichilalu, T. Mathaba, and X. Xia, "Optimal control of a wind–PV-hybrid powered heat pump water heater," *Appl. Energy*, vol. 185, pp. 1173–1184, 2017, doi: 10.1016/j.apenergy.2015.10.072.

[29] F. Behrooz, N. Mariun, M. H. Marhaban, M. A. M. Radzi, and A. R. Ramli, "Review of Control Techniques for HVAC Systems — Nonlinearity Approaches Based on Fuzzy," *Energies*, vol. 11, no. 495, pp. 1–41, 2018, doi: 10.3390/en11030495.

[30] S. M. Sichilalu, "Optimal Control of Renewable Energy/Grid Hybrid Systems With Heat Pump Load," University of Pretoria, 2016.

[31] J Terry Cousins and TLC Engineering Solutions, "Using Time of Use (Tou) tariffs in Industrial , Commercial and Residential applications effectively.," 2009.

[32] L. Yang, C. Dong, C. L. J. Wan, and C. T. Ng, "Electricity time-of-use tariff with consumer behavior consideration," *Int. J. Prod. Econ.*, vol. 146, no. 2, pp. 402–410, 2013, doi: 10.1016/j.ijpe.2013.03.006.

[33] A. K. Aliyu, B. Modu, and C. W. Tan, "A review of renewable energy development in Africa: A focus in South Africa, Egypt and Nigeria," *Renew. Sustain. Energy Rev.*, vol. 81, pp. 2502–2518, 2018, doi: 10.1016/j.rser.2017.06.055.

[34] D. Mariano-Hernández, L. Hernández-Callejo, A. Zorita-Lamadrid, O. Duque-Pérez, and F. Santos García, "A review of strategies for building energy management system: Model predictive control, demand side management, optimization, and fault detect & diagnosis," *J. Build. Eng.*, vol. 33, pp. 1–12, 2021, doi: 10.1016/j.jobe.2020.101692.

[35] F. Pallonetto, S. Oxizidis, F. Milano, and D. Finn, "The effect of time-of-use tariffs on the demand response flexibility of an all-electric smart-grid-ready dwelling," *Energy Build.*, vol. 128, pp. 56–67, 2016, doi: 10.1016/j.enbuild.2016.06.041.

[36] A. Arteconi, N. J. Hewitt, and F. Polonara, "Domestic demand-side management (DSM): Role of heat pumps and thermal energy storage (TES) systems," *Appl. Therm. Eng.*, vol. 51, pp. 155–165, 2013, doi: 10.1016/j.applthermaleng.2012.09.023.

[37] J. Hong, C. Johnstone, J. Torriti, and M. Leach, "Discrete demand side control performance under dynamic building simulation : A heat pump application," *Renew. Energy*,

vol. 39, no. 1, pp. 85–95, 2012, doi: 10.1016/j.renene.2011.07.042.

[38] F. E. Lephuthing, "Intervention mechanisms to reduce energy consumption of air-conditioning and illumination systems for commercial buildings," Cape Peninsula University of Technology, 2013.

[39] B. Alimohammadisagvand, J. Jokisalo, and K. Sirén, "Comparison of four rule-based demand response control algorithms in an electrically and heat pump-heated residential building," *Appl. Energy*, vol. 209, pp. 167–179, 2018, doi: 10.1016/j.apenergy.2017.10.088.

[40] A. R. Jordehi, "Optimisation of demand response in electric power systems, a review," *Renew. Sustain. Energy Rev.*, vol. 103, pp. 308–319, 2019, doi: 10.1016/j.rser.2018.12.054.

[41] J. Thakur and B. Chakraborty, "Demand side management in developing nations: A mitigating tool for energy imbalance and peak load management," *Energy*, vol. 114, pp. 895–912, 2016, doi: 10.1016/j.energy.2016.08.030.

[42] X. Yuan, Z. Chen, Y. Liang, Y. Pan, J. Jokisalo, and R. Kosonen, "Heating energy-saving potentials in HVAC system of swimming halls: A review," *Build. Environ.*, vol. 205, pp. 1–18, 2021, doi: 10.1016/j.buildenv.2021.108189.

[43] J. Peng, H. He, and R. Xiong, "Rule based energy management strategy for a series – parallel plug-in hybrid electric bus optimized by dynamic programming," *Appl. Energy*, vol. 185, pp. 1633–1643, 2017, doi: 10.1016/j.apenergy.2015.12.031.

[44] E. Atam and L. Helsen, "Ground-coupled heat pumps: Part 1 – Literature review and research challenges in modeling and optimal control," *Renew. Sustain. Energy Rev.*, vol. 54, pp. 1653–1667, 2016, doi: 10.1016/j.rser.2015.10.007.

[45] Y. M. Zhao, W. F. Xie, and X. W. Tu, "Performance-based parameter tuning method of model-driven PID control systems," *ISA Trans.*, vol. 51, no. 3, pp. 393–399, 2012, doi: 10.1016/j.isatra.2012.02.005.

[46] S. Andrew Putrayudha, E. C. Kang, E. Evgueniy, Y. Libing, and E. J. Lee, "A study of photovoltaic/thermal (PVT)-ground source heat pump hybrid system by using fuzzy logic control," *Appl. Therm. Eng.*, vol. 89, pp. 578–586, 2015, doi:

10.1016/j.applthermaleng.2015.06.019.

[47] L. Olatomiwa, S. Mekhilef, M. S. Ismail, and M. Moghavvemi, "Energy management strategies in hybrid renewable energy systems: A review," *Renew. Sustain. Energy Rev.*, vol. 62, pp. 821–835, 2016, doi: 10.1016/j.rser.2016.05.040.

[48] D. Burns and C. Laughman, "Extremum Seeking Control for Energy Optimization of Vapor Compression Systems," in *International Refrigeration and Air Conditioning Conference*, 2012, pp. 1–7.

[49] L. Xia, Z. Ma, G. Kokogiannakis, S. Wang, and X. Gong, "A model-based optimal control strategy for ground source heat pump systems with integrated solar photovoltaic thermal collectors," *Appl. Energy*, vol. 228, pp. 1399–1412, 2018, doi: 10.1016/j.apenergy.2018.07.026.

[50] T. Q. Péan, J. Salom, and R. Costa-castelló, "Review of control strategies for improving the energy flexibility provided by heat pump systems in buildings," *J. Process Control*, vol. 74, pp. 35–49, 2019, doi: 10.1016/j.jprocont.2018.03.006.

[51] B. Paris, J. Eynard, S. Grieu, T. Talbert, and M. Polit, "Heating control schemes for energy management in buildings," *Energy Build.*, vol. 42, no. 10, pp. 1908–1917, 2010, doi: 10.1016/j.enbuild.2010.05.027.

[52] C. Verhelst, F. Logist, J. Van Impe, and L. Helsen, "Study of the optimal control problem formulation for modulating air-to-water heat pumps connected to a residential floor heating system," *Energy Build.*, vol. 45, pp. 43–53, 2012, doi: 10.1016/j.enbuild.2011.10.015.

[53] M. Zanon, A. Boccia, V. G. S. Palma, S. Parenti, and I. Xausa, "Chapter 3: Direct optimal control and model predictive control," in *Lecture Notes in Mathematics*, vol. 2180, 2017, pp. 263–382.

[54] O. Ibrahim, F. Fardoun, R. Younes, and H. Louahlia-Gualous, "Review of water-heating systems: General selection approach based on energy and environmental aspects," *Build. Environ.*, vol. 72, pp. 259–286, 2014, doi: 10.1016/j.buildenv.2013.09.006.

[55] P. A. Hohne and K. Kusakana, "A survey of domestic water heating technologies," in *Proceedings of the 25th Southern African Universities Power Engineering*, 2017, pp. 1–5.

[56] Global Energy Partners LLC, "Electric Tankless Water Heating: Competitive Assessment," Lafayette, CA, 2005.

[57] A. Hepbasli and Y. Kalinci, "A review of heat pump water heating systems," *Renew. Sustain. Energy Rev.*, vol. 13, no. 6–7, pp. 1211–1229, 2009, doi: 10.1016/j.rser.2008.08.002.

[58] H. D. Fu, G. Pei, J. Ji, H. Long, T. Zhang, and T. T. Chow, "Experimental study of a photovoltaic solar-assisted heat-pump/heat-pipe system," *Appl. Therm. Eng.*, vol. 40, pp. 343–350, 2012, doi: 10.1016/j.applthermaleng.2012.02.036.

[59] P. Mabina and P. Mukoma, "Energy Optimization and Management of Electric Water Heaters using Direct Load Control," in *The Southern African Energy Efficiency Confederation Conference (2019SAEEC)*, 2019, pp. 1–5.

[60] G. Shen, Z. E. Lee, A. Amadeh, and K. M. Zhang, "A data-driven electric water heater scheduling and control system," *Energy Build.*, vol. 242, pp. 1–13, 2021, doi: 10.1016/j.enbuild.2021.110924.

[61] M. Khosa, S. P. D. Chowdhury, L. Ngoma, and R. Roux, "Household energy management by efficient use of smart geyser," *2020 6th IEEE Int. Energy Conf.*, vol. 6, pp. 226–230, 2020, doi: 10.1109/ENERGYCon48941.2020.9236451.

[62] M. J. Booysen, J. A. A. Engelbrecht, M. J. Ritchie, M. Apperley, and A. H. Cloete, "How much energy can optimal control of domestic water heating save?," *Energy Sustain. Dev.*, vol. 51, pp. 73–85, 2019, doi: 10.1016/j.esd.2019.05.004.

[63] M. J. Ritchie, J. A. A. Engelbrecht, and M. J. Booysen, "Impact of node count on energy-optimal control of stratified vertical water heaters in smart grid applications," 2021, doi: https://doi.org/10.31224/osf.io/gbvc9.

[64] M. Roux and M. J. Booysen, "Use of smart grid technology to compare regions and days of the week in household water heating," in *2017 International Conference on the Domestic Use of Energy (DUE)*, 2017, pp. 1–8, doi: 10.23919/DUE.2017.7931855.

[65] S. Tangwe, M. Simon, and E. Meyer, "Mathematical modeling and simulation application to visualize the performance of retrofit heat pump water heater under first hour heating rating," *Renew. Energy*, vol. 72, pp. 203–211, 2014, doi: 10.1016/j.renene.2014.07.011.

[66] M. S. Buker and S. B. Riffat, "Solar assisted heat pump systems for low temperature water heating applications: A systematic review," *Renew. Sustain. Energy Rev.*, vol. 55, pp. 399–413, 2016, doi: 10.1016/j.rser.2015.10.157.

[67] S. K. Chaturvedi, V. D. Gagrani, and T. M. Abdel-Salam, "Solar-assisted heat pump - A sustainable system for low-temperature water heating applications," *Energy Convers. Manag.*, vol. 77, pp. 550–557, 2014, doi: 10.1016/j.enconman.2013.09.050.

[68] H. Willem, Y. Lin, and A. Lekov, "Review of energy efficiency and system performance of residential heat pump water heaters," *Energy Build.*, vol. 143, pp. 191–201, 2017, doi: 10.1016/j.enbuild.2017.02.023.

[69] L. Zhang, T. Fujinawa, and M. Saikawa, "A new method for preventing air-source heat pump water heaters from frosting," *Int. J. Refrig.*, vol. 35, no. 5, pp. 1327–1334, 2012, doi: 10.1016/j.ijrefrig.2012.04.004.

[70] M. Simon, "Performance optimization of an air source heat pump water heater using mathematical modelling," *96 J. Energy South. Africa*, vol. 26, no. 1, pp. 96–105, 2015.

[71] E. M. Wanjiru, S. M. Sichilalu, and X. Xia, "Model predictive control of heat pump water heater-instantaneous shower powered with integrated renewable-grid energy systems," *Appl. Energy*, vol. 204, pp. 1333–1346, 2017, doi: 10.1016/j.apenergy.2017.05.033.

[72] S. L. Tangwe, M. Simon, and R. Mhundwa, "The performance of split and integrated types air-source heat pump water heaters in South Africa," *J. Energy South. Africa*, vol. 29, no. 2, pp. 12–20, 2018, doi: 10.17159/2413-3051/2018/v29i2a4358.

[73] W. C. Kukard and M. Van Eldik, "The optimized scheduling of a sanitary water heating system for commercial high rise apartment buildings," in *Proceedings of the 24th Conference on the Domestic Use of Energy, DUE 2016*, 2016, pp. 1–9, doi: 10.1109/DUE.2016.7466698.

[74] S. Sadhishkumar and T. Balusamy, "Performance improvement in solar water heating systems - A review," *Renew. Sustain. Energy Rev.*, vol. 37, pp. 191–198, 2014, doi: 10.1016/j.rser.2014.04.072.

[75] P. Olczak, D. Matuszewska, and J. Zabagło, "The comparison of solar energy

gaining effectiveness between flat plate collectors and evacuated tube collectors with heat pipe: Case study," *Energies*, vol. 13, no. 7, 2020, doi: 10.3390/en13071829.

[76] K. Hudon, "Chapter 20: Solar Energy - Water Heating," in *Future Energy: Improved, Sustainable and Clean Options for our Planet*, M. L. Trevor, Ed. Elsevier, 2014, pp. 433–451.

[77] P. A. Hohne, K. Kusakana, and B. P. Numbi, "Operation cost and energy usage minimization of a hybrid solar / electrical water heating system," in *2018 International Conference on the Domestic Use of Energy (DUE)*, 2018, pp. 1–7, doi: 10.23919/DUE.2018.8384387.

[78] E. C. Joubert, S. Hess, and J. L. Van Niekerk, "Large-scale solar water heating in South Africa: Status, barriers and recommendations," *Renew. Energy*, vol. 97, pp. 809–822, 2016, doi: 10.1016/j.renene.2016.06.029.

[79] R. S. Kamel, A. S. Fung, and P. R. H. Dash, "Solar systems and their integration with heat pumps: A review," *Energy Build.*, vol. 87, pp. 395–412, 2015, doi: 10.1016/j.enbuild.2014.11.030.

[80] N. Gowda, B. P. B. Gowda, and R. Chandrashekar, "Investigation of Mathematical Modelling to Assess the Performance of Solar Flat Plate Collector," *Int. J. Renew. Energy Res.*, vol. 4, no. 2, pp. 255–260, 2014.

[81] S. A. Kalogirou, "Chapter 3 - Solar Energy Collectors," in *Solar Energy Engineering*, Second Edi., 2014, pp. 125–220.

[82] R. Shukla, K. Sumathy, P. Erickson, and J. Gong, "Recent advances in the solar water heating systems: A review," *Renew. Sustain. Energy Rev.*, vol. 19, pp. 173–190, 2013, doi: 10.1016/j.rser.2012.10.048.

[83] B. K. Naik, A. Varshney, P. Muthukumar, and C. Somayaji, "Modelling and Performance Analysis of U Type Evacuated Tube Solar Collector Using Different Working Fluids," *Energy Procedia*, vol. 90, pp. 227–237, 2016, doi: 10.1016/j.egypro.2016.11.189.

[84] S. Ahmad and S. Alam, "Design of Solar Evacuated Tube Collector for Low Intensity Thermal Energy," *Int. J. Appl. Eng. Res.*, vol. 13, no. 12, pp. 10310–10315, 2018.

[85] S. Gerber, A. J. Rix, and M. J. Booysen, "Combining grid-tied PV and intelligent water heater control to reduce the energy costs at schools in South Africa," *Energy Sustain.*

*Dev.*, vol. 50, pp. 117–125, 2019, doi: 10.1016/j.esd.2019.03.004.

[86] E. Nshimyumuremyi and W. Junqi, "Thermal efficiency and cost analysis of solar water heater made in Rwanda _ Enhanced Reader.pdf," *Energy Explor. Exploit.*, vol. 3, no. 37, pp. 1147–1161, 2019.

[87] B. Batidzirai, E. H. Lysen, S. Van Egmond, and W. G. J. H. M. Van Sark, "Potential for solar water heating in Zimbabwe," *Renew. Sustain. Energy Rev.*, vol. 13, pp. 567–582, 2009, doi: 10.1016/j.rser.2008.01.001.

[88] M. Jahangiri, E. T. Akinlabi, and S. M. Sichilalu, "Assessment and Modeling of Household-Scale Solar Water Heater Application in Zambia: Technical, Environmental, and Energy Analysis," *Int. J. Photoenergy*, vol. 2021, pp. 1–13, 2021, doi: https://doi.org/10.1155/2021/6630338 Research.

[89] M. Kakaza and K. A. Folly, "Effect of solar water heating system in reducing household energy consumption," *IFAC-PapersOnLine*, vol. 48, no. 30, pp. 468–472, 2015, doi: 10.1016/j.ifacol.2015.12.423.

[90] A. Del Amo, A. Martínez-Gracia, A. A. Bayod-Rújula, and M. Cañada, "Performance analysis and experimental validation of a solar-assisted heat pump fed by photovoltaic-thermal collectors," *Energy*, vol. 169, pp. 1214–1223, 2019, doi: 10.1016/j.energy.2018.12.117.

[91] J. Cai, Z. Li, J. Ji, and F. Zhou, "Performance analysis of a novel air source hybrid solar assisted heat pump," *Renew. Energy*, vol. 139, pp. 1133–1145, 2019, doi: 10.1016/j.renene.2019.02.134.

[92] P. D. Malali, S. K. Chaturvedi, and T. M. Abdel-Salam, "An approximate method for prediction of thermal performance of direct expansion-solar assisted heat pump (DX-SAHP) systems for water heating applications," *Energy Convers. Manag.*, vol. 127, pp. 416–423, 2016, doi: 10.1016/j.enconman.2016.09.017.

[93] G. Wang, Y. Zhao, Z. Quan, and J. Tong, "Application of a multi-function solar-heat pump system in residential buildings," *Appl. Therm. Eng.*, vol. 130, pp. 922–937, 2018, doi: 10.1016/j.applthermaleng.2017.10.046.

[94] L. Croci, L. Molinaroli, and P. Quaglia, "Dual Source Solar Assisted Heat Pump

Model Development, Validation and Comparison to Conventional Systems," *Energy Procedia*, vol. 140, pp. 408–422, 2017, doi: 10.1016/j.egypro.2017.11.153.

[95] Y. H. Kuang and R. Z. Wang, "Performance of a multi-functional direct-expansion solar assisted heat pump system," *Sol. Energy*, vol. 80, no. 7, pp. 795–803, 2006, doi: 10.1016/j.solener.2005.06.003.

[96] X. Q. Kong, D. Zhang, Y. Li, and Q. M. Yang, "Thermal performance analysis of a direct-expansion solar-assisted heat pump water heater," *Energy*, vol. 36, no. 12, pp. 6830–6838, 2011, doi: 10.1016/j.energy.2011.10.013.

[97] K. V. Kumar, L. Paradeshi, M. Srinivas, and S. Jayaraj, "Parametric Studies of a Simple Direct Expansion Solar Assisted Heat Pump Using ANN and GA," *Energy Procedia*, vol. 90, pp. 625–634, 2016, doi: 10.1016/j.egypro.2016.11.231.

[98] M. Mohanraj, Y. Belyayev, S. Jayaraj, and A. Kaltayev, "Research and developments on solar assisted compression heat pump systems – A comprehensive review (Part A: Modeling and modifications)," *Renew. Sustain. Energy Rev.*, vol. 83, pp. 90–123, 2018, doi: 10.1016/j.rser.2017.08.022.

[99] D. Jonas, G. Frey, and D. Theis, "Simulation and performance analysis of combined parallel solar thermal and ground or air source heat pump systems," *Sol. Energy*, vol. 150, pp. 500–511, 2017, doi: 10.1016/j.solener.2017.04.070.

[100] W. Lerch, A. Heinz, and R. Heimrath, "Direct use of solar energy as heat source for a heat pump in comparison to a conventional parallel solar air heat pump system," *Energy Build.*, vol. 100, pp. 34–42, 2015, doi: 10.1016/j.enbuild.2015.03.006.

[101] Y. Wang, Z. Rao, J. Liu, and S. Liao, "An optimized control strategy for integrated solar and air-source heat pump water heating system with cascade storage tanks," *Energy Build.*, vol. 210, pp. 1–14, 2020, doi: 10.1016/j.enbuild.2020.109766.

[102] E. Zanetti, M. Aprile, D. Kum, R. Scoccia, and M. Motta, "Energy saving potentials of a photovoltaic assisted heat pump for hybrid building heating system via optimal control," *J. Build. Eng.*, vol. 27, pp. 1–14, 2020, doi: 10.1016/j.jobe.2019.100854.

[103] S. Sichilalu, X. Xia, and J. Zhang, "Optimal Scheduling Strategy for a Grid-connected Photovoltaic System for Optimal scheduling strategy for a grid-connected

photovoltaic system for heat pump water heaters," *Energy Procedia*, vol. 61, pp. 1511–1514, 2014, doi: 10.1016/j.egypro.2014.12.158.

[104] U. Çakir, K. Çomakli, Ö. Çomakli, and S. Karsli, "An experimental exergetic comparison of four different heat pump systems working at same conditions: As air to air, air to water, water to water and water to air," *Energy*, vol. 58, pp. 210–219, 2013, doi: 10.1016/j.energy.2013.06.014.

[105] X. Guo and A. P. Goumba, "Air source heat pump for domestic hot water supply: Performance comparison between individual and building scale installations," *Energy*, vol. 164, pp. 794–802, 2018, doi: 10.1016/j.energy.2018.09.065.

[106] K. J. Chua, S. K. Chou, and W. M. Yang, "Advances in heat pump systems: A review," *Appl. Energy*, vol. 87, no. 12, pp. 3611–3624, 2010, doi: 10.1016/j.apenergy.2010.06.014.

[107] A. E. Kabeel, A. Khalil, S. S. Elsayed, and A. M. Alatyar, "Modified mathematical model for evaluating the performance of water-in-glass evacuated tube solar collector considering tube shading effect," *Energy*, vol. 89, pp. 24–34, 2015, doi: 10.1016/j.energy.2015.06.072.

[108] O. Ozgener and A. Hepbasli, "Performance analysis of a solar-assisted ground-source heat pump system for greenhouse heating: An experimental study," *Build. Environ.*, vol. 40, no. 8, pp. 1040–1050, 2005, doi: 10.1016/j.buildenv.2004.08.030.

[109] G. Martínez-Rodríguez, A. L. Fuentes-Silva, and M. Picón-Núñez, "Solar thermal networks operating with evacuated-tube collectors," *Energy*, vol. 146, pp. 26–33, 2018, doi: 10.1016/j.energy.2017.04.165.

[110] M. B. Elsheniti, A. Kotb, and O. Elsamni, "Thermal performance of a heat-pipe evacuated-tube solar collector at high inlet temperatures," *Appl. Therm. Eng.*, vol. 154, pp. 315–325, 2019, doi: 10.1016/j.applthermaleng.2019.03.106.

[111] "SAURAN - Southern African Universities Radiometric Network." https://sauran.ac.za/ (accessed Aug. 03, 2021).

[112] D. Chen and H. W. Chen, "Using the Köppen classification to quantify climate variation and change: An example for 1901-2010," *Environ. Dev.*, vol. 6, no. 1, pp. 69–79,

2013, doi: 10.1016/j.envdev.2013.03.007.

[113] C. D. Lynch, "'Mammalian distribution patterns in the Orange Free State : inter-relationship between community types.' Navorsinge van die Nasionale Museum : Researches of the National Museum," Bloemfontein, 1985.

[114] M. C. Makoae, "Investigating the possibility of using groundwater associated with dolerite structures to augment the municipal water supply to the city of Bloemfontein – Investigations in the Central Business District," University of the Free State, 2018.

[115] P. A. Hohne, "Optimal energy management of a hybrid solar water heating system with grid connection under time-based pricing," Central University of Technology, Free State, 2017.

[116] H. J. Vermeulen and S. Fast, "Electrical energy consumption analysis for sanitary water heating in student residences," in *Proceedings of the 24th Conference on the Domestic Use of Energy, DUE 2016*, 2016, pp. 1–6, doi: 10.1109/DUE.2016.7466710.

[117] S. Tangwe and K. Kusakana, "Application of Modelling and Statistical Inferences To Compare Performance of Hot Water Heating Devices in the Residence of University Campus," in *AIUE Proceedings of the 18th Industrial and Commercial Use of Energy Conference 2020*, 2021, pp. 1–6, doi: 10.2139/ssrn.3735366.

[118] A. Morales and G. San Vicente, "Chapter 4 - A new generation of absorber tubes for concentrating solar thermal (CST) systems," in *Advances in Concentrating Solar Thermal Research and Technology*, Elsevier Ltd, 2017, pp. 59–73.

[119] R. A. Coetzee, A. Mwesigye, and Z. Huan, "Optimal slope angle selection of an evacuated tube collector for domestic solar water heating," *J. Energy South. Africa*, vol. 28, no. 1, p. 104, 2017, doi: 10.17159/2413-3051/2017/v28i1a1621.

[120] ITS Heat Pumps and Solar Manufacturer, *ITS - Evacuated Tube Specifications Technical Data - Evacuated Tube Heat Pipe Collectors*. 2021, pp. 1–2.

[121] Jinyi solar is a solar water heater manufacturer, "U Pipe Solar Collectors, U Solar collector - Jinyi Solar," *Jinyi solar is a solar water heater manufacturer*, 2021. https://www.jinyi-solar.com/u-pipe-solar-collector.html (accessed Aug. 23, 2021).

[122] G. L. Morrison, T. Anderson, and M. Behnia, "Seasonal performance rating of heat

pump water heaters," *Sol. Energy*, vol. 76, no. 1–3, pp. 147–152, 2004, doi: 10.1016/j.solener.2003.08.007.

[123] S. Tangwe and K. Kusakana, "Evaluation of the coefficient of performance of an air source heat pump unit and an air to water heat pump," *J. Energy South. Africa*, vol. 32, no. 1, pp. 27–40, 2021.

[124] 4 Seasons Solar and Plumbing Supplies CC, "Vertical hot water vessels for bulk heating of water," *4 Seasons Solar and Plumbing Supplies CC*. http://www.4seasonssolar.co.za/VHWV1.html (accessed Oct. 26, 2021).

[125] K. Kusakana, "Prospective energy cost savings in CUT facilities equipped with wall mounted instant water boilers," in *2018 International Conference on the Domestic Use of Energy, DUE 2018*, 2018, pp. 1–5, doi: 10.23919/DUE.2018.8384396.

[126] South African Bureau of Standards (SABS) Division, "Grid Interconnection of Embedded Part 2 : Small-scale embedded generation Section 3 : Simplified utility connection criteria for low-voltage connected generators," 2014.

[127] "Compare Product Prices South Africa | Online Shopping | PriceCheck." https://www.pricecheck.co.za/ (accessed Nov. 26, 2021).

[128] P. A. Hohne, K. Kusakana, and B. P. Numbi, "Scheduling and economic analysis of hybrid solar water heating system based on timer and optimal control," *J. Energy Storage*, vol. 20, pp. 16–29, 2018, doi: 10.1016/j.est.2018.08.019.

[129] Statista, "South Africa: Inflation rate from 1986 to 2026." https://www.statista.com/statistics/370515/inflation-rate-in-south-africa/ (accessed Nov. 20, 2021).

[130] P. A. Hohne, K. Kusakana, and B. P. Numbi, "Energy and cost analysis of an optimally controlled grid-connected Hybrid Solar Water Heating System in Bloemfontein," no. September, 2018.

# APPENDICES

## APPENDIX A: WALK-THROUGH AUDIT DATA COLLECTION

Table A1: Geysers and boilers specifications and their hours of operation

| Residences | Geysers / boilers | Type | Resistive elements | Water storage tank (in litres) | Hours per day | System control |
|---|---|---|---|---|---|---|
| Loggies | geysers ×5 | standard | 4 kw | 200 | 24 | isolator switch |
| | geyser ×4 | eco 200 | 4 kw | 200 | 24 | isolator switch |
| | boiler | N/A | 9 kw x2 | 2000 | 24 | control box |
| | hydro boil ×2 | standard | 2 kw | 15 | 24 | isolator switch |
| | geyser | eco 50 | 2 kw | 50 | 24 | isolator switch |
| Huis Technikon | bt 102\103 ×14 | eco 200 | 4 kw | 200 | 24 | isolator switch |
| | 100\101\kitchen ×11 | standard | 4 kw | 200 | 24 | N/A |
| | hydro boil | es45 | 2 kw | 15 | 24 | isolator switch |
| | geyser ×3 | eco 150 | 3 kw | 150 | 24 | isolator switch |
| | over sink geyser | standard | 2 kw | 15 | 24 | isolator switch |
| Welgemoet | geyser ×13 | eco 200 | 4 kw | 200 | 24 | isolator switch |
| | geyser | standard | 3 kw | 150 | 24 | isolator switch |
| | geyser ×2 | standard | 2 kw | 100 | 24 | isolator switch |
| | hydro boil ×2 | eco 15 | 2 kw | 15 | 24 | isolator switch |
| Eendrag | geyser ×22 | eco 200 | 4 kw | 200 | 24 | isolator switch |
| | geyser ×3 | standard | 3 kw | 150 | 24 | isolator switch |
| | hydro boil ×3 | standard | 2 kw | 15 | 24 | isolator switch |
| | boiler | standard | 9 kw x2 | 1600 | 24 | control box |

| | | | | | | |
|---|---|---|---|---|---|---|
| Manheim Ladies | geyser ×3 | standard | 4 kw | 200 | 24 | isolator switch |
| | geyser ×4 | eco 200 | 4 kw | 200 | 24 | isolator switch |
| | hydro boil ×3 | standard | 2 kw | 15 | 24 | isolator switch |
| | geyser | standard | 2 kw | 100 | 24 | isolator switch |
| Manheim Men | boiler ×2 | standard | 9 kw x2 | 1600 | 24 | control box |
| | boiler | standard | 18 kw | 2000 | 24 | isolator switch |
| | geyser | eco 200 | 4 kw | 200 | 24 | isolator switch |
| | hydro boil | standard | 2 kw | 15 | 24 | isolator switch |
| | hydro boil | standard | 3 kw | 25 | 24 | isolator switch |
| Gymnos | boiler | standard | 18 kw x2 | 2000 | 24 | control box |
| | hydro boil | standard | 2 kw | 15 | 24 | isolator switch |

Table A2: The maximum estimated energy usage of the residences in an hour based on the survey data.

| Residences | Energy consumption (kwh) |
|---|---|
| Loggies | 60 |
| Huis Technikon | 113 |
| Welgemoet | 63 |
| Eendrag | 103 |
| Manheim Ladies | 54 |
| Manheim Men | 63 |
| Gymnos | 38 |
| **Total** | **494** |

# APPENDIX B: EXOGENOUS DATA (20-MINUTE AVERAGED)

Appendix B1: Winter data

| Time | Global horizontal irradiance [W/m²] | Direct normal irradiance [W/m²] | Diffuse horizontal irradiance [W/m²] | Ambient air temperature [°C] | Inlet water temperature [°C] | Hot water consumption [L] |
|---|---|---|---|---|---|---|
| 0:00 | 0 | 0 | 0 | 0.052 | 12 | 9.94 |
| 0:20 | 0 | 0 | 0 | -0.1 | 12 | 5.28 |
| 0:40 | 0 | 0 | 0 | -0.198 | 12 | 3.42 |
| 1:00 | 0 | 0 | 0 | 0.062 | 12 | 4.98 |
| 1:20 | 0 | 0 | 0 | 0.084 | 12 | 3.42 |
| 1:40 | 0 | 0 | 0 | -0.156 | 12 | 1.56 |
| 2:00 | 0 | 0 | 0 | -0.412 | 12 | 0 |
| 2:20 | 0 | 0 | 0 | -0.763 | 12 | 0 |
| 2:40 | 0 | 0 | 0 | -0.908 | 11 | 0 |
| 3:00 | 0 | 0 | 0 | -0.756 | 11 | 0 |
| 3:20 | 0 | 0 | 0 | -0.725 | 11 | 0 |
| 3:40 | 0 | 0 | 0 | -0.684 | 11 | 0 |
| 4:00 | 0 | 0 | 0 | -0.788 | 11 | 0 |
| 4:20 | 0 | 0 | 0 | -1.068 | 11 | 9.33 |
| 4:40 | 0 | 0 | 0 | -1.351 | 11 | 16.78 |
| 5:00 | 0 | 0 | 0 | -1.555 | 11 | 19.89 |
| 5:20 | 0 | 0 | 0 | -2.028 | 11 | 23 |
| 5:40 | 0 | 0 | 0 | -2.061 | 10 | 26.73 |
| 6:00 | 0 | 0 | 0 | -2.264 | 10 | 29.83 |
| 6:20 | 0 | 0 | 0 | -2.21 | 10 | 60.92 |
| 6:40 | 0 | 0 | 0 | -1.79 | 10 | 116.85 |

| | | | | | | |
|---|---|---|---|---|---|---|
| 7:00 | 0 | 0 | 0.101619 | -1.436 | 10 | 179 |
| 7:20 | 268.7533 | 9.07445 | 19.56133 | -0.875 | 10 | 182.11 |
| 7:40 | 504.0331 | 19.5337 | 70.6567 | -0.452 | 10 | 181.18 |
| 8:00 | 660.5361 | 27.27914 | 137.4347 | -0.603 | 11 | 176.51 |
| 8:20 | 744.415 | 32.80811 | 205.3087 | -0.119 | 11 | 157.87 |
| 8:40 | 807.264 | 37.75703 | 276.2584 | -0.062 | 11 | 131.76 |
| 9:00 | 856.3865 | 41.18162 | 342.2437 | 0.316 | 11 | 106.9 |
| 9:20 | 896.0777 | 42.2008 | 404.4359 | 1.759 | 11 | 103.8 |
| 9:40 | 915.7459 | 44.48463 | 459.3573 | 2.96 | 11 | 91.68 |
| 10:00 | 937.6204 | 46.62388 | 513.6011 | 4.064 | 11 | 74.58 |
| 10:20 | 950.1722 | 49.19342 | 560.515 | 4.418 | 11 | 83.91 |
| 10:40 | 964.4706 | 50.14903 | 603.8051 | 5.755 | 11 | 81.11 |
| 11:00 | 975.1052 | 51.34577 | 639.2039 | 6.33 | 11 | 67.12 |
| 11:20 | 978.2744 | 51.26279 | 664.3071 | 7.438 | 11 | 76.45 |
| 11:40 | 985.4963 | 51.75318 | 685.8186 | 8.32 | 11 | 72.72 |
| 12:00 | 990.9766 | 51.31373 | 698.8984 | 9.01 | 12 | 57.18 |
| 12:20 | 981.1829 | 54.76762 | 700.2568 | 9.16 | 12 | 47.86 |
| 12:40 | 978.8789 | 54.25362 | 696.4173 | 10.21 | 12 | 38.54 |
| 13:00 | 992.2296 | 52.11921 | 693.0816 | 10.12 | 12 | 32.31 |
| 13:20 | 985.3871 | 51.50127 | 672.4406 | 10.29 | 12 | 61.84 |
| 13:40 | 982.0522 | 50.81474 | 648.7031 | 10.77 | 12 | 67.43 |
| 14:00 | 975.9212 | 48.95206 | 616.4742 | 11.37 | 12 | 47.24 |
| 14:20 | 969.0346 | 48.42316 | 578.624 | 11.19 | 12 | 42.58 |
| 14:40 | 944.1416 | 43.99123 | 522.6065 | 11.99 | 12 | 35.12 |
| 15:00 | 928.1752 | 43.07912 | 472.7091 | 12.34 | 12 | 27.35 |
| 15:20 | 909.636 | 40.93139 | 416.9634 | 12.45 | 12 | 21.13 |
| 15:40 | 879.9061 | 36.56019 | 355.4168 | 13.08 | 12 | 23.01 |
| 16:00 | 824.7355 | 35.64042 | 288.9364 | 12.51 | 12 | 32.31 |

| | | | | | | |
|---|---|---|---|---|---|---|
| 16:20 | 762.5556 | 32.87503 | 219.8702 | 12.23 | 12 | 30.77 |
| 16:40 | 669.892 | 26.10575 | 146.859 | 12.49 | 12 | 35.43 |
| 17:00 | 536.3097 | 19.5186 | 80.61623 | 12.34 | 12 | 44.75 |
| 17:20 | 320.8759 | 9.458782 | 25.78414 | 11.68 | 12 | 43.2 |
| 17:40 | 0.1644439 | 0 | 0 | 10.44 | 12 | 58.11 |
| 18:00 | 0 | 0 | 0 | 9.89 | 11 | 84.53 |
| 18:20 | 0 | 0 | 0 | 9.4 | 11 | 61.22 |
| 18:40 | 0 | 0 | 0 | 9.6 | 11 | 38.85 |
| 19:00 | 0 | 0 | 0 | 7.348 | 11 | 24.87 |
| 19:20 | 0 | 0 | 0 | 6.355 | 11 | 48.18 |
| 19:40 | 0 | 0 | 0 | 6.359 | 11 | 60.29 |
| 20:00 | 0 | 0 | 0 | 5.696 | 11 | 57.18 |
| 20:20 | 0 | 0 | 0 | 4.565 | 11 | 71.17 |
| 20:40 | 0 | 0 | 0 | 3.718 | 11 | 78.62 |
| 21:00 | 0 | 0 | 0 | 4.152 | 11 | 77.07 |
| 21:20 | 0 | 0 | 0 | 3.597 | 11 | 44.45 |
| 21:40 | 0 | 0 | 0 | 4.199 | 11 | 31.39 |
| 22:00 | 0 | 0 | 0 | 4.731 | 11 | 42.26 |
| 22:20 | 0 | 0 | 0 | 4.528 | 11 | 25.17 |
| 22:40 | 0 | 0 | 0 | 3 | 12 | 23.87 |
| 23:00 | 0 | 0 | 0 | 2.553 | 12 | 38.79 |
| 23:20 | 0 | 0 | 0 | 3.507 | 12 | 26.36 |
| 23:40 | 0 | 0 | 0 | 3.505 | 12 | 11.82 |

Appendix B2: Summer data

| Time | Global horizontal irradiance [W/m²] | Direct normal irradiance [W/m²] | Diffuse horizontal irradiance [W/m²] | Ambient air temperature [°C] | Inlet water temperature [°C] | Hot water consumption [L] |
|---|---|---|---|---|---|---|
| 0:00 | 0.006845 | 0 | 0 | 21.96 | 22 | 8.85 |
| 0:20 | 0.2738012 | 0 | 0 | 21.51 | 22 | 4.7 |
| 0:40 | 0 | 0 | 0 | 21.14 | 22 | 3.05 |
| 1:00 | 0 | 0 | 0 | 20.68 | 22 | 4.43 |
| 1:20 | 0 | 0 | 0 | 20.41 | 22 | 3.05 |
| 1:40 | 0 | 0 | 0 | 19.83 | 22 | 1.39 |
| 2:00 | 0 | 0 | 0 | 19.14 | 22 | 0 |
| 2:20 | 0 | 0 | 0 | 19.12 | 22 | 0 |
| 2:40 | 0 | 0 | 0 | 18.87 | 22 | 0 |
| 3:00 | 0 | 0 | 0 | 18.59 | 21 | 0 |
| 3:20 | 0 | 0 | 0 | 18.67 | 21 | 0 |
| 3:40 | 0 | 0 | 0 | 18.55 | 21 | 0 |
| 4:00 | 0 | 0 | 0 | 18.58 | 21 | 0 |
| 4:20 | 0 | 0 | 0 | 18.24 | 21 | 8.3 |
| 4:40 | 0 | 0 | 0 | 17.96 | 21 | 14.94 |
| 5:00 | 0 | 0 | 0 | 17.9 | 21 | 17.7 |
| 5:20 | 0 | 0 | 0 | 17.88 | 21 | 20.47 |
| 5:40 | 0 | 15.22147 | 15.08478 | 17.64 | 21 | 23.79 |
| 6:00 | 335.5685 | 31.13482 | 63.93767 | 18.11 | 20 | 26.55 |
| 6:20 | 494.5685 | 46.04919 | 129.3213 | 18.18 | 20 | 54.21 |
| 6:40 | 592.139 | 64.36671 | 207.8722 | 18.48 | 20 | 104 |
| 7:00 | 671.0402 | 106.0943 | 318.119 | 18.71 | 20 | 159.31 |
| 7:20 | 726.9453 | 115.9576 | 397.8902 | 19.45 | 20 | 162.08 |

| | | | | | | |
|---|---|---|---|---|---|---|
| 7:40 | 434.8187 | 172.0262 | 369.9471 | 19.59 | 20 | 161.24 |
| 8:00 | 194.7393 | 232.9366 | 337.4386 | 19.89 | 20 | 157.09 |
| 8:20 | 746.0349 | 190.1847 | 629.1271 | 20.68 | 20 | 140.5 |
| 8:40 | 881.474 | 148.8412 | 722.781 | 21.42 | 20 | 117.27 |
| 9:00 | 912.2477 | 105.2413 | 752.3268 | 21.82 | 20 | 95.14 |
| 9:20 | 927.9118 | 103.4122 | 812.1363 | 22.29 | 20 | 92.38 |
| 9:40 | 942.8919 | 106.4517 | 875.4613 | 22.89 | 20 | 81.6 |
| 10:00 | 839.9965 | 126.9494 | 850.323 | 22.98 | 20 | 66.38 |
| 10:20 | 967.8378 | 106.6356 | 975.8386 | 24.06 | 20 | 74.68 |
| 10:40 | 980.7048 | 107.0933 | 1021.026 | 24.65 | 20 | 72.19 |
| 11:00 | 987.0703 | 108.0165 | 1056.703 | 25.48 | 20 | 59.74 |
| 11:20 | 1002.06 | 105.6507 | 1091.615 | 24.77 | 20 | 68.04 |
| 11:40 | 1007.616 | 105.6671 | 1112.633 | 25.01 | 20 | 64.72 |
| 12:00 | 1008.719 | 101.9173 | 1120.529 | 27.11 | 21 | 50.89 |
| 12:20 | 1012.996 | 102.5969 | 1129.354 | 27.4 | 21 | 42.59 |
| 12:40 | 1013.471 | 98.91734 | 1122.349 | 27.95 | 21 | 34.3 |
| 13:00 | 1010.156 | 99.42525 | 1111.806 | 27.63 | 21 | 28.76 |
| 13:20 | 1009.398 | 114.2371 | 1111.801 | 27.15 | 21 | 55.04 |
| 13:40 | 1009.532 | 133.3908 | 1110.691 | 28.08 | 21 | 60.02 |
| 14:00 | 996.3516 | 159.7342 | 1098.896 | 29.48 | 21 | 42.04 |
| 14:20 | 826.9774 | 268.9741 | 1021.338 | 30.29 | 21 | 37.89 |
| 14:40 | 108.5542 | 271.5633 | 344.8483 | 28.86 | 21 | 31.26 |
| 15:00 | 392.555 | 205.0055 | 495.0047 | 29.48 | 21 | 24.34 |
| 15:20 | 0.4718932 | 215.5987 | 215.6529 | 29.25 | 21 | 18.81 |
| 15:40 | 233.7721 | 207.7375 | 387.8535 | 29.02 | 21 | 20.47 |
| 16:00 | 402.9854 | 262.8528 | 537.6998 | 30.53 | 21 | 28.76 |
| 16:20 | 752.8419 | 197.0441 | 661.3769 | 28.66 | 21 | 27.39 |
| 16:40 | 676.3504 | 137.7759 | 504.0948 | 29.71 | 21 | 31.53 |

| | | | | | | |
|---|---|---|---|---|---|---|
| 17:00 | 143.9888 | 138.3427 | 198.3929 | 29.02 | 21 | 39.83 |
| 17:20 | 763.7689 | 105.9392 | 427.0865 | 29.12 | 21 | 38.45 |
| 17:40 | 2.496357 | 71.68157 | 73.16638 | 28.6 | 21 | 51.72 |
| 18:00 | 610.944 | 76.38116 | 244.9391 | 28.99 | 21 | 75.23 |
| 18:20 | 497.4384 | 49.4411 | 150.122 | 28.99 | 22 | 54.49 |
| 18:40 | 214.3877 | 34.74383 | 63.07903 | 28.38 | 22 | 34.57 |
| 19:00 | 198.3638 | 19.36589 | 31.62829 | 28.07 | 22 | 22.13 |
| 19:20 | 0.0068402 | 0.4212284 | 0.5883917 | 27.24 | 22 | 42.87 |
| 19:40 | 0 | 0 | 0 | 27.02 | 22 | 53.66 |
| 20:00 | 0 | 0 | 0 | 27.45 | 22 | 50.89 |
| 20:20 | 0 | 0 | 0 | 26.7 | 22 | 63.34 |
| 20:40 | 0 | 0 | 0 | 27.63 | 22 | 69.98 |
| 21:00 | 0 | 0 | 0 | 27.35 | 22 | 68.59 |
| 21:20 | 0 | 0 | 0 | 24.94 | 22 | 39.56 |
| 21:40 | 0 | 0 | 0 | 25.82 | 22 | 27.94 |
| 22:00 | 0 | 0 | 0 | 26 | 22 | 37.61 |
| 22:20 | 0 | 0 | 0 | 23.48 | 22 | 22.4 |
| 22:40 | 0 | 0 | 0 | 22.96 | 22 | 21.25 |
| 23:00 | 0 | 0 | 0 | 22.46 | 22 | 34.52 |
| 23:20 | 0 | 0 | 0 | 23.39 | 22 | 23.46 |
| 23:40 | 0 | 0 | 0 | 24.75 | 22 | 10.52 |

## APPENDIX C: ANNUAL ENERGY AND CUMULATIVE COSTS (LCC)

| Year | ESTWH energy cost after each year (ZAR) | IDX-SAHP energy cost after each year (ZAR) | O & M ESTWH cost after each year (ZAR) | O & M IDX-SAHP cost after each year (ZAR) | ESTWH (Annual cumulative cost) (ZAR) | IDX-SAHP (Annual cumulative cost) (ZAR) |
|---|---|---|---|---|---|---|
| 0 | - | - | - | - | 108 375.00 | 215 554.00 |
| 1 | 181 132.42 | 43 879.17 | 1 083.75 | 2 155.54 | 290 591.17 | 261 588.71 |
| 2 | 380 378.09 | 92 146.26 | 2 227.00 | 4 429.42 | 490 980.08 | 312 129.68 |
| 3 | 599 548.32 | 145 240.06 | 3 433.01 | 6 828.13 | 711 356.33 | 367 622.19 |
| 4 | 840 635.57 | 203 643.23 | 4 705.23 | 9 358.54 | 953 715.80 | 428 555.77 |
| 5 | 1 105 831.55 | 267 886.73 | 6 047.30 | 12 027.86 | 1 220 253.85 | 495 468.59 |
| 6 | 1 397 547.12 | 338 554.57 | 7 463.05 | 14 843.73 | 1 513 385.17 | 568 952.30 |
| 7 | 1 718 434.26 | 416 289.20 | 8 956.52 | 17 814.19 | 1 835 765.77 | 649 657.39 |
| 8 | 2 071 410.10 | 501 797.29 | 10 531.98 | 20 947.73 | 2 190 317.09 | 747 594.11 |
| 9 | 2 459 683.54 | 595 856.19 | 12 193.94 | 24 253.30 | 2 580 252.47 | 844 958.59 |
| 10 | 2 886 784.31 | 699 320.98 | 13 947.13 | 27 740.35 | 3 009 106.45 | 951 910.42 |
| 11 | 3 356 595.16 | 813 132.25 | 15 796.58 | 31 418.83 | 3 480 766.75 | 1 069 400.18 |
| 12 | 3 873 387.10 | 938 324.65 | 17 747.56 | 35 299.27 | 3 999 509.67 | 1 198 473.01 |
| 13 | 4 441 858.23 | 1 076 036.28 | 19 805.65 | 39 392.74 | 4 570 038.89 | 1 340 278.11 |
| 14 | 5 067 176.48 | 1 227 519.08 | 21 976.73 | 43 710.94 | 5 197 528.21 | 1 496 079.11 |
| 15 | 5 755 026.55 | 1 394 150.16 | 24 267.01 | 48 266.21 | 6 084 802.68 | 1 939 706.19 |
| 16 | 6 511 661.63 | 1 577 444.35 | 26 683.02 | 53 071.57 | 6 843 853.77 | 2 137 379.83 |
| 17 | 7 343 960.21 | 1 779 067.96 | 29 231.66 | 58 140.73 | 7 678 701.00 | 2 344 072.60 |
| 18 | 8 259 488.65 | 2 000 853.92 | 31 920.23 | 63 488.20 | 8 596 918.01 | 2 571 206.04 |
| 19 | 9 266 569.94 | 2 244 818.49 | 34 756.40 | 69 129.24 | 9 606 835.47 | 2 820 811.64 |
| 20 | 10 374 359.36 | 2 513 179.51 | 37 748.28 | 75 079.98 | 10 695 941.76 | 3 052 012.60 |
| Salvage | - | - | - | - | -21 675.00 | -43 110.80 |
| LCC | - | - | - | - | 10 695 941.76 | 3 052 012.60 |